Acinetobacter baumannii in Norwegian chicken farms:

A One Health perspective

Per Kristian Thorén Edvardsen

Master Thesis

Department of Biosciences

Faculty for Mathematics and Natural Sciences

University of Oslo

June 2020

2020

Acinetobacter baumannii in Norwegian chicken farms: A One Health perspective

http://www.duo.uio.no

Trykk: Reprosentralen, Universitetet i Oslo

Abstract

The Gram-negative bacterium, *Acinetobacter baumannii*, is one of the leading causes of drug resistant hospital-acquired infections in humans. Owing to its ability to easily acquire resistance genes and to survive in the hospital environment for long periods of time, *A. baumannii* has become a major problem worldwide. Despite much effort trying to find out where it naturally resides, less is known about its native habitat or the reservoirs for the isolates found in the clinic. Thus, in this thesis, multilocus sequence typing (MLST) was performed on a collection of environmental *A. baumannii* isolates sampled from Norwegian chicken farms in 2016, to uncover the phylogenetic diversity and the relationship between the isolates. The isolates were screened for resistance toward selected clinically relevant antimicrobials using both a disc diffusion and broth microdilution method, in order to investigate whether Norwegian chicken farms could constitute potential reservoirs of carbapenem resistant isolates. Additionally, the isolates were examined for their ability to switch from the opaque to translucent colony morphology, a newly discovered phenomenon in *A. baumannii* believed to constitute a phase variation mechanism. The MLST analysis revealed both close and distant relationships between the chicken farm isolates, and 36 novel and 18 previously known sequence types were identified. A possible connection between some of the chicken farm isolates and a clinical *A. baumannii* isolate retrieved from a Norwegian hospital was found. Only one allelic mismatch separated some of the chicken farm isolates from the clinical isolate, harboring the same sequence type as the international clonal lineage 8. Furthermore, it was determined that none of the isolates from chicken farms were resistant to any of the antibiotics tested, putatively indicating that Norwegian chicken farms do not constitute reservoirs of carbapenem resistant *A. baumannii*. This study presents the first data showing that non-clinical isolates of *A. baumannii* can switch from the opaque to translucent colony phase, and that frequencies of switching can be highly variable from one isolate to another. Altogether, this study indicates that chicken farms may be an important source of *A. baumannii* and that phase variation may be a natural inherent mechanism of this species.

Acknowledgements

First, I would like to express my profound gratitude to my main supervisor Professor Ole Andreas Løchen Økstad, for giving me the opportunity to work on this project. Thank you for your support and guidance. The time spent in your group have been very educational.

My sincere thanks also go to my supervisor Professor Dirk Linke for his advice and always being accessible and helpful when needed.

I would like to express my deepest gratitude to my friend, colleague, and PhD candidate Claus Michael Goul Larsen, who have guided me through this project. Thank you for your collaboration, time, and advice.

A special thanks to Beata, Mona, Sarah, Roger and Truls for your assistance and always being helpful when needed. Beata, thank you for the laughs shared and the continuous encouragement.

To my friends and family, thank you for your everlasting support. I am indebted to my friends for always cheering me up and for the wonderful moments together.

Finally, I want to thank Kristine for her support and for always being there for me. I am forever grateful for all the craziness we have shared together!

Abbreviations

AAC	aminoglycosides acetyltransferase
AAD	aminoglycoside adenyltransferase
Acb	*Acinetobacter calcoaceticus-baumannii* complex
ADC	*Acinetobacter*-derived cephalosporinase
AGP	antibiotic growth promoter
AME	aminoglycoside-modifying enzymes
AMR	antimicrobial resistance
APH	aminoglycoside phosphotransferase
BLAST	basic local alignment search tool
BURST	based upon related sequence type
CARB	carbenicillinases
CC	clonal complex
CFU	colony forming units
CIP	ciprofloxacin
CLSI	Clinical and Laboratory Standards Institute
CPE	carbapenemase-producing *Enterobacterales*
DEPC	diethyl pyrocarbonate
dH_2O	distilled water
DLV	double-locus variant
DNA	deoxyribonucleic acid
dNTP	deoxynucleotide
EDTA	ethylenediaminetetraacetic acid
ESBL	extended spectrum β-lactamase
EUCAST	European committee on antimicrobial susceptibility testing
GEN	gentamicin
GDP	gross deomestic product
goeBURST	global optimal eBURST
HGT	horizontal gene transfer
IC	international clone
IPM	imipenem
IS	insertion sequence
LB	Luria-Bertani

MALDI-TOF	matrix-assisted laser desorption/ionization time of flight
MBL	metallo-β-lactamase
MDR	multidrug-resistant
MEM	meropenem
MH	Mueller-Hinton
MHB	Mueller-Hinton broth
MIC	minimum inhibitory concentration
MLST	multilocus sequencing typing
MRSA	methicillin-resistant *Staphylococcus aureus*
MSA	multiple sequence alignment
MSIS	Norwegian Surveillance System for Communicable Diseases
MST	minimum spanning tree
OD	optical density
OXA	oxacillinase
PBP	penicillin-binding protein
PCR	polymerase chain reaction
RCF	relative centrifugal force
RND	resistance-nodulation-division
RPM	rounds per minute
SLV	single-locus variant
spp.	species
ST	sequence type
TAE	tris-acetate-EDTA
TOB	tobramycin
UPGMA	unweighted pair group method with arithmetic mean
VRE	vancomycin-resistant *Enterococcus*
WHO	World Health organization

Table of Contents

1 Introduction

1.1 The One Health concept

The One Health concept is a concept built upon the realization that the health of people, animals and our environment are inextricably interconnected (Figure 1). It is an approach that reflects our understanding that we are a part of a larger highly dynamic system (American Veterinary Medical Association, 2008). The One Health approach has been defined by the American Veterinary Medical Association as "the collaborative efforts of multiple disciplines working locally, nationally, and globally, to attain optimal health for people, animals, and our environment". Central to this concept is the management of infectious diseases. Most of the new emerging infectious diseases are zoonotic, reflecting the ever-increasing contact with animals (American Veterinary Medical Association, 2008; Cantas and Suer, 2014). Humans have probably never been as exposed to zoonotic diseases as today (Cantas and Suer, 2014). There is no doubt that zoonotic diseases have a major impact on global health.

Every indication suggests that infectious diseases will continue to impact the health of humans globally. We will continue to share the world and its environment with other inhabitants including animals and microbial pathogens. Consequently, zoonotic diseases will occur and therefore a better understanding of what drives the emergence and spread of infectious diseases is needed. Globalization and climate change are some of the factors contributing to this (American Veterinary Medical Association, 2008). Factors like these are not likely to stop in the near future and therefore a One Health approach to handling the problem is needed. As Dr. Gro Harlem Brundtland, former director of World Health Organization (WHO), stated in one of her speeches "In an interconnected and interdependent world, bacteria and viruses travel almost as fast as email messages" (Brundtland, 2003). With globalization this is true, there are no health sanctuaries, as clearly evidenced by the recent SARS-CoV-2 pandemic. However, this is not only true for humans but also for animals and the environment (American Veterinary Medical Association, 2008; Calistri *et al.*, 2013).

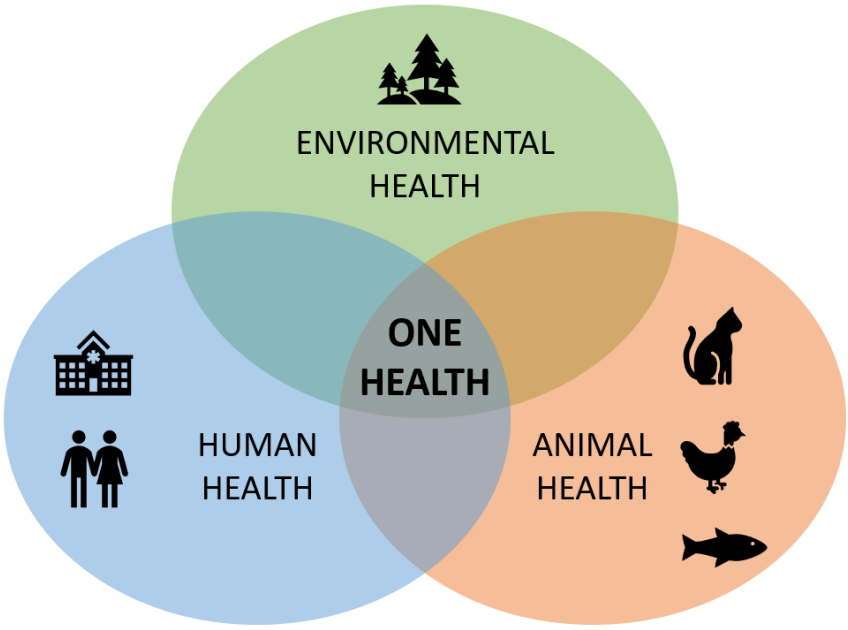

Figure 1. The One Health concept: an interconnected approach of health.

1.2 Antibiotic resistance

In the late 1920s Alexander Fleming discovered one of the first antibiotics, penicillin. A drug discovered by sheer luck, proved to be a discovery of a lifetime. Fleming (2019) stated that an accidental contamination of a culture plate of *Staphylococcus* bacteria by a mold, was the origin behind the discovery of penicillin. Fleming discovered that many of the common human pathogens were killed by penicillin. The success and discovery of penicillin led to an intensive research into antibacterial compounds to combat infectious bacteria. In 1945 Alexander Fleming was awarded the Nobel prize for his work. However, in 1945 while giving his Nobel Lecture he stated a warning: "The time may come when penicillin can be bought by anyone in the shops. Then there is the danger that the ignorant man may easily underdose himself and by exposing his microbes to non-lethal quantities of the drug make them resistant…." (*Sir Alexander Fleming – Nobel Lecture*, 2019). As Fleming predicted, resistance has emerged at a large scale for many antimicrobials.

Today antimicrobial resistance (AMR) is regarded as one of the most important threats to global public health (WHO, 2014, 2015). The extensive and reckless usage of antibiotics has accelerated the development and emergence of drug-resistant bacteria (WHO, 2015). The development of antibacterial resistance mechanisms giving resistance to whole classes of drugs, leave few or no antibiotics to treat certain multidrug-resistant (MDR) bacteria (i.e. bacteria resistant towards several antibiotics) today. Development of resistance limits the

lifespan of antibiotics and a constant introduction of new compounds is needed. The situation is on the way becoming critical and there is a desperate need for novel antibiotics. Antibiotic resistance is rising much faster than new antibiotics are developed and approved (O'Neill, 2014; WHO, 2014; Tacconelli *et al.*, 2018).

What is antibiotic resistance? Antibiotic resistance is the ability of bacteria to resist the effects of antibiotics and makes bacteria able to grow in the presence of these compounds. Though antibiotic resistance can develop as a result of natural selection, misuse of antibiotics greatly accelerates its development and spread (O'Neill, 2014; Zaman *et al.*, 2017). In fact, resistance to penicillin was reported in bacteria before it got widely used, however the extensive use of the drug accelerated the rate at which bacteria became resistant against it (Abraham and Chain, 1940; Lobanovska and Pilla, 2017). The misuse of antibacterial drugs in both humans and animals has resulted in the selection and spread of resistant bacteria (WHO, 2014; IACG, 2019). In human health, poor prescribing practices, low regulation and over-the-counter sales have contributed greatly to the problem (IACG, 2019). In animals, antibiotics have been used as growth promoters which greatly favors the selection of resistant bacteria (WHO, 2014; IACG, 2019). Consequently, antibiotics are becoming less effective which is a major concern for global health. In the absence of effective antibiotics, routine operations and cancer treatments become riskier and could potentially become life-threatening due to infections (WHO, 2014).

The consequence of antibiotic resistance in humans is not fully known, however estimates suggest that resistant bacteria that cause infections are responsible for at least 700 000 deaths every year and may rise to 10 million by 2050 (O'Neill, 2014). Furthermore, antibiotic resistance also threatens the global economy according to a report by the World Bank (2017). Increased morbidity, mortality, infection control and hospitalization will contribute to more costs. More resources will be used to cope with bacterial infections and the society will be affected by a reduction in effective labor supply (World Bank, 2017). In livestock production, increased morbidity and mortality will lead to a lower supply of livestock products. Simulations performed by the World Bank estimate the impact of antimicrobial resistance on the global economy by 2050. In a low impact-AMR scenario the global gross domestic product (GDP) was estimated to fall annually by 1.1 % by 2050, and in a high impact-AMR scenario by 3.8 % annually. The loss in annual global GDP may be comparable or even worse than the losses of the 2008-2009 financial crisis. However, investing 0.2 trillion dollars

until 2050 in AMR containment, will bring global benefits between 10-27 trillion dollars, assuming that 50 % of AMR costs can be avoided (World Bank, 2017).

The use of antibiotics to prevent disease has revolutionized the modern era of medicine and is probably the most successful and important chemotherapeutic drug ever to be found. If we are to continue its use as "wonder drugs" to combat bacteria, tighter regulation and surveillance of its use needs to be implemented. The current global response to antibiotic resistance is inadequate. There is no time to wait, it is time to react.

1.2.1 The use of antibiotics in food animals and its impact on resistance

For an ever-growing human population, more food is needed and as a result more meat is produced. The usage of antibiotic growth promoters (AGP) to enhance the production of meat has been implemented since the 1950s, to both speed up animal growth and to improve the feed-to-weight ratio of food animals (Cogliani, Goossens and Greko, 2011; Marshall and Levy, 2011). Since the first AGPs were approved for use, several studies have established a link between the use of AGPs and the emergence and spread of antimicrobial resistance. It is now clear that the continuous application of low doses of AGPs over an extended period of time selects for resistance in bacteria. Moreover, not only is resistance against the antibiotic administered selected for but also for other antibiotics as well (Cogliani, Goossens and Greko, 2011; Marshall and Levy, 2011).

The introduction of avoparcin as a feed additive clearly demonstrated that the use of AGPs selects for resistance in food animals. An increase in isolation of vancomycin-resistant enterococci (VRE) was observed in farm animals and humans, after its introduction (Cogliani, Goossens and Greko, 2011; Marshall and Levy, 2011). Both vancomycin and avoparcin are glycopeptides and their structure are similar, hence resistance against avoparcin also affected vancomycin (Marshall and Levy, 2011). Vancomycin is often regarded as one of the drugs of last resort against both Methicillin-resistant *Staphylococcus aureus* (MRSA) and *Enterococcus* species and therefore resistance against vancomycin in this species is very serious. Following the ban of avoparcin in the late 1995 in Denmark and 1997 in EU, a reduction in the prevalence of VRE in animals was seen (Marshall and Levy, 2011). In Denmark, the frequencies of isolation fell from 73-80 % to 5-6 %, which is an enormous reduction in isolation rate. Furthermore, a dramatic reduction was also seen in humans; VRE

colonization declined from 13 % to 4% from 1994 to 1998 in Germany (Marshall and Levy, 2011).

Since the banning of several AGPs in 1990s and the ban of all AGPs in the EU in 2006, there were concerns that the incidence of disease in animals would rise. However, no lasting negative effects have been seen (Marshall and Levy, 2011). Between 1992 and 2008, Danish farmers increased their production of swine with 47 %. During this period, antimicrobial use in swine was reduced by 51 %. The therapeutic use of antibiotics was also reduced by 90 % (Cogliani, Goossens and Greko, 2011). This demonstrates that the ban of AGPs does not need to have major consequences for animal health, and that production can increase without its use.

What about human health? Does the use of antibiotics in food animals have an impact on our health? More and more evidence does seem to indicate that this is the case. Farm workers and veterinarians, which are in close contact with animals daily, are directly at risk of picking up resistant bacteria from animals. These people represent an entry point for resistance genes. Such genes may be transferred to the community and hospital environments where further spread of these genes is possible (Marshall and Levy, 2011). For example, the *mecA* gene copies from animal isolates, responsible for resistance against methicillin and other β-lactam antibiotics in *Staphylococcus aureus*, were found to be identical to those found in human isolates in Korea according to Marshall and Levy (2011). Furthermore, there is also evidence to support that human consumption of food exposes humans to resistant bacteria and their genes. However, demonstrating that food-products are a reservoir of resistant bacteria is not an easy task because of the long and complex route from the farms to the consumers. Several genes found in food bacteria have later been found in human isolates (Marshall and Levy, 2011). However, this does only indirectly prove that the food chain is a source of resistant bacteria. Evidence for human infections as a result of food carrying antibiotic-resistant bacteria have also been reported (Marshall and Levy, 2011). For example, an outbreak of multidrug-resistant *Salmonella enterica* serovar *Typhimurium* in Arizona in 1985 was traced back to a person who consumed raw milk (Marshall and Levy, 2011). Resistance to nourseothricin (an AGP) in Germany was also traced back to isolates of *Salmonella* and *Shigella* found in humans with diarrhea. Nourseothricin was only used for growth promotion in swine, and after only 2 years of its use, resistance arose and resistant bacteria was transferred to humans (Marshall and Levy, 2011).

In a recent study by Richardson *et al.* (2018), it was found that gene exchange in different species has driven the success of MRSA. Different isolates of *S. aureus* have been able to undergo host-switching events and adapt to different species by acquiring new genes. Humans are thought of as being the major reservoir of *S. aureus* (Richardson *et al.*, 2018). However, the domestication of animals and the intensification of farming has provided several opportunities for transfer of bacteria such as *S. aureus* to animals from humans (Richardson *et al.*, 2018). Because *S. aureus* has been able to jump and switch between hosts, the bacterium can now be found in several animals in addition to humans. The capacity of *S. aureus* to switch between hosts is a major reason for why it has become such a major threat to human health (Richardson *et al.*, 2018). These host transitions are associated with horizontal acquisition of genes encoding for resistance against antibiotics. Evidence suggests that there are different gene pools associated with different animals and that resistance to specific classes of antibiotics is specific to each host (Richardson *et al.*, 2018). For example, resistance genes for aminoglycosides, such as streptomycin, and for tetracyclines and antiseptics are believed to derive from pigs. Aminoglycosides and tetracyclines are used much more in farmed animals than in human medicine (Richardson *et al.*, 2018). The use of antibiotics in food animals such as pigs has therefore contributed to the emergence of resistance because of the selective pressure it exerts. Richardson and colleagues (2018) imply that host-specific accessory gene pools are probably present in the microbiota of the host species which then promote host-adaptive evolution of *S. aureus*. This, together with its ability to jump between different species, has created what we today know as MRSA.

The evidence provided here shows that food animals can be a reservoir of resistance genes which can ultimately be transferred to humans. By limiting the use of AGPs, the selection pressure on bacteria to gain resistance is lessened. Moreover, it also helps in the preservation of future antibiotics in a world with few new compounds with antimicrobial activity in development. Additionally, minimizing the leaching of unmetabolized antibiotics into the environment from animals will also help in lowering resistance in environmental bacteria (Marshall and Levy, 2011). Overall limiting the use of AGPs is imperative.

1.2.2 Antibiotic resistance and sales in Norway

The occurrence of antibiotic resistance in Norway is low in both humans and food-producing animals (NORM, 2019). This also holds true when comparing the frequency of antibiotic resistance in Norway to other countries as well. The low occurrence of resistance reflects the low usage and tight regulation of antibiotics in the country. Antibiotics in Norway are only made available by prescriptions (NORM, 2019).

Sales of active substances of antibacterial agents in Norway in the period of 2005-2018 have remained between 50 and 60 tons. Out of the total sales, sales for human use accounted for 89 %, animals for 9 % and fish only 2 %. Since 2012, the sales have decreased by 6 %. The total antibiotic usage in humans has decreased by 24 % since 2012, and 84 % of the total sales of antibacterial agents are used in primary care i.e. used by persons at home (NORM, 2019). The most used antibiotic group in primary care in Norway in 2018, are the penicillins followed by tetracyclines. The penicillins are also the most widely used antibacterial agent in major food-producing animals, cattle, goat, pigs and sheep, accounting for 85.8 % of the antibacterial agents used (NORM, 2019).

In veterinary medicine, the sales of antibacterial veterinary medicinal products (VMPs) have declined by 46 % in the period of 1993-2018 (Figure 2). The estimated reduction in sales from 2013 to 2018 in major food-producing animals including poultry, was 17 % (NORM, 2019). At the same time, sales of antibacterial VMPs for companion animals was reduced by 34 %. The sales of antibacterial VMPs for group treatment of the terrestrial food-producing animals, only accounted for 4 % of the total sales. In aquaculture, the sales of antibacterial VMPs have declined significantly since the mid-1980s (Figure 3). In 2018, 871 kg of antibacterial agents was used for farmed fish. This is a reduction of more than 99 % compared to 1987, mainly due to the introduction of vaccines against bacterial diseases in salmon and rainbow trout (NORM, 2019).

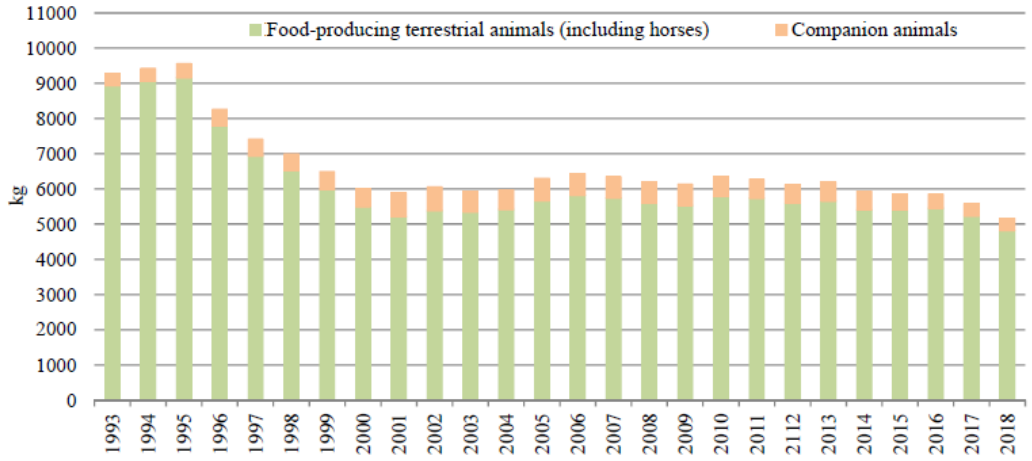

Figure 2. Total sales in kg of antibacterial veterinary medicinal products for therapeutic use in Norway from the period 1993-2018. The sales include both food-producing animals and companion animals. Source: NORM, 2019.

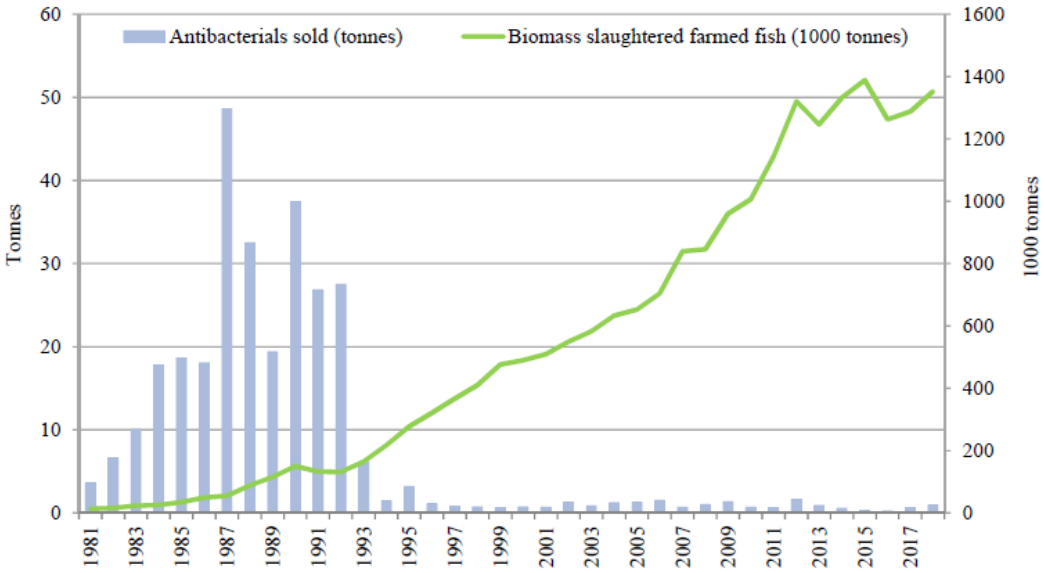

Figure 3. Total sales in tonnes of antibacterial veterinary medicinal products for therapeutic use in farmed fish and biomass of slaughtered farmed fish in tonnes, in Norway from the period of 1981-2018. Source: NORM, 2019.

1.3 The *Acinetobacter* genus

The genus *Acinetobacter*, derived from the Greek word “akinetos” meaning non-motile, belongs phylogenetically to the class of *Gammaproteobacteria*, under the order of *Pseudomonadales* in the family of *Moraxellaceae* (Garrity *et al.*, 2005, p. 425-437). Bacteria belonging to this genus are characterized by being gram-negative, obligately aerobic, catalase-positive, oxidase-negative, nonsporulating coccobacilli (Baumann, Doudoroff and Stanier, 1968; Garrity *et al.*, 2005, p. 425-437). Strains of *Acinetobacters* are often misidentified as gram-positive bacteria because they are often difficult to destain during

Gram staining. *Acinetobacter spp*. are considered as commensals of humans but some species may act as opportunistic pathogens. Most strains grow between 20-37°C, having an tempature optima at 33-35°C. However, the clincal strains readily grow at temperature from 37-44°C. *Acinetobacter spp.* grow well on defined media such as tryptic soy agar and sheep blood agar (Garrity *et al.*, 2005, p. 425-437; Seifert and Dijkshoorn, 2008).

The natural habitat of *Acinetobacter* species is not well defined, although it is believed that they occur naturally in soil and water, and that the environment is their main reservoir (Garrity *et al.*, 2005; Seifert and Dijkshoorn, 2008; Doughari *et al.*, 2011; Atrouni *et al.*, 2016). However, not all members of this group seem to have their natural habitat in the environment. Different species of this genus have been isolated from several origins including humans, animals, vegetables and meat, to mention some (Seifert and Dijkshoorn, 2008; Atrouni *et al.*, 2016). Evidence indicates that the human body may be a residence for some of the *Acinetobacter* species (Doughari *et al.*, 2011; Atrouni *et al.*, 2016). They seem to have an ability to inhabit almost any surface or habitat (Garrity *et al.*, 2005; Seifert and Dijkshoorn, 2008; Doughari *et al.*, 2011; Atrouni *et al.*, 2016). In general the members of this genus are said to be ubiquitous in nature (Garrity *et al.*, 2005; Seifert and Dijkshoorn, 2008; Atrouni *et al.*, 2016).

There has been a lot of confusion regarding the taxonomy of the genus *Acinetobacter*. Over the last 50-60 years the genus has undergone many taxonomic modifications. The oxidase-negative bacteria representing this group today was originally grouped into the genus of *Moraxella* (Baumann, Doudoroff and Stanier, 1968; Seifert and Dijkshoorn, 2008). At one time the species of *Acinetobacter* was assigned to 15 different genera because of all the confusion regarding the classification and the nomenclature of the group (Baumann, Doudoroff and Stanier, 1968). In 1968, the study by Baumann, Doudoroff and Stanier concluded and confirmed that the group of *Acinetobacter* was in fact a group of its own. However, they suggested that all species should be named and referred to as *Acinetobacter calcoaceticus*. This suggestion was made because differentiating the species by physiological characters was proving to be a difficult task at that time (Baumann, Doudoroff and Stanier, 1968). Even as of today differentiating species of *Acinetobacter* by microbial characteristics is still quite difficult (Seifert and Dijkshoorn, 2008).

The work of Baumann, Doudoroff and Stanier (1968) was later shown to be consistent with the work of J. Johnsons and co-workers, that oxidase negative bacteria of *Moraxella* belonged in a separate genus (Johnson, Anderson and Ordal, 1970). Johnson, Anderson and Ordal (1970) used DNA-DNA hybridization to confirm the homologies among *Acinetobacter's*, and to prove that they were distinct from the oxidase positive bacteria of *Moraxella*. However, it was not until the year of 1986 that different species within the genus of *Acinetobacter* were to be described. 12 different genomic species were recognized and assigned numbers; some were given names (Bouvet and Grimont, 1986; Seifert and Dijkshoorn, 2008). The *Acinetobacter* genus today consists of 60 species with validdly published names and several unnamed species (Nemec, 2018)

1.4 The *Acinetobacter calcoaceticus-baumannii* complex

The *Acinetobacter calcoaceticus-baumannii* (Acb) complex is a group consisting of six *Acinetobacter* species: *A. baumannii, A. calcoaceticus, Acinetobacter lactucae* (*Acinetobacter dijkshoorniae*), *Acinetobacter nosocomialis, Acinetobacter pitti* and *Acinetobacter seifertii*. They are more closely related to each other than to the other species of the *Acinetobacter* genus as seen in Figure 4 (Gerner-Smidt, Tjernberg and Ursing, 1991; Seifert and Dijkshoorn, 2008; Touchon *et al.*, 2014; Nemec *et al.*, 2015; Cosgaya *et al.*, 2016; Rooney, Dunlap and Flor-Weiler, 2016; Dunlap and Rooney, 2018). These species, except for *A. calcoaceticus* which is an environmental species, are the most clinically significant species of the genus (Howard *et al.*, 2012).

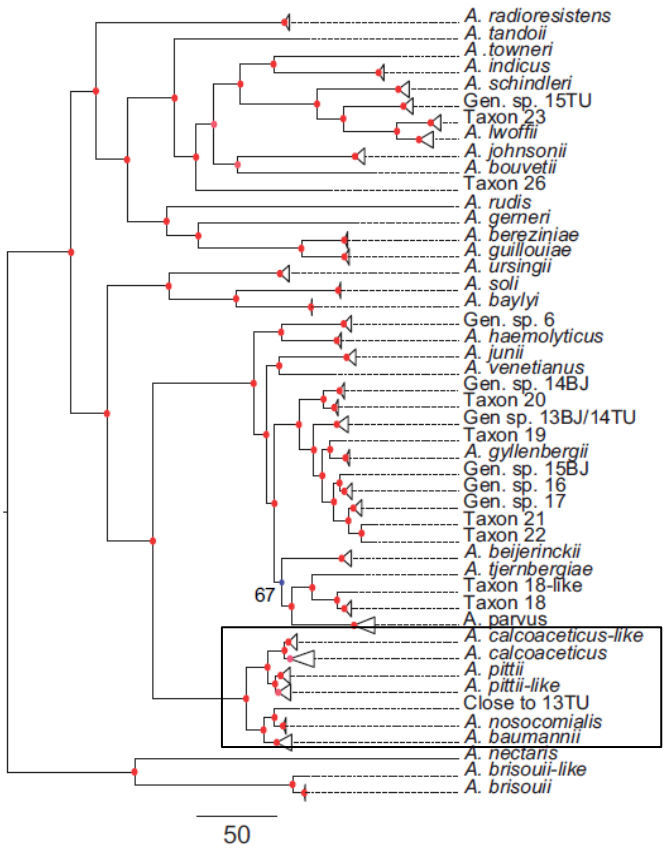

Figure 4. The phylogenetic relationship between the species in the *Acinetobacter* genus based on the alignment of 950 families of proteins found in the core genome. The triangles marks taxa containing several isolates belonging to the same species. The Acb complex is marked with a black square. Close to 13TU is *Acinetobacter seifertii* and *A. pitii-like* is *Acinetobacter lactucae* (also known as *Acinetobacter dijkshoorniae*). Source: Touchon et al., 2014.

1.4.1 *Acinetobacter baumannii*

The most notable and important species of the *Acinetobacter* genus and the Acb complex is *A. baumannii*. This bacterium is an opportunistic pathogen associated with hospital-acquired infections all over the world (Perez *et al.*, 2007; Lee *et al.*, 2017). Ranked by WHO as one of the three most critical bacteria which new antibiotics are urgently needed for treatment, carbapenem-resistant *A. baumannii* has emerged as a big problem in modern healthcare facilities (Lee *et al.*, 2017; Tacconelli *et al.*, 2018). Originally susceptible to most antibiotics up to the early years of the 1970s, resistance increased in *A. baumannii* during the 1980s and 1990s (Doi, Murray and Peleg, 2015). Due to the accumulation of several resistance mechanisms, the number of available antibiotics to treat infections with this bacterium has decreased gradually over the past few decades (Lee *et al.*, 2017). *A. baumannii* has become resistant to drugs such as carbapenems and colistin, which is why new treatments are urgently needed (Moffatt *et al.*, 2010; Doi, Murray and Peleg, 2015; Lee *et al.*, 2017). *A. baumannii* strains resistant to most or all known antibiotics have also been found and its clinical

significance is mainly due to its ability to acquire resistance determinants (Peleg, Seifert and Paterson, 2008; Doi, Murray and Peleg, 2015; Lee *et al.*, 2017). This organism has also proved to be an extraordinarily robust bacterium, tolerant to a wide range of temperatures, pH, and humidity. *A. baumannii* has been shown to survive on dry surfaces for five months, demonstrating how robust this organism can be (Gootz and Marra, 2008). Its ability to acquire resistance and to survive for prolonged periods of time in the hospital environment, makes this bacterium a serious concern.

The immunocompromised represent a high-risk group for infection of this bacterium, especially those with prolonged hospital stay (Gootz and Marra, 2008; Howard *et al.*, 2012). The majority of *A. baumannii* infections are usually caused by MDR *A. baumannii,* which complicates the treatment of the infections caused by the bacterium (Gootz and Marra, 2008). Mortality from *A. baumannii* infections is usually high, especially if it involves isolates resistant to antibiotics such as carbapenems. The mortality rate of those infected with carbapenem-resistant isolates ranges from 16-76 %. Risk factors for obtaining MDR isolates include recent exposure to antibiotics, usage of catheters or ventilators, duration of hospital stay and surgery (Doi, Murray and Peleg, 2015).

Despite a lot of effort trying to find the natural habitat of *A. baumannii,* it remains to be determined where it naturally resides. The bacterium has been isolated from several sources including humans, soil, water, food, companion animals and wildlife (Dijkshoorn, Nemec and Seifert, 2007; Lupo *et al.*, 2014; Pailhoriès *et al.*, 2015; Rafei, Hamze, *et al.*, 2015; Wilharm *et al.*, 2017). *A. baumannii* seems to be distributed widely in nature, however, not much is known about the reservoirs of the resistant isolates found in the clinics.

1.4.2 Epidemiology of *A. baumannii*

Multilocus sequence typing as a typing method

Multilocus sequencing typing (MLST), is a typing method used to characterize different isolates within the same species based on comparison of nucleotide sequences. The underlying principle of MLST is built upon the assumption that housekeeping genes, essential genes required for basic cellular function, are conserved throughout evolution (Urwin and Maiden, 2003). Since these so-called housekeeping genes are conserved, it is

expected that these genes evolve rather slowly and therefore few mutations will occur. Because genes under stabilizing selection for conservation have few mutations, they can be used to indicate genetic relationships between isolates more reliably than genes under positive selection (Urwin and Maiden, 2003). In the absence of genetic exchange, genetic variation is confined to mutations and to the descendants in which it occurred. These variations are recorded in the DNA and therefore may be used to determine relationships between bacteria of the same species. However, genes under positive selection pressure, such as genes conferring antibiotic resistance, are less suited to predict closely related species (Urwin and Maiden, 2003). The reason for this is that selection pressure forces evolution to keep up, accelerating the development of favorable mutations which arise rapidly. Such genes are not suitable for analysis of evolutionary relationships because they evolve too fast becoming less conserved. In addition, such genes are frequently transferred between bacteria making antibiotic resistance genes even less useful in predicting relationships (Urwin and Maiden, 2003).

The MLST approach, summarized in Figure 5, identifies variation by determining the nucleotide sequences of housekeeping genes, commonly seven, which is done by PCR and DNA sequencing. In MLST, all unique sequences are assigned an allele number and the different sequences are combined into an allelic profile for the seven genes, which is assigned a sequence type (ST). Relationships are compared using the allelic profile of each isolate: closely related isolates have identical STs or STs that differ minimally, and unrelated isolates have largely distinct STs. It is important to keep in mind that bacteria with same the ST or bacteria that belong to the same clonal complex are not necessarily identical but are genetically related (Urwin and Maiden, 2003).

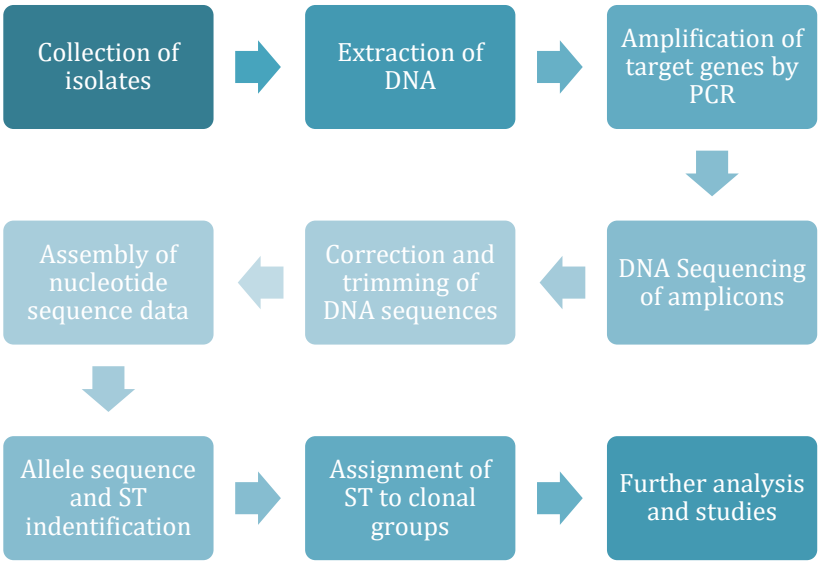

Figure 5. A schematic and simplified illustration of the general workflow of MLST.

The great advantage of MLST is that the allelic profiles of each isolate can be compared to those in a large database (pubMLST) in contrast to most typing procedures which involve comparing DNA fragment sizes on gels. In addition, materials needed for MLST are portable and can be easily exchanged and the technique itself is highly reproducible. MLST provides a powerful discriminatory power to differentiate between isolates. The method itself can be applied for detecting transmission routes, outbreaks and spread of disease, emergence of antibiotic resistance within a species and the relationship between bacteria (Urwin and Maiden, 2003).

MLST schemes for *Acinetobacter*

For *Acinetobacter* species there are two schemes used to study their epidemiology, the Pasteur scheme, and the Oxford scheme. Both schemes use seven genes to characterize different isolates, and the schemes have three genes in common: *cpn60*, *gltA* and *recA*. However, the existence and usage of two schemes has somewhat reduced the advantage of the MLST nomenclature, especially for *A. baumannii* (Gaiarsa *et al.*, 2019). One common scheme is probably more suitable for comparison and does not complicate the communication on genotypes.

There are different advantages and disadvantages associated with each scheme. The Pasteur scheme seems to be less discriminant for closely related strains but is less affected by recombination and more precise for assigning strains to different clonal complexes (CC)

(Gaiarsa *et al.*, 2019). On the other hand, the Oxford scheme possess a higher discriminator power for closely related strains but seem to be affected by recombination and have issues with artificial STs. Despite this, both schemes seem to be in agreement in their classification. A recent study by Gaiarsa *et al.*, (2019) recommended the usage of the Pasteur scheme for *Acinetobacter* species. They concluded that this scheme should be used because it is not affected by recombination or artificial STs. Furthermore, the scheme is better at assigning strains to clonal complexes.

MLST-based global phylogeny of *A. baumannii*

A. baumannii has an extraordinary capability to cause outbreaks in hospitals and the occurrence of *A. baumannii* outbreaks have been reported worldwide (Dijkshoorn, Nemec and Seifert, 2007; Peleg, Seifert and Paterson, 2008). Comparative MLST typing of different *A. baumannii* strains scattered all over the world, has demonstrated the occurrence of several successful clones of *A. baumannii* called international clones (IC) 1, 2, 3, 4, 5, 6, 7 and 8 (Higgins *et al.*, 2009, 2017; Diancourt *et al.*, 2010; Schleicher *et al.*, 2013). All the clonal lineages have been associated with multidrug resistance (Higgins *et al.*, 2009; Diancourt *et al.*, 2010; Giannouli *et al.*, 2010; Da Silva *et al.*, 2018; Abhari *et al.*, 2019; Cerezales *et al.*, 2019). However, IC2 seem to be the most widespread clonal lineage, and is frequently associated with carbapenem resistance (Higgins *et al.*, 2009; Schleicher *et al.*, 2013).

1.4.3 Mechanisms of drug resistance in *A. baumannii*

Owing to the ability to acquire resistance determinants through horizontal gene transfer (HGT), *A. baumannii* has the possibility to assemble a whole arsenal of resistance mechanisms by which it can protect itself against antimicrobials, some of which are described below (Doi, Murray and Peleg, 2015; Lee *et al.*, 2017).

β-lactams. There are four main mechanisms underlying resistance to β-lactams in *A. baumannii*: (i) hydrolysis of β-lactams, (ii) changes in penicillin-binding proteins (PBPs), (iii) alterations in the structure and number of porins and (iv) efflux pumps (Perez *et al.*, 2007). The most common mechanism in *A. baumannii* is enzymatic degradation by β-lactamase enzymes (Peleg, Seifert and Paterson, 2008).

Class A narrow- and extended-spectrum β-lactamases have been found in *A. baumannii*. Narrow-spectrum β-lactamases are enzymes that hydrolyze narrow-spectrum penicillins. Extended-spectrum β-lactamases (ESBLs) confer resistance to penicillins and expanded-spectrum cephalosporins. The genes encoding these enzymes are acquired and are not intrinsic to *A. baumannii* (Perez *et al.*, 2007; Bonnin, Nordmann and Poirel, 2013; Lee *et al.*, 2017). Narrow-spectrum β-lactamases such as TEM-1, TEM-2, carbenicillinase-4 (CARB-4), SHV-1 have been reported, which are inhibited by the β-lactamase inhibitor clavulanic acid (Bonnin, Nordmann and Poirel, 2013; Lee *et al.*, 2017). Narrow-spectrum β-lactamases resistant to clavulanic acid such as oxacillinase-21 (OXA-21) and OXA-37 have also been found (Bonnin, Nordmann and Poirel, 2013). ESBLs that have been identified in *A. baumannii* are variants of PER-1, VEB-1, CTX-M enzymes, TEM-92, SHV-12 and more (Perez *et al.*, 2007; Bonnin, Nordmann and Poirel, 2013; Lee *et al.*, 2017).

Class B β-lactamases also known as metallo-β-lactamases (MBLs) are enzymes with a broad spectrum of substrates. Unlike class A, C and D which are serine dependent, MBLs have a zinc or another metal ion in their active site which is responsible for the catalysis. Furthermore, MBLs are capable of not only hydrolyzing carbapenems, but also every other β-lactam antibiotic except for aztreonam (Lee *et al.*, 2017). MBLs do not constitute the major family of carbapenemases in *A. baumannii* but have been frequently reported(Perez *et al.*, 2007; Bonnin, Nordmann and Poirel, 2013; Lee *et al.*, 2017).

Intrinsic to all *A. baumannii* is the AmpC β-lactamase also called *Acinetobacter*-derived cephalosporinase (ADC) (Bonnin, Nordmann and Poirel, 2013). This is the only class C β-lactamase found in *A. baumannii* (Lee *et al.*, 2017). This enzyme is usually expressed at low levels, however the presence of an insertion sequence (IS), such as ISAba1 upstream of AmpC, causes overexpression of the gene and results in resistance to expanded-spectrum cephalosporins (Bonnin, Nordmann and Poirel, 2013; Doi, Murray and Peleg, 2015). Oxacillinases (OXA), which represent class D β-lactamases, are enzymes that hydrolyze carbapenems at low levels (Bonnin, Nordmann and Poirel, 2013; Lee *et al.*, 2017). These enzymes are the major contributors of carbapenem resistance in *A. baumannii* (Doi, Murray and Peleg, 2015; Lee *et al.*, 2017). In fact, the OXA-51 like β-lactamases occurs naturally and universally in *A. baumannii* (Doi, Murray and Peleg, 2015). Only the $bla_{\text{OXA-51-like}}$ genes are found ubiquitously in *A. baumannii*, while the other bla_{OXA} genes are usually found on mobile elements such as transposons or plasmids (Perez *et al.*, 2007; Bonnin, Nordmann and

Poirel, 2013; Lee *et al.*, 2017). If the *bla*$_{OXA}$ genes are coupled with more efficient promotors upstream, such as ISAba1 mentioned above, the susceptibility to carbapenems may be lowered dramatically (Doi, Murray and Peleg, 2015).

As mentioned earlier, resistance to β-lactams can also be conferred by nonenzymatic mechanisms. Reduced expression of PBP-2 has been described as a source of resistance to carbapenems (Perez *et al.*, 2007). However, not many studies have been performed regarding resistance by modifications of PBPs in *A. baumannii*, so how PBPs may potentially play a role in resistance is not fully known. Reduced expression or loss of some porins including CarO and various outer membrane proteins is also associated with resistance to carbapenems (Perez *et al.*, 2007; Lee *et al.*, 2017). The chromosomally encoded resistance-nodulation-division (RND) efflux pump AdeABC is as well shown to play a role in resistance to β-lactams, including carbapenems (Gootz and Marra, 2008; Bonnin, Nordmann and Poirel, 2013).

Aminoglycosides. The AdeABC pump mentioned above do not only pump β-lactams, but also aminoglycosides, tetracyclines, fluoroquinolones, and chloramphenicol and others (Gootz and Marra, 2008; Peleg, Seifert and Paterson, 2008; Xu, Bilya and Xu, 2019). This constitutes the intrinsic resistance mechanism towards aminoglycosides found in *A. baumannii* (Peleg, Seifert and Paterson, 2008; Lee *et al.*, 2017). However, resistance is mainly due to aminoglycoside-modifying enzymes (AMEs), that inactivate aminoglycosides by addition of specific substrates (Bonnin, Nordmann and Poirel, 2013; Lee *et al.*, 2017). The acquisition of several AMEs can lead to resistance against all aminoglycosides (Bonnin, Nordmann and Poirel, 2013). Another mechanism of resistance that is emerging is a 16S rRNA methyltransferase called ArmA (Bonnin, Nordmann and Poirel, 2013; Doi, Murray and Peleg, 2015). This enzyme methylates the binding site of aminoglycosides in the A-site of the ribosome, preventing the aminoglycosides to bind and exert its effect on the ribosome (Bonnin, Nordmann and Poirel, 2013.

Fluoroquinolones. Fluoroquinolones inhibit bacterial replication by binding to DNA gyrase (encoded by *gyrA* and *gyrB*) and DNA topoisomerase IV (encoded by *parA* and *parC*). The most common mechanism of resistance against fluoroquinolones is target modification by amino acid substitutions, which is caused by mutations in the genes encoding these enzymes (Peleg, Seifert and Paterson, 2008; Bonnin, Nordmann and Poirel, 2013). Intrinsic resistance

caused by the efflux pumps AdeABC, AdeIJK, AdeM and AdeFHG contribute to resistance against ciprofloxacin (Bonnin, Nordmann and Poirel, 2013). Plasmid-mediated resistance to fluoroquinolones has so far not been identified in *A. baumannii* (Peleg, Seifert and Paterson, 2008; Bonnin, Nordmann and Poirel, 2013).

Tetracyclines and glycylcyclines. Resistance to tetracyclines and their derivates in *A. baumannii* is mainly caused by efflux or ribosomal protection (Bonnin, Nordmann and Poirel, 2013; Doi, Murray and Peleg, 2015). Efflux is mediated by Tet proteins such as TetA and TetB, found in transposons, or the intrinsic Ade-type pumps. Protection of the ribosome is mediated by the TetM determinant. Neither Tet efflux proteins nor TetM seem to hinder the action of tigecycline (Bonnin, Nordmann and Poirel, 2013). However, resistance can be developed by the overexpression of the Ade-type pumps (Bonnin, Nordmann and Poirel, 2013; Doi, Murray and Peleg, 2015).

Colistin. Colistin (polymyxin E) is a polycationic peptide belonging to the group of polymyxins that binds to lipid A (Doi, Murray and Peleg, 2015; Lee *et al.*, 2017). By binding to lipid A and phospholipids in the inner membrane, colistin disrupts and permeabilizes the membranes of gram-negative bacteria (Bonnin, Nordmann and Poirel, 2013). Unfortunately, the number of colistin-resistant *A. baumannii* strains has increased worldwide, which is quite serious because colistin serves as the last line of defense against extremely drug-resistant bacteria (Lee *et al.*, 2017). Resistance mechanisms to colistin include loss of LPS and addition of phosphoethanolamine to lipid A (Moffatt *et al.*, 2010; Lee *et al.*, 2017). However, the most important mechanism seems to be addition of phosphoethanolamine to lipid A as loss of LPS is not that beneficial or common in clinical isolates (Moffatt *et al.*, 2010; Doi, Murray and Peleg, 2015).

1.4.4 *A. baumannii* in Norway

The true prevalence of *A. baumannii* infections in Norway is to the best of my knowledge not known. No full record exists, and only carbapenemase-producing *Acinetobacter* spp. are registered in the Norwegian Surveillance System for Communicable Diseases (MSIS), which is a unit of the Norwegian Institute of Public Health. In Norway, only two minor outbreaks of *A. baumannii* have been reported, the first one reported in 1998, whereby a Norwegian patient was transferred from Spain to a Norwegian hospital in Bergen carrying a multidrug-

resistant *A. baumannii*. The strain was resistant towards several β-lactam antibiotics, meropenem, imipenem, ciprofloxacin, netilmicin and Trimethoprim/sulfamethoxazole (Onarheim *et al.*, 2000). The second outbreak occurred in 2016 in the same hospital, and the strain was also reported to be multi-drug resistant (Helse-Bergen, 2016).

In a study by Karah, Haldorsen, Hegstad, *et al.*, (2011) only 10 out of the 113 (8.8 %) *Acinetobacter* spp. blood culture isolates from 2005-2007 contained *A. baumannii*, indicating that only a few people are infected by *A. baumannii* in Norway. According to a report from NORM (2019), the number of carbapenemase-producing *Enterobacterales* (CPE), *Pseudomonas aeruginosa* and *Acinetobacter* spp. have increased slowly from the year 2007. However, clinical isolates in Norway carrying carbapenem resistance, including *A. baumannii*, are mostly associated with import of strains (Karah, Haldorsen, Hermansen, *et al.*, 2011; NORM, 2019). A total of 21 carbapenemase-producing *Acinetobacter* spp. isolates were detected in 2018 - 19 isolates were found in patients, compared to eight in 2017. Twelve of the cases were linked to an infection, and 13 of the isolates were carbapenemase-producing *A. baumannii*, of which 11 harbored the $bla_{\text{OXA-23}}$ gene. All isolates were associated with import except for one isolate. One isolate of *A. baumannii* contained the $bla_{\text{OXA-72}}$ gene and another isolate contained $bla_{\text{OXA-58}}$ plus NDM. The isolate harboring $bla_{\text{OXA-72}}$ was associated with import. Additionally, eight NDM positive isolates of *Acinetobacter* spp. were detected in seven patients (NORM, 2019).

1.5 Phase variation

Traditionally the expression of most genes in bacteria is believed to be controlled at the level of transcription or indirectly with translation. However, bacteria have a method to deal with stressful and varying environments, without transcription or by acquiring mutations. One such mechanism is called phase variation and involves the differential expression of a gene or genes in a reversible or irreversible ON-OFF fashion (Henderson, Owen and Nataro, 1999).

To exemplify how phase variation may work, the phase variation system in *Salmonella enterica* serovar Typhimurium are shown in Figure 6. In the case of *S. Typhimurium* this type of system is used to evade the host immune system. Two types of flagellar proteins called H1 and H2, can be expressed. These proteins are encoded by the *fljB* gene (H2) and the *fliC* gene (H1). When *S. Typhimurium* transcribes the *fljB* gene and the *fljA* gene, repressor of H1, only

the H2 flagellin of is produced, since the H1 repressor represses transcription of *fliC*. However, if the DNA segment containing the promoter (flanked by two hix sites) is inverted by site-specific recombination, the repressor of H1 is no longer transcribed, and the H1 flagellin can be expressed by the cell. By alternating the expression of the two different flagellar antigens, a subset of the bacteria may escape or go undetected by the immune system. This system can be described as going from an ON_{H2}/OFF_{H1} state to an ON_{H1}/OFF_{H2} state (Henderson, Owen and Nataro, 1999; Wisniewski-Dyé and Vial, 2008).

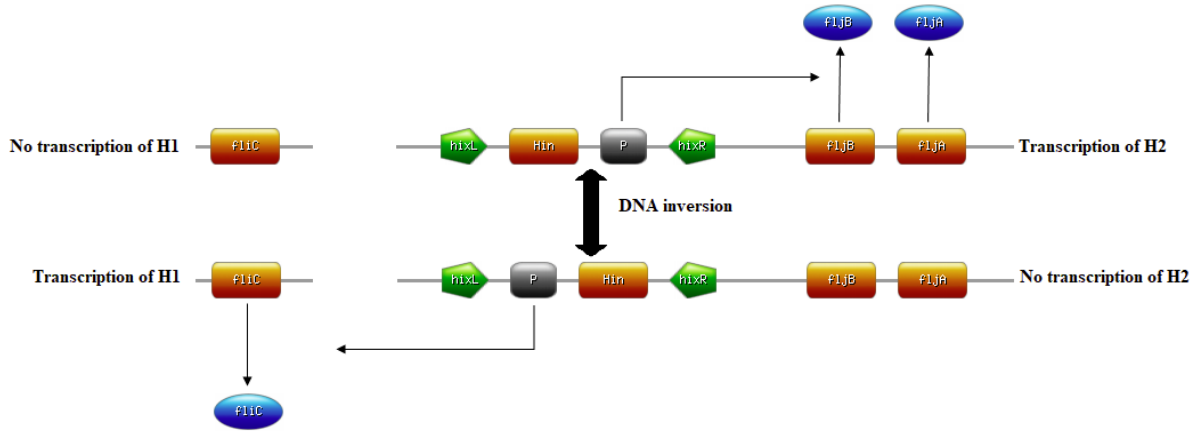

Figure 6. Phase variation – site specific inversion in *S. Typhimurium*. Inversion of the promoter causes either transcription of *fljA* (repressor of H1) and *fljB* (H2) or *fliC* (H1). The orange squares represent the genes, the blue circles proteins, the grey squares the promoter and the green pentagons the hix sites.

1.5.1 Phase variation in *A. baumannii*

In 2015 Tipton and co-workers described a phase-variable mechanism in *A. baumannii* for the first time (Tipton, Dimitrova and Rather, 2015). By using a stereo microscope under oblique light, the authors were able to identify a in the colony types based on their opacity. According to their opacity they named the two distinct colony types opaque and translucent (see Figure 7). The frequency of phase variation in *A. baumannii* within colonies and in liquid medium have been shown to increase in a cell density-dependent manner. Evidence also indicates that there is an extracellular signal involved in the colony switching (Tipton, Dimitrova and Rather, 2015).

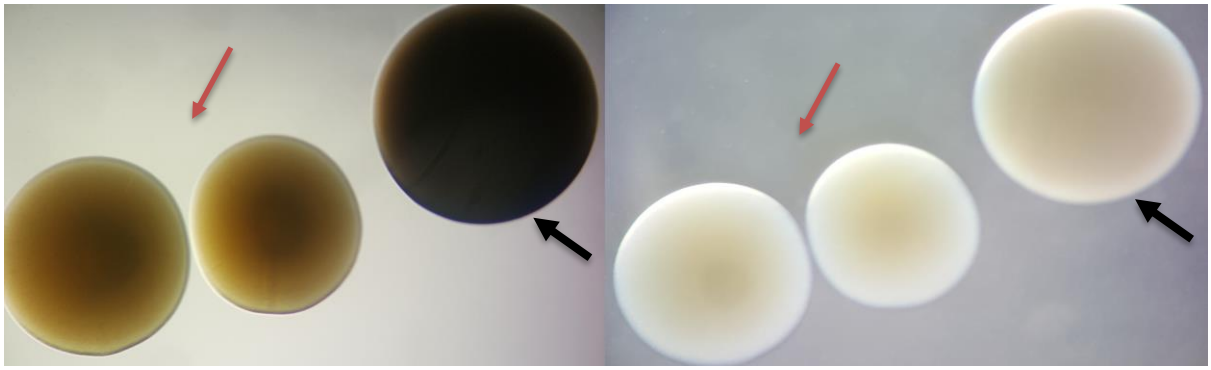

Figure 7. Opaque and translucent colony variants of *A. baumannii* chicken farm isolate A31. To the left, the colonies are viewed under oblique lightning. To the right, the colonies are viewed under oblique lightning but with less light. The black arrow shows the opaque colony, while the red arrows shows the translucent colonies.

There are also certain phenotypic differences between the two colony types: (i) **Cell shape**. When the two different types are grown to stationary phase, the opaque variant has a coccobacilli morphology while the translucent variant has a more elongated shape. (ii) **Motility.** The opaque variant seems to be more motile than the translucent variant. (iii) **Biofilm formation.** The translucent cells are better suited to form biofilm than their opaque counterpart. (iv) **Pathogenicity.** The opaque variant is more virulent than the translucent variant. The opaque cells are better equipped to infect and cause death in waxworm and mice models. (v) **Resistance.** The opaque variant seems to be more resistant than the translucent variant against several different molecules including aminoglycosides, lysozyme, hydrogen peroxide and disinfectants. They are also more resistant towards desiccation (Tipton, Dimitrova and Rather, 2015; Chin *et al.*, 2018).

How exactly phase variation is regulated in *A. baumannii* is yet to be elucidated. However, a predicted TetR-type of transcriptional regulator, ABUW_1645, seems to be involved. It has been shown that overexpression of ABUW_1645 in opaque cells leads the cells into a translucent state. When both opaque and translucent cells overexpressed the predicted TetR-regulator, they both got locked in the translucent state without the ability to switch to the opaque state. Additionally, overexpression of ABUW_1645 in the opaque variant completely reversed the resistance against antimicrobials, disinfectants, and desiccation. When mice were infected with the opaque cells overexpressing this gene, only the translucent cells were recovered from the mice. These results highly suggest that the predicted regulator has a role in phase variation (Chin *et al.*, 2018).

Whether the mechanism is known or not, the few studies that have been conducted on phase variation has provided interesting insight into how *A. baumannii* deals with different environments. The opaque variant seems to be selected to cause disease in humans and to persist in the hospital environment. The translucent variant on the other hand may be more suitable to accommodate the natural environment of *A. baumannii* (Chin *et al.*, 2018). It seems like *A. baumannii* has found several ways to persist and survive in a whole set of different environments. However, since few studies have investigated phase variation and its role in *A. baumannii*, more studies are needed to fully understand this mechanism in this species.

1.6 Aims of the project

Knowledge about the natural reservoirs and the epidemiology of *A. baumannii* is limited and is needed obtain a more complete understanding of the bacterium. The lack of knowledge is due to the fact that most studies on *A. baumannii* have focused on clinical isolates. Therefore, my work has focused on studying non-clinical isolates of *A. baumannii*, in order to provide new insights about the natural reservoirs and the epidemiology of the pathogen outside of hospitals. The first goal of this project was to map the relatedness between a set of *A. baumannii* isolates from Norwegian chicken farms, and to investigate a possible role of chicken farms in the epidemiology of the pathogen. The second aim of the project was to determine whether Norwegian chicken farms could represent a possible reservoir of carbapenem resistance. Furthermore, this work aims to get a better understanding of how whether resistant *A. baumannii* isolates may circulate in chicken farms in Norway and potentially establish a possible link to human carriage and the establishment as a nosocomial pathogen. In light of the recent discovery that phase variation is present in clinical isolates of *A. baumannii*, the third aim of the project was to determine if the non-clinical chicken farm isolates of *A. baumannii* can switch from the opaque to translucent colony type and to determine with what frequency this switch occurs. This in return, might give an indication whether phase variation is present in environmental isolates and further provide insight into the importance of this mechanism outside the hospital setting and whether this is an inherent mechanism of the species.

2 Materials and Methods

2.1 Isolation and species identification of *A. baumannii*

Isolation and identification of *A. baumannii* isolates was done by the Norwegian Veterinary Institute. Samples were collected from 2213 flocks of chickens from Norwegian chicken farms between May and October 2016. The bacteria were collected by sock sampling, whereby veterinarians go into the chicken farms and sample the chicken farm environment by using boot swabs. This sampling method targets the litter of the chicken. Since these isolates are samples from the environment of the chicken farms, they will be classified as environmental samples (see discussion). However, for simplicity, the isolates will be referred to as chicken farm isolates. A total of 783 isolates were identified as *A. baumannii* from the chicken flocks. The isolates were grown on McConkey agar, containing either 0.06 mg/L ciprofloxacin, 1 mg/L cefotaxime or 2 mg/L ceftazidime, and identified using the Bruker Biotyper MALDI-TOF MS system (Bruker Daltonics) under the control of the FlexControl 3.4.119 software. The MASS spectra were processed using the Bruker database version 6.0. A subselection of 200 of these isolates were given to the host laboratory of Professor Ole Andreas Løchen Økstad. These isolates were randomly selected but are representative of the geographical spread of the sampled farms.

2.2 DNA preparation of isolates of *A. baumannii* from chicken farms

DNA used for screening the $bla_{\text{OXA-51}}$ gene and MLST, was extracted from liquid cultures of different isolates of *A. baumannii*. A loop containing a colony from a 24 hours plate culture of the bacteria was resuspended in 200 µL of DEPC-treated water and incubated at 96 °C for 10 minutes. Afterwards the solution was centrifuged for 5 minutes at 13000 rpm. The supernatant was transferred into a 1.5 mL Eppendorf tube. Altogether 200 DNA preps were made. The DNA extraction was performed by guest researcher Varsha Naidu (Macquarie University), who contributed to establishing the MLST system for *A. baumannii* in the host laboratory of Professor Ole Andreas Løchen Økstad.

2.3 Screening for the *bla*$_{\text{OXA-51}}$ gene

Since the species in the Acb complex can be difficult to differentiate by MALDI-TOF alone (Šedo *et al.*, 2013), an additional screening of the *bla*$_{\text{OXA-51}}$ gene was performed by PCR to confirm if all the given isolates were in fact *A. baumannii*. Only the strains of *A. baumannii* contain the *bla*$_{\text{OXA-51}}$ gene, and this gene is intrinsic to this species (Turton *et al.*, 2006). The screening for the *bla*$_{\text{OXA-51}}$ gene was done by PCR and agarose gel electrophoresis and was performed by PhD candidate Claus Michael Goul Larsen.

2.4 MLST

MLST is method that uses a combination of PCR amplification of housekeeping genes and DNA sequencing to represent a description of the phylogenetic position of an isolate. The general outline and workflow of MLST is depicted in Figure 5. The Pasteur MLST scheme was used (https://pubmlst.org/bigsdb?db=pubmlst_abaumannii_pasteur_seqdef&page=schemeInfo&scheme_id=2) .

2.4.1 Polymerase chain reaction (PCR)

PCR is a technique used to amplify nucleotide sequences. This technique relies on thermal cycling, whereby the reagents are exposed to repeated cycles of heating and cooling. A cycle usually consists of three steps. The first step is denaturation, in which the double stranded DNA is separated into two single stranded DNA molecules by heat. In the second step called annealing oligonucleotide primers anneal to the single stranded DNA by lowering the temperature of the reaction. The third and final step is the elongation step whereby the single stranded DNA is copied and amplified by a heat-stable DNA polymerase, which generates a new double stranded DNA molecule. By repeating such a cycle 25-40 times the DNA of interest can be amplified more than a trillion times, providing high amounts of the target DNA. In MLST, PCR is used to amplify selected housekeeping genes followed by DNA sequencing as described in the introduction under MLST.

Protocol - PCR

PCR reactions were performed according to the manufacturer's protocols (Thermo Fisher Scientific). A 50 µL reaction mix was made of 41.3 µL DEPC-treated water, 5.0 µL 10x

DreamTaq buffer, 1.0 µL of 10 µM forward and reverse primers (Appendix 2), 0.5 µL 100 mM dNTP solution, 0.2 µL DreamTaq polymerase and 2.0 µL of the DNA preps from section 2.2. All reagents and their respective suppliers used for the PCR reactions, are listed in Table 1. More information about the contents of buffers and solutions and the primer sequences used, can be found in Appendix 1 and 2. Details regarding the PCR program is found below.

Table 1. Overview of the reagents used for PCR and their respective concentration and supplier.

Reagent	Concentration	Supplier
DreamTaq DNA Polymerase	5 U/µL	Thermo Fisher Scientific
DreamTaq Buffer (contains KCl, $(NH_4)_2SO_4$ and $MgCl_2$)	10X	Thermo Fisher Scientific
DEPC-treated water	-	Thermo Fisher Scientific
Oligonucleotide primers	100 µM	Thermo Fisher Scientific
dNTP	100 mM	Thermo Fisher Scientific
DNA samples (DNA from chicken farm isolates)	-	Norwegian Veterinary Institute

PCR program

1 cycle:

Initial denaturation: 94 °C 2 minutes

↓

35 cycles

Denaturation: 94 °C 30 seconds

Primer annealing: 52 °C 30 seconds

Elongation: 72 °C 30 seconds

↓

1 cycle

Final elongation: 72 °C 5 minutes

↓

Hold at 4 °C ∞

2.4.2 Agarose Gel Electrophoresis

Gel electrophoresis is a technique used to separate DNA molecules based on their negative charge. DNA molecules can be separated according to their size and conformation when exposed to an electric field through a porous material such as agarose, which forms the gel matrix (Watson *et al.*, 2013, p. 148). The negatively charged DNA will migrate through the gel when exposed to an electrical field and move towards the anode. Since agarose produces pores in the gel, smaller DNA molecules migrate further than larger DNA molecules after a given amount of time as larger molecules have more difficulty passing through the pores compared to smaller DNA molecules, resulting in larger DNA molecules migrating more slowly through the gel.

For MLST DNA sequencing, it is important to have pure sample of DNA without any side products. To confirm that only one specific product of the expected size had been amplified in the PCR reactions, a small sample of the DNA amplified from a selected set of the isolates was run on an agarose gel. A 1 % agarose gel was made from agarose powder dissolved in 1x TAE buffer. The agarose powder was dissolved in the buffer by the aid of a microwave oven. Then 1 µL of GelRed™ or Ethidium bromide was added and gently mixed for every 10 mL of agarose solution made (1:10000 dilution), and the solution was poured into a gel caster. A comb was placed in the caster to create the wells which samples are loaded into. The agarose solution was left to solidify for 20-30 minutes, before being transferred into an electrophoresis chamber containing 1x TAE buffer. DNA samples (4 µL) were mixed with 3 µL of orange mix and 3 µL of DEPC-treated water. The samples were loaded directly into the wells and 5 µl of Generuler™ 1 kb DNA ladder (Thermo Fisher Scientific) was used as a marker. The gel was run for 45-60 minutes depending on the electrophoresis chamber and voltage used. When finished, the gel was transferred to a chamber with a UV transilluminator, and a picture was taken with the aid of a computer. All reagents and their respective suppliers used for making the agarose gel, are listed in Table 2. All buffer and solution recipes can be found in Appendix 1.

Table 2. Overview of the reagents used for gel electrophoresis and their respective concentration and supplier.

Reagent	Concentration (stock solution)	Supplier
UltraPure™ Agarose	-	Life Technologies (Thermo Fisher Scientific)
SeaKem™ LE Agarose	-	FMC bioproducts
Trizma™ base (Tris base)	-	Sigma-Aldrich (Merck)
Acetic Acid	-	VWR
EDTA (Ethylenediaminetetraacetic acid)	-	-
Ficoll 400	-	Sigma-Aldrich (Merck)
Orange G	-	Sigma-Aldrich (Merck)
GelRed™	10000X in water	Biotium
Ethidium bromide	5 mg/mL	Sigma-Aldrich (Merck)
DEPC-treated water	-	Thermo Fisher Scientific
Generuler™ 1 kb DNA ladder, ready to use	0.1 µg/µL	Thermo Fisher Scientific

2.4.3 DNA sequencing of genes

Sequencing and purification of the PCR products was performed by Eurofins, using the forward (F) primer for each gene. PCR products for each of the seven genes amplified from each chicken farm isolate were added to a 96-well plate and then dispatched to Eurofins by mail. Each PCR product (15 µL) was transferred by a multichannel pipette to a standard 96-well microtiter plate (Figure 8), and wells were closed and sealed with PCR lids/caps before shipment. Each F primer (15 µL, 10 pmol/µL) was supplied in a separate Eppendorf tube.

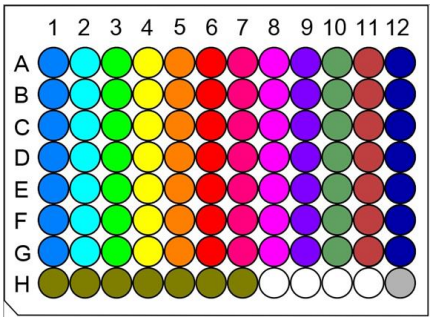

Figure 8. An overview of the 96-well microtiter plate showing where samples were added. Each color represents an isolate except for wells H8-H12. A-F represents the different genes e.g. row A is cpn60 from each isolate. In the bottom row, H1-H7 is also an isolate with its genes, while wells H8-H12 contains quality controls.

2.4.4 Analysis and correction of sequences

Using Jalview (Waterhouse *et al.*, 2009), a multiple sequence alignment (MSA) was made using the Clustal logarithm for comparison of the different genes from the isolates to the template sequences. The template sequences, which can be found in Appendix 3, are sequences used to recognize the corresponding sequences found in the same genes for different strains of *A. baumannii*. The template sequences were retrieved from the pubMLST database. The sequences of the PCR products were only accepted if the phred quality score was 20 or above, corresponding to a base call accuracy of at least 99 %. Not all the sequences were of good enough quality to satisfy this criterion, however these sequences were then submitted for resequencing. The sequences for the template DNA and the sequences for the isolates, retrieved from Eurofins, were copied into Jalview. An MSA was made using the Clustal logarithm with default settings (Web Service →Alignment →Clustal→With defaults). The sequences were colored after % identity (Color→ % Identity). By comparing the sequence template to the sequences from the chicken farm isolates, sequences were trimmed with the aid of chromatograms specific for each isolate and their corresponding genes. Due to the generally low quality of the *recA* sequences near one end of the PCR product, both the forward and the reverse strand of *recA* was sequenced. Consequently, the forward and the reverse strands were aligned with each other to create the full-length sequence of the *recA* gene. By doing this, complete *recA* sequences with good quality were assembled. This was done as follows: the forward and the reverse strands of *recA* were trimmed as described above, and the sequences of *recA* reverse strand were reverse complemented using the following website: http://reverse-complement.com/. The template DNA sequence for *recA* forward was then copied into Jalview. For each isolate the *recA* forward sequence and the reverse complemented *recA* reverse sequence, were aligned. The first part of the sequence from *recA* reverse was then manually added to the *recA* forward sequence to create the full-length sequence. This was performed for all isolates.

Resequencing of genes

Due to the poor quality and uncertainty of some base calls in some of the sequences retrieved from Eurofins, some genes were submitted for a second round of sequencing. This time, GATC was used instead of Eurofins, employing their LightRun™ sequencing service. With this service, purification of the PCR reactions was required before sending in the samples to GATC.

Purification of the PCR reactions were done using the E.Z.N.A.® Gel Extraction Kit from Omega Bio-Tek, in accordance with the protocol from the manufacturer supplied with the kit. Briefly, a 1:1 volume of XP2 Binding Buffer was added (15 µL:15 µL) to completed PCR mixture and mixed by vortexing. The solution was added to the HiBind® DNA Mini Column and centrifuged at 10,000 RCF (x g) for one minute. The flow-through was discarded and the column was placed back into the collection tube. SPW buffer (700 µL) was added to the column and the solution was centrifuged for one minute at 13,000 RCF (g) for one minute. The flow-through was discarded and the column was placed back into the collection tube. 700 µL of SPW buffer was added to the column a second time and the solution was centrifuged for at 13,000 RCF (g) for one minute. The flow-through was discarded and the column was placed back into the collection tube. The empty HiBind® DNA Mini Column was centrifuged for an additional two minutes for complete removal of any residual ethanol from the wash buffer. The HiBind® DNA Mini Column was transferred to an Eppendorf tube and 30-50 µL of elution buffer was added directly to the column. The column was left on the bench for two minutes, and then centrifuged at 13,000 RCF (g) for one minute to elute DNA from the column.

Submission of the DNA samples to GATC for sequencing was done by first adding 5 µl of the PCR product (10-80 ng/µl) and 5 µl of the forward primer (5 µM) into a 1.5 mL Eppendorf tube. A barcode sticker was affixed horizontally to each tube. The samples were deposited at the nearest GATC pick-up point. Out of the 47 of the *rpoB* sequences that were sent in for resequencing, 10 were purified and submitted personally, while the remaining 37 *rpoB* PCR products were purified and submitted by PhD candidate Claus Michael Goul Larsen.

2.4.5 Registration of the MLST data to the pubMLST database

Registration of new STs and isolate data to the pubMLST database for *A. baumannii* (https://pubmlst.org/bigsdb?db=pubmlst_abaumannii_pasteur_seqdef) was done by PhD candidate Claus Michael Goul Larsen.

2.4.6 Construction of phylogenetic trees

The trees were created with PHYLOViZ version 2.0 based on the STs from the MLST data. All MLST data was extracted from the pubMLST database for *A. baumannii* (https://pubmlst.org/bigsdb?db=pubmlst_abaumannii_pasteur_seqdef). A clonal complex was defined as sharing six of the seven alleles in the Pasteur scheme (Feil *et al.*, 2004).

Construction of the minimum spanning tree

A minimum spanning tree (MST) was created using the global optimal eBURST (goeBURST) algorithm (Francisco *et al.*, 2009). First, the typing data was loaded into the program by using a tab separated file containing the STs and the allelic profile of each isolate included in the analysis (Files →Load dataset). Under dataset type, MLST was chosen. After the data was loaded into the program, the MST was created by right clicking the 'MLST data' under 'dataset' and clicking on 'compute' and then 'goeBURST full MST'. Clonal complexes were identified using the goeBURST algorithm with the criterion of one allelic mismatch.

UPGMA dendrograms

Unweighted Pair Group Method Using Arithmetic Average or simply UPGMA, is a ultrameric method (assumes that the sequences evolve at a constant rate) which builds a tree by arranging clusters in a hierarchy (Xiong, 2006, p. 143). Given that a distance matrix is used, the method starts by initially grouping the two taxa with the shortest pairwise distance to each other. A node is then placed in the midpoint between the two taxa so that they become joined. The matrix then becomes reduced because the new cluster is now considered a group. The distance between the new group and the remaining sequences, is now the average distance between the sequences and the original distance to the two taxa from the original matrix. For example, two isolates (a and b) are grouped, then the average of the distance between a to c (a third isolate) and b to c is taken as the distance between a-b and c. The distances between this joined group and the remaining taxa are then calculated such that a reduced matrix is made. The same process is repeated for other groups and new reduced matrixes are created. This process continues until all the taxa are placed on the tree (Xiong, 2006, p. 143).

After loading the STs and the allelic profiles of each isolate, as described above, the UPGMA dendrograms were created by right clicking the 'MLST data' button under 'dataset' and clicking on 'compute' and then 'hierarchical clustering'. For distance measurement the hamming distance was chosen, and under 'method', 'UPGMA' was chosen.

2.5 Antibiotic susceptibility testing

2.5.1 Disc diffusion

Antimicrobial susceptibility testing of the *A. baumannii* chicken farm isolates was done using the disc diffusion method. Commonly a petri dish containing a specific agar medium is inoculated by an evenly spread suspension of a liquid culture containing the bacteria of interest. Subsequently, paper discs containing known amounts of one or a combination of antimicrobial agents, are placed aseptically on the agar. During the incubation period, the antimicrobial agents diffuses from the discs into the agar, establishing a gradient. The concentration of a given agent is high near the disc and lower as it diffuses farther into the agar. At some given distance, the minimum inhibitory concentration (MIC) is reached, the smallest amount of antimicrobial agent needed to inhibit the organism tested. A zone of inhibition can be seen where the bacteria do not grow, and the diameter of the zone can be measured. The diameter of the zone is proportional to the effectiveness of the agent and tells us how effective a certain drug is against an isolate of a bacterium. The MIC will differ for each test organism and the MIC can tell us if the organism is susceptible or resistant against a certain antibiotic.

Protocol - Disc-diffusion

The following protocol was performed according to the procedure described by the European Committee on Antimicrobial Susceptibility Testing (EUCAST)(Matuschek, Brown and Kahlmeter, 2014). All reagents and their respective suppliers used for disc diffusion, are found in Table 3. All solution recipes can be found in Appendix 1. Mueller-Hinton (MH) agar plates were made following the instructions of the manufacturer (Sigma-Aldrich/Merck), and stored in a cold room at 4 °C. The isolates were streaked out on LB agar plates and incubated overnight at 37 °C. The next day several colonies of *A. baumannii* were picked with a sterile inoculation loop and suspended in 3 mL of 0.85 % saline solution in a 15 mL falcon tube. The suspension was vortexed to an even turbidity. The turbidity was measured at

625 nm and adjusted, if needed, to an optical density (OD) of 0.08 to 0.13 (corresponding to 0.5 McFarland). The 0.85 % saline solution was used as blank. 2 mL of the saline solution containing bacteria was added to the MH agar plates. Excess fluid was removed, and the plates were left for 15 minutes to dry. A sterile tweezer was then used to place the different antimicrobial disc on the plates. The plates were incubated overnight at 35 °C ± 1 °C for 18 ± 2 hours. After incubation, the zone of inhibition was measured with a ruler.

Table 3. Overview of the reagents used for disc diffusion and their respective supplier.

Reagent	**Supplier**
Tryptone	Oxoid (Thermo Fisher Scientific)
Yeast extract	Oxoid (Thermo Fisher Scientific)
Agar	Oxoid (Thermo Fisher Scientific)
NaCl	VWR
Mueller-Hinton Agar 2	Sigma-Aldrich (Merck)
dH_2O	-
Ceftazidime discs (10 µg)	Oxoid (Thermo Fisher Scientific)
Ciprofloxacin discs (5 µg)	Oxoid (Thermo Fisher Scientific)
Gentamicin discs (10 µg)	Oxoid (Thermo Fisher Scientific)
Imipenem discs (10 µg)	Oxoid (Thermo Fisher Scientific)
Meropenem discs (10 µg)	Oxoid (Thermo Fisher Scientific)
Tobramycin discs (10 µg)	Oxoid (Thermo Fisher Scientific)

2.5.2 Broth microdilution

A. baumannii chicken farm isolates that were considered resistant by the disc diffusion method were tested again by the broth microdilution method. In this method, the MIC is measured in liquid cultures, and the antimicrobial agents are diluted by a 2-fold serial dilution series. To establish the MIC for a given agent, a series of wells, when using a microtiter plate, are inoculated with the same amount of the organism. Each well contains medium in addition to a given concentration of the antimicrobial agent tested for. After incubation, the plate is checked for growth and the MIC is determined.

Determination of correct inoculum size

According to EUCAST (EU) and the Clinical and Laboratory Standards Institute (CLSI, US), the correct inoculum size to use for broth microdilution is 2-8 x 10^5 CFU/mL. To ensure that the correct inoculum was used, a viable colony count was performed of all the isolates before being tested for their susceptibility using the broth microdilution method. The inoculum for

each isolate tested was prepared by picking several colonies of *A. baumannii* with a sterile loop and suspending the colony material in 3 mL of 0.85 % saline solution in a 15 mL falcon tube. The suspension was vortexed to an even turbidity. The density of the solution was adjusted equivalent to a 0.5 McFarland standard (corresponding roughly to $5 \times 10^7 - 1 \times 10^8$ CFU/ml of *A. baumannii*). The turbidity was measured at 625 nm and adjusted, if needed, to an optical density (OD) of 0.08 to 0.13 (corresponding to 0.5 McFarland). The 0.85 % saline solution was used as blank. 10 µL of the cell suspension was then transferred to a new 15 mL falcon tube and diluted with 1.0 mL of 0.85 % saline solution. Afterwards, 0.5 mL of this bacterial suspension was further diluted with 1.0 mL of 0.85 % saline solution in a new 15 mL falcon tube. 10 µL of the diluted suspension was then removed and again diluted with 10 mL of 0.85 % saline solution in a new 15 mL falcon tube (in total a dilution of 1:200.000). 100 µL of the final solution was mixed and spread onto LB agar plates. After 18-24 hours of incubation at 35 °C ± 1 °C, the number of colonies were counted. The number of colonies counted should be in the range of 20 – 80 colonies, corresponding to $2\text{-}8 \times 10^5$ CFU/mL

Protocol – Broth microdilution

The following protocol was performed according to the recommendations given by the EUCAST and according to the procedures described by CLSI. All reagents and their respective suppliers used for the broth microdilution method, are listed in Table 4. All buffer and solution recipes can be found in Appendix 1. Un-supplemented cation-adjusted Mueller-Hinton broth (MHB) was prepared following the instructions of the manufacturer and stored in a cold room at 4 °C before use. The isolates tested, were streaked out on LB agar plates, and incubated overnight at 37 °C. The next day, the antibiotic stock solution of tobramycin (10.88 mg/mL) and/or gentamicin (12.94 mg/mL) was diluted in 1 mL of MHB to a concentration of 256 µg/mL in Eppendorf tubes. 100 µL of MHB was transferred with a multichannel pipette to all the wells needed in a standard 96-well microtiter plate. 200 µL of MHB was transferred to the wells used as negative control. 100 µL of the diluted tobramycin and/or gentamicin solution was transferred to row A for the columns used. A two-fold dilution series of the given antibiotic solution was performed from row A to H (Table 5). The final volume in row H after the dilution series was 200 µL, and since only 100 µL was needed, 100 µL got removed and discarded.

The direct colony suspension method was used for inoculum preparation. The inoculum for each isolate tested was prepared by picking several colonies of *A. baumannii* with a sterile

loop and suspending the colony material in 3 mL of 0.85 % saline solution in a 15 mL falcon tube. The suspension was vortexed to an even turbidity. The turbidity was measured at 625 nm and adjusted, if needed, to an optical density (OD) of 0,08 to 0,13 (corresponding to 0.5 McFarland), preferably to an OD of 0.11-0.13 to ensure usage of correct amount of inoculum. 0.85 % saline solution was used as blank. Transferred 50 µL of the 0.5 McFarland suspension into a new 15 mL falcon tube and diluted the suspension with 5.0 mL of MHB. 100 µL of the prepared bacterial suspensions were added with a multichannel pipette to the wells in the designated column for each isolate in the microtiter plate. Another 100 µL of each isolate was also added to a separate column containing 100 µL of MHB, serving as a positive control. The inoculum for two of the isolates was checked, by removing 10 µL from the positive-control wells immediately after inoculation and diluted in 10 mL of 0.85 % saline solution in a 15 mL falcon tube. 100 µL of the bacterial suspension was spread onto LB agar plates. The microtiter plate was covered with a sealing film and incubated at 35 °C ± 1 °C for 18 ± 2 hours, and the results were analyzed by visual examination the next day.

Table 4. Overview of the reagents used for broth microdilution and their respective concentration and supplier.

Reagent	**Concentration**	**Supplier**
Tryptone	-	Oxoid (Thermo Fisher Scientific)
Yeast extract	-	Oxoid (Thermo Fisher Scientific)
Agar	-	Oxoid (Thermo Fisher Scientific)
NaCl	-	VWR
Mueller-Hinton broth	-	Sigma-Aldrich (Merck)
dH_2O	-	-
Tobramycin	10.88 mg/mL	Sigma-Aldrich (Merck)
Gentamicin	12.94 mg/mL	Sigma-Aldrich (Merck)

Table 5. Layout of the 96-well microtiter plate for the broth microdilution method when nine isolates were tested at the same time. The range of the concentrations (µg/mL) were the same for both tobramycin and gentamicin. The final volume of each well was 200 µL. POS = Positive, NEG = Negative and CTRL = Control.

	1	2	3	4	5	6	7	8	9	10	11	12
A	64	64	64	64	64	64	64	64	64	MH + BACTERIA POS CTRL	MH+ BACTERIA POS CTRL	MH NEG CTRL
B	32	32	32	32	32	32	32	32	32			
C	16	16	16	16	16	16	16	16	16			
D	8	8	8	8	8	8	8	8	8			
E	4	4	4	4	4	4	4	4	4			
F	2	2	2	2	2	2	2	2	2			
G	1	1	1	1	1	1	1	1	1			
H	0.5	0.5	0.5	0.5	0.5	0.5	0.5	0.5	0.5			

2.6 Phase variation

2.6.1 Establishment of a modified protocol for measuring opaque to translucent switching frequencies

The current protocol that exists for studying phase variation in *A. baumannii* has only been used and tested on clinical isolates. The protocol instructs to dilute overnight cultures and let the diluted culture grow to an OD_{600} between 1.8 and 4.0 (early stationary phase), before performing a tenfold serial dilution of the culture (Tipton, Dimitrova and Rather, 2015; Anderson and Rather, 2019). A modified version of this protocol was established within this work. This protocol was used to measure the switching frequency from opaque- to translucent colony type for each of the chicken farm isolates. The switching frequency from translucent- to opaque colonies was not determined within this work. All reagents and their respective suppliers used for phase variation, are listen in Table 6. All solution recipes can be found in Appendix 1.

Growth curves

Using a sterile loop, chicken farm isolate A1, A63, A98 and *A. baumannii* ATCC 17978 were streaked out on LB agar plates and incubated overnight at 37 °C. The next day a single opaque colony from each isolate was picked with a sterile loop and suspended in 6 mL of LB medium in separate 50 mL falcon tubes. The next morning, the overnight cultures were diluted to OD_{600} of 0.05 in 6 mL LB medium. The OD_{600} of the cultures was measured every hour for 12 hours, using a spectrophotometer. Aliquots from the bacterial suspensions (200 µL) were diluted 1:5 in LB medium. The OD_{600} was measured 24 hours and 48 hours was. The liquid cultures were incubated at 37 °C with shaking (180 rpm).

Checking the isolates for switching from opaque to translucent colony phase

Using a sterile loop, chicken farm isolates A1, A63, A98 and *A. baumannii* ATCC 17978 were streaked out on LB agar plates and incubated overnight at 37 °C. The next day a single colony from each isolate was picked with a sterile loop and suspended in 6 mL of LB medium in separate 50 mL falcon tubes. On the next day, a photometric device was used to measure the OD of the overnight cultures. The cultures were diluted to an OD_{600} = 0.05 in 6 mL of LB medium in new 50 mL falcon tubes. The cultures were incubated at 37 °C with shaking (180 rpm). Samples were taken from each of the liquid cultures after 6, 24, and 48

hours and diluted to OD_{600nm} = 1, and a serial dilution series was made for each sample from 10^{-1} to 10^{-6} x dilution (20 µL of bacteria was diluted in 180 µL of LB medium for each 10-fold dilution step). 100 µL of the 10^{-4} and 10^{-6} dilutions were spread out on LB agar plates, and the LB agar plates were incubated at 37 °C for 24, 48 and 72 hours. The number of opaque and translucent colonies was determined after each incubation period.

$$\boldsymbol{Frequency} = \frac{(\boldsymbol{number\ of\ translucent\ colonies}) \times (\mathbf{10^4})}{(\boldsymbol{number\ of\ colonies\ of\ both\ phentoypes}) \times (\mathbf{10^6})} \times \mathbf{100}\%$$

2.6.2 The final protocol

An optimized protocol was used to measure the switching frequency from opaque- to translucent colonies of the chicken farm isolates. The isolates tested, were streaked out on LB agar plates, and incubated overnight at 37 °C. The next day the streaked isolates were examined for their ability to switch from the opaque to translucent colony phase using a stereo microscope. Single opaque colonies from each *A. baumannii* isolate was picked with a sterile loop and suspended in 5 mL of LB medium in separate 50 mL falcon tubes. The cultures were incubated overnight at 37 °C with shaking (180 rpm). On the next day, a photometric device was used to measure the OD of the overnight cultures. The cultures were diluted to an OD_{600} = 0.05 in 5 mL of LB medium in new 50 mL falcon tubes. The cultures were incubated at 37 °C for approximately 48 hours with shaking (180 rpm). After two days of incubation, the cultures were diluted to an OD_{600} = 0.1 in 1 mL of LB medium, serially diluted in LB medium (10 x dilution steps), and 100 µL of the 10^{-3} and 10^{-5} dilutions were spread out on LB agar plates. The plates were incubated at 37 °C over night. After approximately 20-24 hours, the number of opaque and translucent colonies were counted by using a stereo microscope. The switching frequency was determined by the following equation:

$$\boldsymbol{Frequency} = \frac{(\boldsymbol{number\ of\ translucent\ colonies}) \times (\mathbf{10^3})}{(\boldsymbol{number\ of\ colonies\ of\ both\ phentoypes}) \times (\mathbf{10^5})} \times \mathbf{100}\%$$

Table 6. Overview of the reagents used for measuring the switching frequencies and their respective supplier.

Reagent	**Supplier**
Tryptone	Oxoid (Thermo Fisher Scientific)
Yeast extract	Oxoid (Thermo Fisher Scientific)
NaCl	VWR
Agar	Oxoid (Thermo Fisher Scientific)
dH_2O	-

3 Results

3.1 Investigating the phylogenetic relationships and epidemiology of *A. baumannii* isolates from Norwegian chicken farms

Identifying bacterial species by MALDI-TOF are not always fully reliable for closely related species as in the Acb complex. Consequently, the *A. baumannii* isolates were also screened for the presence of the *bla*$_{\text{OXA-51}}$ gene since this gene is only found in *A. baumannii*. The goal of the *bla*$_{\text{OXA-51}}$ screening was to confirm that all the *A. baumannii* isolates provided by the Veterinary Institute were in fact *A. baumannii*, and not closely related species from the Acb complex. This was done by PCR by PhD candidate Claus Michael Goul Larsen. Of all the 200 *A. baumannii* isolates retrieved from the Norwegian Veterinary Institute, 180 (90 %) of these isolates tested positive for *bla*$_{\text{OXA-51}}$. The following chicken farm isolates tested negative for *bla*$_{\text{OXA-51}}$: A2, A4, A10, A11, A17, A27, A35, A36, A55, A59, A91, A95, A99, A144, A185, A187, A189, A196, A197 and A199.

3.1.1 PCR and agarose gel electrophoresis

The first step of the MLST analysis was to PCR amplify (methods section 2.4.1) the seven housekeeping genes of the Pasteur scheme (*cpn60*, *fusA*, *gltA*, *pyrG*, *recA*, *rpiB* and *rpoB*) for each of the A1-A100 strains that were positive for the *bla*$_{\text{OXA-51}}$ gene. The following strains were not included in the PCR because they were *bla*$_{\text{OXA-51}}$ negative: A2, A4, A10, A11, A17, A27, A35, A36, A55, A59, A91, A95, and A99. PCR of the *bla*$_{\text{OXA-51}}$ positive strains of A100-A200 were performed by PhD graduate Claus Michael Goul Larsen. Premade boiling preps (2 µL) containing gDNA was used for each of the seven PCR reactions for each isolate. For each round of PCR, only six isolates with their corresponding seven genes were amplified. From each round, only the PCR amplicons of three of the isolates were run on a gel. Figure 9 shows the results from agarose gel electrophoresis (methods section 2.4.2) analysis of PCR amplicons from three isolates (A76, A77 and A80 respectively), in addition to a no template negative control. This batch consisted of isolates A76, A77, A78, A79, A80 and A81. All the bands in Figure 9 had the expected theoretical sizes, as were observed for all

the other gels. Some smearing was observed in some of the wells in the gels, as seen in all the wells containing the *rpoB* amplicons in Figure 9.

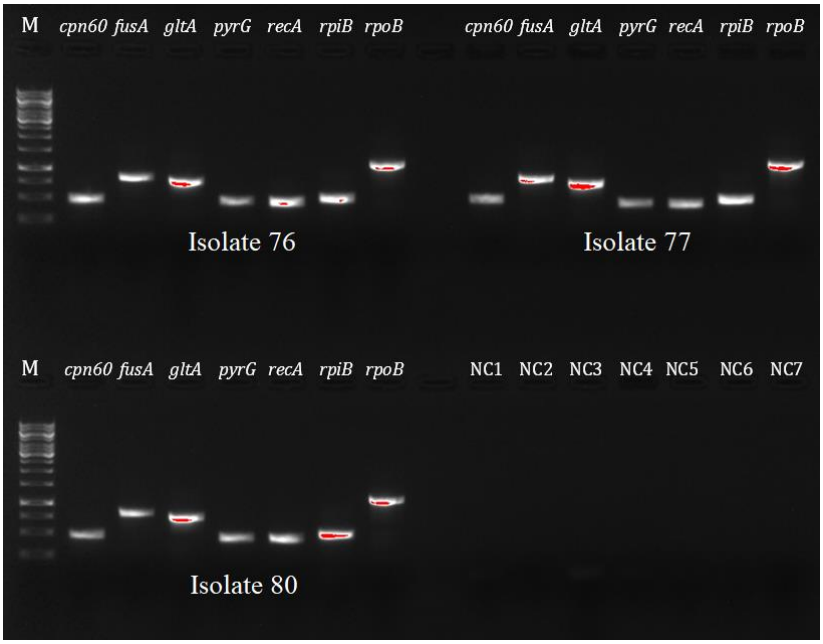

Figure 9. Agarose gel (1 %) electrophoresis of PCR amplicons for isolate A76, A77 and A80 in addition to negative controls reactions for all seven primer sets. Sizes of the PCR amplicon for each gene were approximately: 480 bp (*cpn60*), 802 bp (*fusA*), 723 bp (*gltA*), 434 bp (*pyrG*), 425 bp (*recA*), 475 bp (*rpiB*) and 1076 bp (*rpoB*). NC1: negative control for *cpn60*, NC2: negative control for *fusA*, NC3: negative control for *gltA*, NC4: negative control for *pyrG*, NC5: negative control for *recA*, NC6: negative control for *rpiB* and NC7: negative control for *rpoB*. M: Generuler™ 1 kb DNA ladder, ready to use (Thermo Fisher Scientific). Gels were stained with either EtBr or GelRed and the DNA was visualized under UV light.

3.1.2 The data analysis revealed 36 novel STs

Out of the 180 isolates identified as *A. baumannii* by MALDI-TOF and $bla_{\text{OXA-51}}$ PCR, 170 were included in the MLST analysis below. The remaining 10 isolates (A24, A37, A39, A57, A67, A88, A124, A130, A167, and A180) were left out mainly due to the poor sequence quality for some the housekeeping loci needed for assigning the STs, which may have been the result of the faulty amplification of some of the genes. As mentioned in the methods section (section 2.4.5), registration of new STs and isolate data to the pubMLST database for *A. baumannii* was done by PhD candidate Claus Michael Goul Larsen. A curator verified our novel allele sequences using the sequence chromatograms files and added the new STs to the database.

The data analysis identified 36 unknown STs and 18 known STs for the 170 isolates analyzed (Table 7). The 36 new STs identified found were as follows (n = 129): ST1354 (n = 14), ST1355 (n = 2), ST1356 (n = 11), ST1357 (n = 10), ST1358 (n = 2), ST1359 (n = 1), ST1360 (n = 1), ST1361 (n = 1), ST1362 (n = 1), ST1363 (n = 1), ST1364 (n = 2), ST1365 (n = 1),

ST1366 (n = 1), ST1367 (n = 1), ST1368 (n = 1), ST1369 (n = 26), ST1370 (n = 7), ST1371 (n = 17), ST1372 (n = 6), ST1373 (n = 2), ST1374 (n = 2), ST1375 (n = 4), ST1376 (n = 1), ST1377 (n = 1), ST1378 (n = 1), ST1379 (n = 1), ST1380 (n = 1), ST1381 (n = 1), ST1382 (n = 1), ST1383 (n = 1), ST1384 (n = 1), ST1385 (n = 1), ST1425 (n = 1), ST1426 (n = 1), ST1427 (n = 1) and ST1428 (n = 1). The new STs and their allelic profiles are listed in Table 8. Out of the 170 isolates, 129 (75.9 %) belonged to new STs. Among the new STs found, ST1369 was the dominant one. The remaining 41 isolates (24.1 %) belonged to previously known STs, and 11 of these isolates belonged to ST154. According to the data analysis, none of the 170 isolates analyzed belonged to the same STs of the international clones (IC), which are widely distributed in the world and closely associated with drug resistance.

Table 7. STs and number of isolates belonging to each ST, identified in this work, for the *A. baumannii* isolates from chicken farms. Previously known STs are colored red.

ST	**n**	**ST**	**n**	**ST**	**n**	**ST**	**n**
1369	26	1355	2	926	1	1378	1
1371	17	1358	2	1032	1	1379	1
1354	14	1364	2	1222	1	1380	1
1356	11	1373	2	1359	1	1381	1
154	11	1374	2	1360	1	1382	1
1357	10	575	2	1361	1	1383	1
1370	7	46	1	1362	1	1384	1
1372	6	149	1	1363	1	1385	1
602	5	150	1	1365	1	1425	1
1048	4	155	1	1366	1	1426	1
1375	4	285	1	1367	1	1427	1
961	4	294	1	1368	1	1428	1
138	3	608	1	1376	1		
1036	2	923	1	1377	1		

Table 8. The novel STs identified in this work, and their corresponding allelic profiles.

STs	*cpn60*	*fusA*	*gltA*	*pyrG*	*recA*	*rpiB*	*rpoB*
1354	12	3	5	2	5	1	14
1355	156	2	2	2	9	1	2
1356	3	1	2	2	9	1	5
1357	1	100	2	2	9	1	52
1358	1	3	2	5	3	1	14
1359	27	2	2	7	5	4	14
1360	1	3	17	2	3	1	14
1361	3	2	2	2	5	4	14
1362	27	4	2	2	7	1	2
1363	3	3	7	2	9	4	5
1364	3	1	2	5	29	1	4
1365	6	3	2	2	5	2	2
1366	1	12	11	2	15	9	14
1367	1	2	2	1	9	1	4
1368	25	1	2	3	169	1	2
1369	9	195	2	2	4	1	4
1370	1	3	192	1	4	4	4
1371	9	195	7	2	4	1	4
1372	208	2	3	2	2	110	4
1373	3	3	2	2	206	4	14
1374	209	3	3	2	29	110	8
1375	3	199	7	1	7	1	4
1376	207	2	7	5	11	1	14
1377	3	196	101	2	3	1	14
1378	3	3	7	2	4	2	180
1379	1	197	193	2	18	2	5
1380	1	198	6	2	3	1	54
1381	27	88	167	5	207	109	2
1382	1	53	3	2	208	9	14
1383	1	201	193	2	9	2	5
1384	1	3	194	2	4	4	5
1385	12	200	5	2	5	1	14
1425	1	5	2	2	217	1	8
1426	3	16	13	2	71	2	4
1427	1	3	11	5	3	4	14
1428	1	100	2	2	9	115	52

Using the pubMLST database for *A. baumannii* (https://pubmlst.org/abaumannii/), the data available on the known STs were analyzed. Of the known STs identified in this work, ST46, ST138, ST149, ST150, ST154, ST155, ST285, ST575, ST602, ST608, ST923, ST961 and ST1222 have previously been found in human clinical samples. Also, the following STs have previously been identified in animals: ST138 (goose), ST155 (cattle and red panda), ST285 (cattle), ST294 (bearded dragon), ST923 (white stork), ST926 (white stork), ST961 (pig), ST1032 (cattle), ST1036 (cattle) and ST1048 (fecal sample from cattle). ST46 and ST294 have previously been identified in biogas and water in addition to in human and animal samples, respectively.

3.1.3 Phylogenetic analyses of chicken farm isolates

Only some of the STs identified among the chicken farm isolates were closely related

An MST was generated using the global optimal eBURST (goeBURST) (methods section 2.4.6) algorithm for the STs representing the chicken farm isolates (Figure 10). The lines between the circles containing the STs indicate how many allelic mismatches there are between the connected STs. An allelic mismatch in this context means that one or several of the allele numbers assigned to each ST differ between the STs connected. By analyzing the MST, we can see that there are 6 links with one allelic mismatch, 13 links with two allelic mismatches, 23 links with three allelic mismatches, 10 links with four allelic mismatches and one link with five allelic mismatches. Based upon the links and the allelic mismatches, only some of these STs can be described as being closely related. Overall, there was no close relationship between the STs based upon the MST (Figure 10). However, using the standard criterion of one allelic mismatch to group STs into clonal complexes (Feil *et al.*, 2004), five small clonal complexes were identified (Figure 11). These complexes are the closest relationship seen between the STs analyzed. ST46, ST149 and ST1032 make up the largest clonal complex, whereby ST46 is the central ST. The four other clonal complexes consist of ST923 and ST602, ST1385 and ST1354, ST1369 and 1371, and ST1428 together with ST1357. Although in general no close relationship was seen between all the STs found in this work, the minority of the STs that were considered close contained many of the chicken farm isolates analyzed. In total, the clonal complexes include 11 out of the 54 STs (20.4 %) identified in this work. These 11 STs alone represent 78 out of the 170 (45.9 %) chicken farm isolates analyzed (Table 7). Taken together, almost half of all the chicken farm isolates

examined do have a close relationship to each other, and these isolates are confined to 11 of the STs identified within this work.

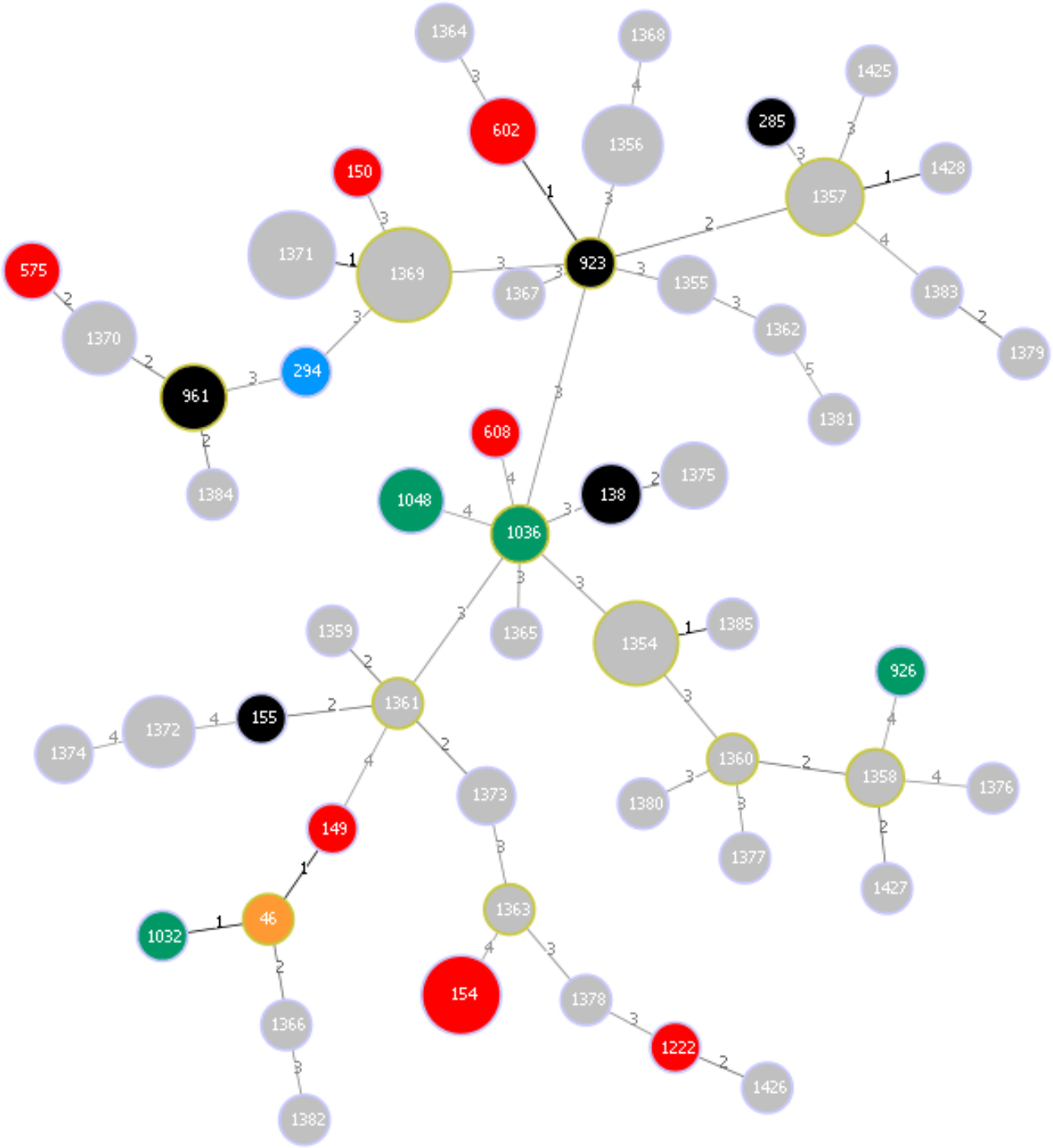

Figure 10. MST generated for the 170 strains using the goeBURST alghorithm in PHYLOViZ 2.0. The size of the circles reflect the number of isolates that are assoicated with the given ST. The numbers between the different STs indicate the number of allelic differences. Thick lines represent SLVs. STs within the nodes with green edges represent central STs that can be thought of as an ancestor or a founder of to two or more STs. Already existing STs that have been identified prior to this work are shown in different colors: clinical samples are found within red circles, samples from animals are within green circles, STs containing both clinical and animal samples are black, STs found to contain a water and animal sample are blue and the orange circle contains isolates from biogas and a clinical sample.

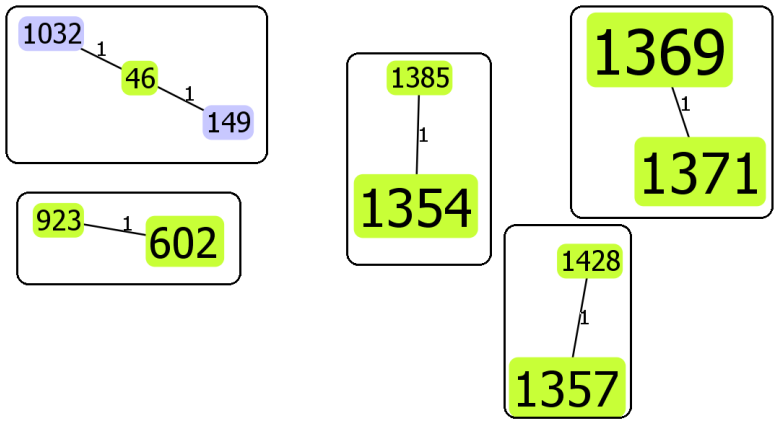

Figure 11. The clonal complexes identified using the goeBURST alghorithm with the criterion of one allelic mismatch (SLV). The remaining STs are regarded as singletons when using this criterion. The numbers listed between the different STs indicate the number of allelic differences. The black squares identify each clonal complex. The green color indicate the founder and the blue color indicate the the clonal STs. The size of the coloured squares (containing the STs) reflect the number of isolates that are assoicated with the given ST.

Analysis of the UPGMA dendrograms reveals a potential close relationship between some of the STs identified among *A. baumannii* chicken farm isolates and international clonal lineage 8

Another way to illustrate the relationship between the chicken farm isolates was to make a phylogenetic dendrogram using the UPGMA algorithm (methods section 2.4.6), as shown in Figure 12. Here, the relationship between the STs is measured by the hamming distance which represents the allelic mismatches between the STs. By analyzing the dendrogram, one can see that only some of the STs could be described as being closely related, and that overall, there are no close relationship between the STs. However, the closest relationships observed between the STs in the UPGMA dendrogram, were between those making up the clonal complexes (as observed for the MST analyses; Figures 10 and 11). ST46, ST149 and ST1032 make up the largest clonal complex, with ST46 grouped with ST149. The closest ST to this group is then ST1032 as seen in (Figure 12). Since this algorithm only groups pairs, ST1032 is not included in the group consisting of ST46 and ST149. In fact, the UPGMA dendrogram indicates that the distance between ST46 and ST149 is one and a half, meaning that ST1032 differ in one and a half locus compared to ST149 and ST46 (in reality ST1032 differ only at one locus compared to ST46, however the UPGMA algorithm calculates the mean pairwise distance from both ST149 and ST46 to ST1032, and while ST46 only differs at one locus compared to ST1032, ST149 differs at two loci compared to ST1032). Since both ST149 and ST1032 have one allelic mismatch compared to ST46, ST1032 could have also been grouped with ST46, instead of ST149.

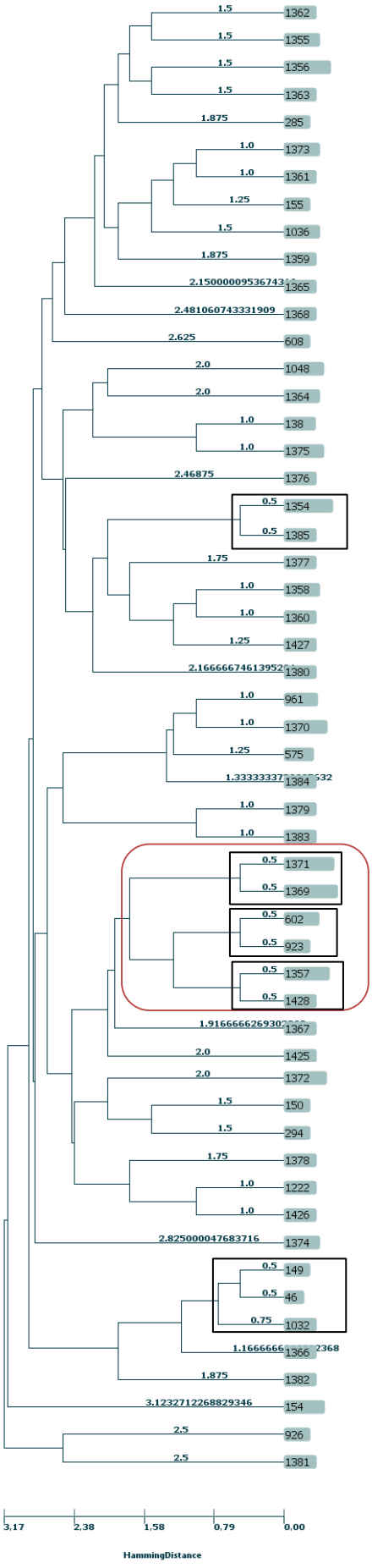
1.5
1362
1.5
1355
1.5
1356
1.5
1363
1.875
285
1.0
1373
1.0
1361
1.25
155
1.5
1036
1.875
1359
1365
2.481060743331909
1368
2.625
608
2.0
1048
2.0
1364
1.0
138
1.0
1375
2.46875
1376
0.5
1354
0.5
1385
1.75
1377
1.0
1358
1.0
1360
1.25
1427
1380
1.0
961
1.0
1370
1.25
575
1384
1.0
1379
1.0
1383
0.5
1371
0.5
1369
0.5
602
0.5
923
0.5
1357
0.5
1428
1367
2.0
1425
2.0
1372
1.5
150
1.5
294
1.75
1378
1.0
1222
1.0
1426
2.825000047683716
1374
0.5
149
0.5
46
0.75
1032
1366
1.875
1382
3.1232712268829346
154
2.5
926
2.5
1381
3.17
2.38
1.58
0.79
0.00
HammingDistance

Figure 12. UPGMA clustering dendrogram showing the relationship between the STs identified in this work. The relationships between the STs are measured by the hamming distance which represents the degree of allelic mismatches between the STs. The black squares indicate the clonal complexes, while the red square signify the close relationship between the three clonal complexes consisting of ST923 and ST602, ST1371 and ST1369, and ST1357 with ST1428. The phylogenetic tree was constructed using PHYLOViZ 2.0.

The four other clonal complexes observed in Figures 10 and 11, are also grouped together in the UPGMA dendrogram; ST923 is grouped with ST602, ST1385 with ST1354, ST1369 with ST1371, and ST1428 together with ST1357. As the hamming distance indicates, they only differ at one locus. Looking closer at the groups consisting of ST923 and ST602, ST1428 and ST135, and ST1369 with ST1371, these three clades seem to be part of a bigger clade, marked with a red rectangle.

To find out if there is any connection between the chicken farm isolates and IC1-8, to which new strains have been grouped after frequently having been isolated in several countries worldwide, a new dendrogram was made. The new dendrogram containing the international clonal lineages is shown in Figure 13. IC1 seems to be very distantly related to the chicken farm isolates and is not closely related to any of the STs identified found in this work. IC2 is related to ST1365, however there are three allelic mismatches between them, indicating no close relationship. IC3 is grouped with ST1036, having only two variable alleles. IC4 is part of a bigger clade but is not closely related to any of the STs in this clade. IC5 is also part of a clade but is not grouped with any of the STs found in this work. IC6 is grouped with ST1380, however there are four allelic mismatches between them indicating no close relationship. On the other hand, IC7 seem to be related to the clade containing ST138 and ST1375, however there is no close relationship with these STs. The last IC, IC8, has clustered with ST575 and ST1370, making a new clade, suggesting a close relationship between these STs. ST575 is grouped with IC8, while the closest ST to this clade is ST1370 as seen in Figure 13. However, both ST575 and ST1370 have only one allelic mismatch compared to IC8. As seen earlier with ST455, ST149 and ST1032, only ST575 is grouped with IC8 while ST1370 is not. However, ST1370 could have also been grouped with IC8. Only of one the STs can be picked to group with IC8, and this is due to the nature of the UPGMA algorithm only grouping two taxa together. In sum, the dendrograms are in agreement with the MST showing that some of the STs do have a close relationship with each other, while the rest of the STs is more distantly related. Furthermore, it is revealed that two of the STs have a potential close relationship to IC8.

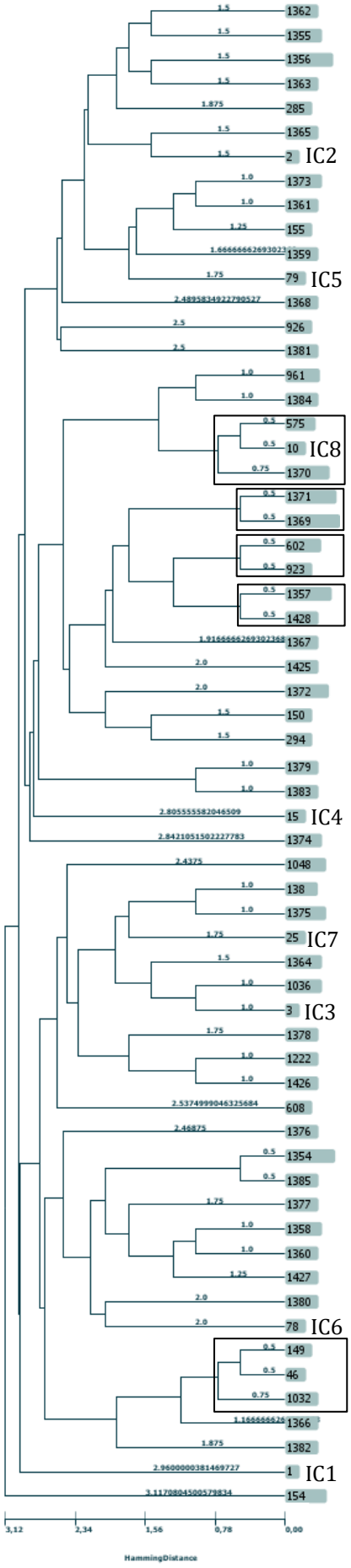
1362
1355
1356
1363
285
1365
2
IC2
1373
1361
155
1359
79
IC5
1368
926
1381
961
1384
575
10
IC8
1370
1371
1369
602
923
1357
1428
1367
1425
1372
150
294
1379
1383
15
IC4
1374
1048
138
1375
25
IC7
1364
1036
3
IC3
1378
1222
1426
608
1376
1354
1385
1377
1358
1360
1427
1380
78
IC6
149
46
1032
1366
1382
1
IC1
154
3,12
2,34
1,56
0,78
0,00
HammingDistance

Figure 13. UPGMA clustering dendrogram showing the relationship between the STs identified for the chicken farm isolates and the STs for the widespread international clones (IC) 1-8. ST1 corresponds to IC1, ST2 to IC2, ST3 to IC3, ST15 to IC4, ST79 to IC5, ST78 to IC6, ST25 to IC7 and ST10 to IC8. The relationship between the STs are measured by the hamming distance which represents the degree of allelic mismatches between the STs. The black squares indicate the clonal complexes found in the MST. The phylogenetic tree was constructed using PHYLOViZ 2.0.

3.2 Profiling for drug resistance

3.2.1 The disc diffusion method shows that some of the chicken farm isolates are resistant towards aminoglycosides

A Kirby-Bauer disc diffusion method was used to identify any drug-resistant isolates among the *A. baumannii* chicken farm isolates (methods section 2.5.1). In general, the chicken farm isolates were susceptible to ciprofloxacin (CIP) (100 %), gentamicin (GEN) (97.2 %), imipenem (IPM) (100 %), meropenem (MEM) (100 %) and tobramycin (TOB) (85.6 %) (Table 9). Conversely, some isolates were resistant to the aminoglycosides GEN (2.8 %) and TOB (14.4 %), as based on the EUCAST clinical breakpoints for the R category (Table 9). Note that the epidemiological cut-off value for TOB is identical to the clinical breakpoint for the R category. As of 25.03.2020, no data are available on the breakpoints of ceftazidime for the disc diffusion method on either EUCAST or The United States Committee on Antimicrobial Susceptibility Testing (USCAST). A picture of the result from a disc diffusion test for three of the isolates is shown in Figure 14. *A. baumannii* strains A085 and ATCC17978 were used for quality control of the antibiotics and media used for disc diffusion. *A. baumannii* strain A085 was resistant towards all tested antibiotics, while *A. baumannii* strain ATCC17978 was susceptible, showing no resistance, as expected

Table 9. Distribution (%) of antimicrobial susceptibility categories of chicken farm isolates of *A. baumannii* (n = 180). The breakpoints are according to the clinical breakpoints reported by EUCAST (last updated 01.01.2020) (EUCAST, 2020a).

	Breakpoints (diameter, mm)		**Proportion of isolates (%)**	
	Susceptible ≥	Resistant <	Susceptible (S)	Resistant (R)
Ceftazidime[1]	-	-	-	-
Ciprofloxacin	50	21	100	-
Gentamicin	17	17	97.2	2.8
Imipenem	24	21	100	-
Meropenem	21	15	100	-
Tobramycin[2]	17	17	85.6	14.4

[1] There are no data available for ceftazidime as of 25.03.2020 on EUCAST or USCAST.
[2] The epidemiological cut-off value for tobramycin is identical to the clinical breakpoint.

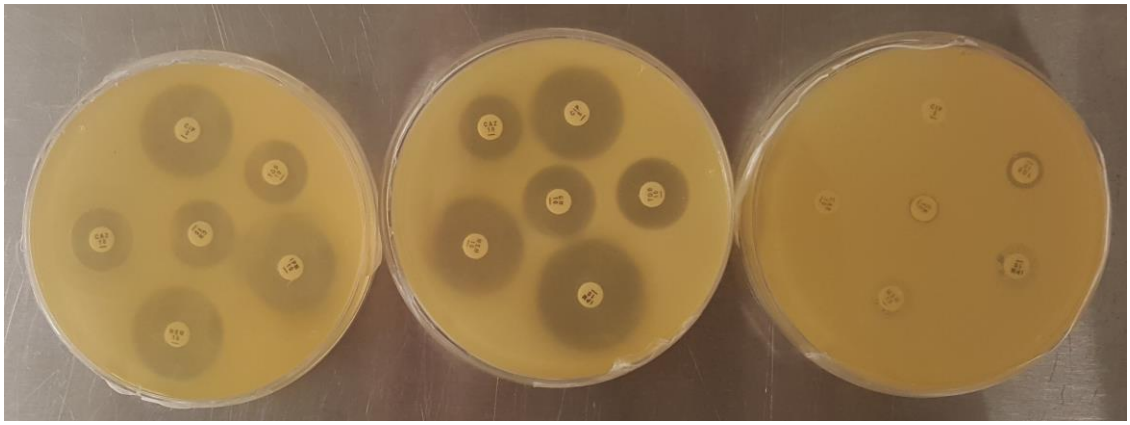

Figure 14. Disc diffusion of chicken farm isolate A51 (to the left) and Isolate A191 (in the middle) in addition to the MDR clinical isolate A085 from Sweden (to the right). All isolates were tested for their susceptibility against TOB, GEN, CAZ, CIP, MEM and IPM.

Figure 15 shows an overview of the distribution of the zone diameter for all the isolates for each antibiotic. For TOB the inhibition zones ranged from 15-20 mm, for GEN 16-22 mm in addition to one isolate having a zone of 24 mm and another one with a zone of 32 mm, for CIP 22-32 mm, for CAZ 15-24 mm in addition to one isolate having a zone with a diameter of 32 mm, for IPM 23-36 mm in addition to one isolate having a zone of 38 mm and another one with 40 mm, and for MEM the range varied from 21-31 mm in addition to one isolate having a zone diameter of 34. The majority of the isolates are clustered in the middle of the zone diameter range, while a few isolates have a low zone diameter and a large zone diameter. For comparison, breakpoints for all the antibiotics are shown in Table 9. The clinical breakpoint for the R category is also indicated by the stippled line in Figure 15, for TOB and GEN. As previously mentioned, all isolates were regarded as susceptible for CIP, IPM and MEM.

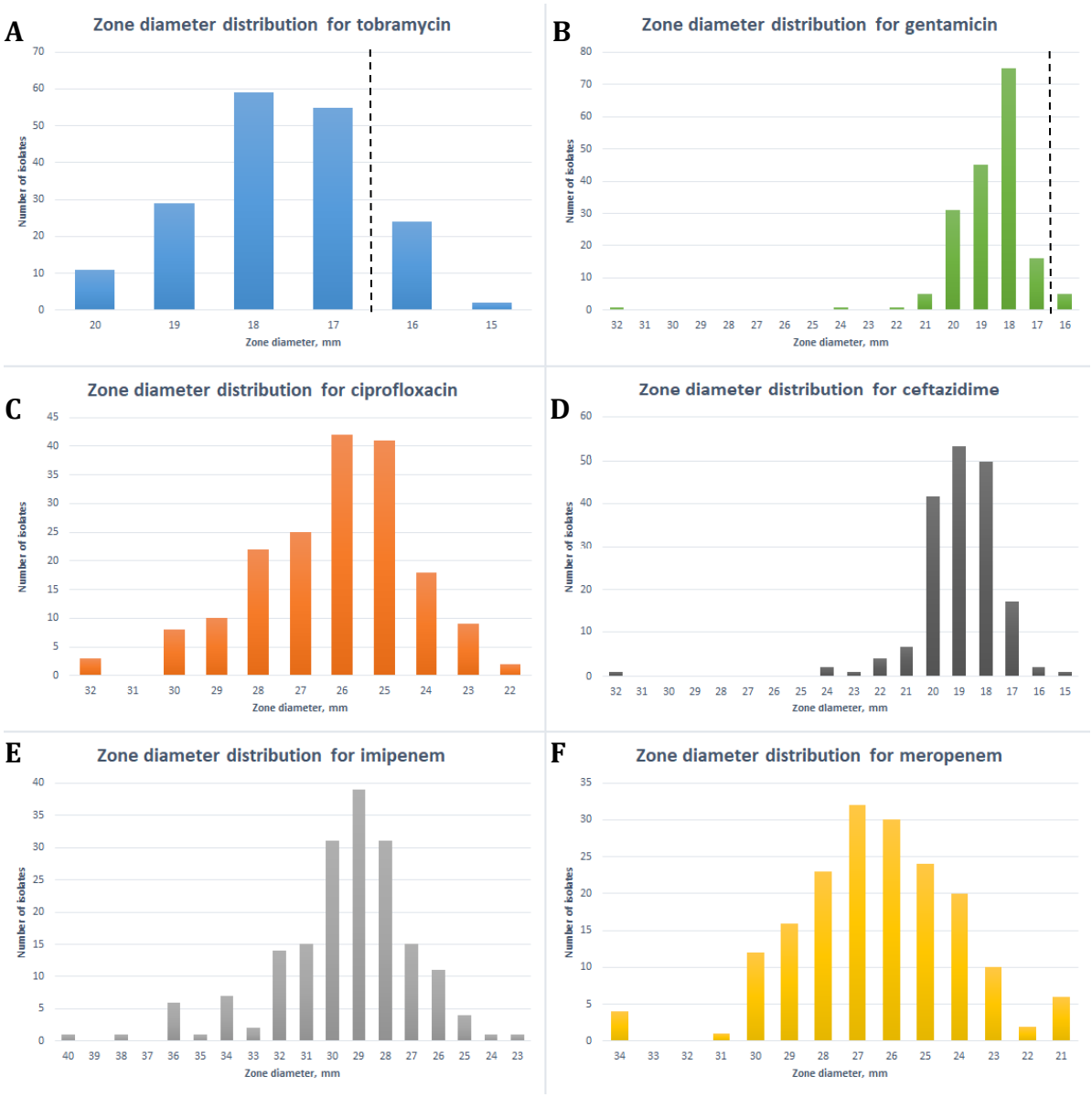

Figure 15. An overview over the distribution of the zone diameters from disc diffusion tests of *A. baumannii* isolates (n = 180). **(**A) TOB, (B) GEN, (C) CIP, (D) CAZ, (E) IPM, (F) MEM. The stippled lines indicate the clinical breakpoints for the R category. The left side of the line represent the susceptible isolates, and to the right the resistant isolates. Where there are no lines, all isolates came out as susceptible.

3.2.2 Broth microdilution MIC testing showed that none of the chicken farm isolates were resistant to aminoglycosides

The goal of the broth microdilution method was to verify and extend the results from the Kirby-Bauer disc diffusion testing. All the isolates displaying resistance towards TOB and GEN using the disc diffusion method had diameters that were close to the clinical breakpoint for the R category. Due to this, an additional drug testing analysis was performed to reveal if the isolates were in fact resistant to the aminoglycosides tested for.

Determination of the correct inoculum size

All the isolates being tested for their susceptibility using the broth microdilution method, were checked for their inoculum size (2 - 8 x 10^5 CFU/ml) using viable counts, before being tested for their susceptibility against TOB and GEN (methods section 2.5.2). The results from the first round of viable counts are shown in Table 10. Most of the isolates were in the range of 20-80 colonies per plate, as desired. However, isolates A51, A96 and A163 were not in the desired range. In addition to these three isolates, isolate A9 was at the borderline of the criterion. Since isolates A9, A51, A96 and A163 did not satisfy the criterion, additional viable counts were performed for these four isolates, and to ensure the proper inoculum size, a higher density of the bacteria was used. The results for the second analysis of these isolates are shown in Table 11. For isolates A9 and A163 a density of 4X 0.5 McFarland were used, while for isolate A98 a density of 10X 0.5 McFarland were used. Isolate A51 required several rounds of viable counts to be in the desired range.

Table 10. Summary of the viable count experiments performed for all the isolates to be mapped for drug resistance using the broth microdilution method. The isolates not being in the desired range are marked red.

Isolate	Number of colonies
A1	49
A9	21
A12	32
A13	41
A14	35
A15	46
A16	58
A25	35
A26	60
A33	65
A42	28
A48	89
A50	59
A51	172
A56	60
A63	46
A69	36
A80	34
A96	8
A100	42
A106	40
A108	51
A109	31
A127	25
A129	39
A155	60
A163	11

Table 11. Results from the second round of viable count experiments performed on isolates A9, A51, A96 and A163 to be mapped for drug resistance using a higher density of the bacteria. The density is measured as 0.5 McFarland

Isolate	Number of colonies replicate 1	Number of colonies replicate 2	0.5 McFarland
A9	42	60	4X
A51	36	50	1X
A96	70	85	10X
A163	37	40	4X

Susceptibility testing using the broth microdilution method

To check whether the chicken farm isolates displaying resistance against TOB and/or GEN by disc diffusion were in fact resistant, the isolates were also tested using the broth microdilution method (methods section 2.5.2). As shown in Table 12, all the isolates tested were susceptible towards TOB and/or GEN by this method, having an MIC value in the range of 2 µg/mL - 4 µg/mL. According to EUCAST, the clinical breakpoint for the R category of both TOB and GEN is R > 4 µg/mL. The epidemiological cut-off value also corresponded to this value. All MIC values lower or equivalent to 4 µg/mL are regarded as susceptible for both antimicrobials. The isolates used as positive controls for the susceptibility testing using the broth microdilution method are shown in Table 13. Most of the isolates satisfied the criterion having colonies between the range of 20-80 colonies in the viable count, except for A33, A96, A109 and A155 which showed 16, 11, 19 and 15 colonies respectively from the viable count. Despite not satisfying the criterion, it was deemed that the small deviation observed was most probably not as substantial as to affect the MIC value significantly. Taken together, the results from the disc diffusion and the broth microdilution experiments indicated that none of the isolates are resistant to any of the clinically antibiotics tested for.

Table 12. An overview of antimicrobial suscpetbility toward TOB and Gen for the isolates (n= 27) that according to the disc diffusion method were resistant to TOB and/or GEN. The epidemiological cut-off value and the clinical breakpoint of EUCAST for TOB and GEN was the same. Two biological replicates were carried out for each isolate.

Isolate	**MIC values (µg/mL)**		**Susceptible ≤ 4 µg/mL**	**Resistant > 4 µg/mL**
	TOB	**GEN**		
A1	4	-	X	
A9	2	-	X	
A12	2	-	X	
A13	2-4	-	X	
A14	4	-	X	
A15	2-4	-	X	
A16	2	-	X	
A25	4	-	X	
A26	2	-	X	
A33	2	-	X	
A42	4	-	X	
A48	2	-	X	
A50	4	-	X	
A51	2-4	4	X	
A56	2	-	X	
A63	4	4	X	
A69	4	4	X	
A80	2-4	-	X	
A96	2-4	-	X	
A100	2-4	-	X	
A106	4	-	X	
A108	4	4	X	
A109	2-4	-	X	
A127	2-4	-	X	
A129	2-4	-	X	
A155	2-4	-	X	
A163	4	4	X	

Table 13. Isolates serving as positive controls for the broth microdilution method. Isolates serving as positive controls were chosen at random, and those used as a positive control twice have two counts separated by a forward slash.

Isolates	Colonies
A9	54
A33	16
A51	31
A56	28
A63	60
A69	40
A96	11/55
A108	21
A109	19
A155	15/21

3.3 Mapping phase variation frequencies in *A. baumannii* chicken farm isolates

3.3.1 Modification of the existing protocol

Growth analysis

Switching between opaque and translucent colony morphologies has been identified as a feature of certain *A. baumannii* strains, affecting various phenotypes such as drug resistance and biofilm formation, but has not been investigated systematically in large sets of environmental isolates. The goal of the following experiments was to establish a slightly modified version of the current protocol for phase variation experiments, so that it could be used to measure the switching frequency from the opaque to translucent colony phase of the chicken farm isolates (methods section 2.6.1). The growth curves for three chicken farm isolates and a reference strain were first determined in a pilot study, in order to determine the timing of the various stages of growth. The growth curves of chicken farm isolate A1, A63, A98 and *A. baumannii* ATCC 17978 are shown in Figure 16, which depicts the growth of the bacteria plotted as OD_{600} versus time. According to Tipton, Dimitrova and Rather (2015), their isolates used for phase variation experiments reached early stationary phase between OD_{600} 1.8 – 4.0. This OD_{600}-range was reached approximately after 4-8 hours for isolate A1, A63, A98 and *A. baumannii* ATCC 17978. However, early stationary phase was not achieved at this point. In our experiments early stationary phase was reached during the time period of

8 – 12 hours growth (Figure 16). The stationary phase was reached after 12 – 16 hours, and after 24 hours all isolates tested had reached late stationary phase. For determining the switching frequency from the opaque to translucent colony phase, aliquots were taken from the liquid cultures after 6, 24 and 48 hours, corresponding to exponential, stationary and late stationary phases of growth.

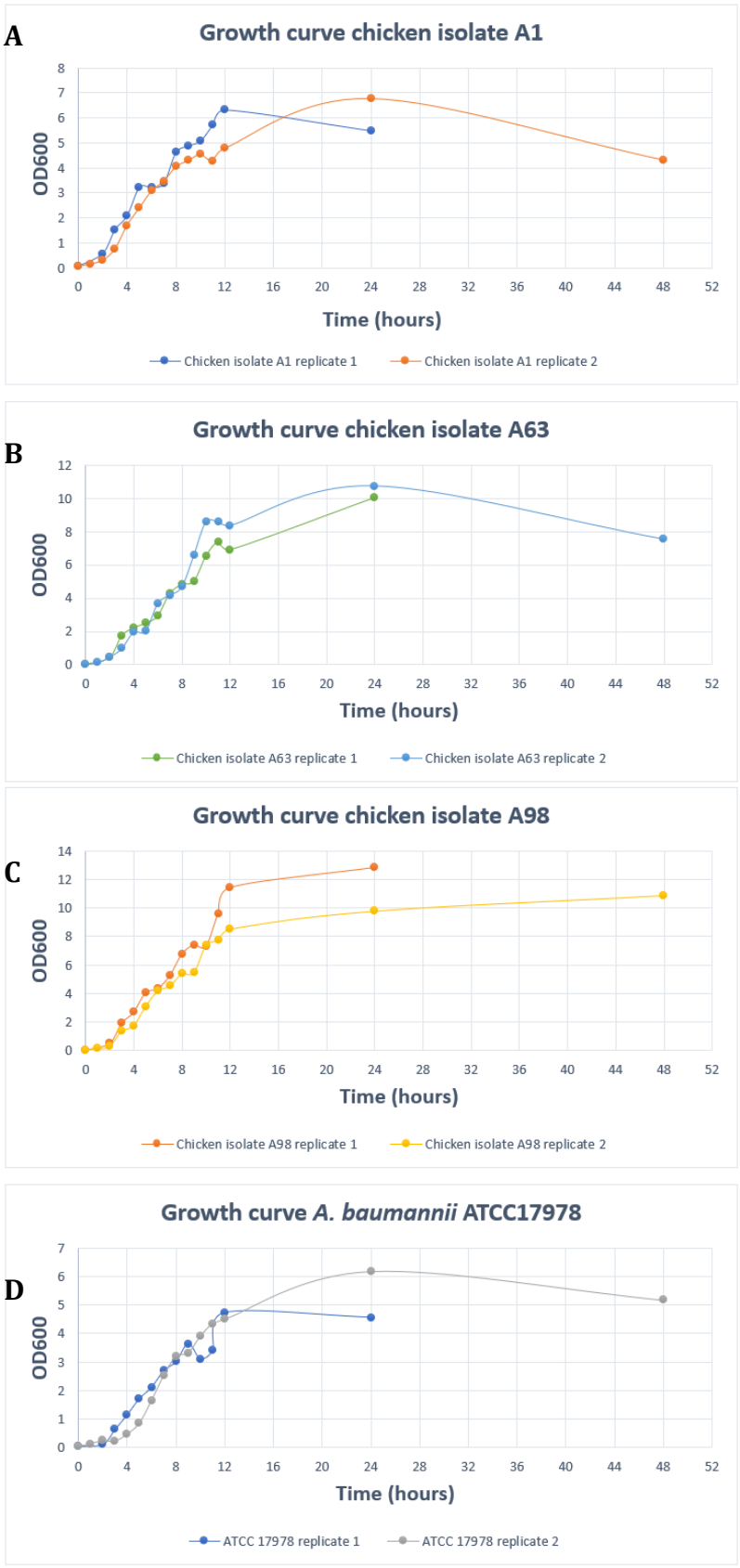

Figure 16. Growth of chicken farm isolates (A) A1, (B) A63, (C) A98 and (D) *A. baumannii* ATCC 17978 in LB at 37 °C with shaking (180 rpm). OD_{600} was plotted versus time. Two biological replicates were performed for each isolate, with the second replicate containing measurements of the OD_{600} after 48 hours. OD was measured at 600 nm.

Examining a selection of the chicken farm isolates for the ability to switch from opaque to translucent colony type

Detecting the switching from opaque to translucent colonies can be difficult if the switching frequency is low. To overcome this obstacle, it was aimed to use conditions to allow every isolate included in establishing the modified protocol to have the highest switching frequency possible. To achieve this, it was decided to optimize both the incubation time of the liquid cultures ahead of plating, as well as the length of incubation of the LB plates. Additionally, both 0.5X and regular LB medium was used to observe if the different types of plates had any effect on the switching frequency. The results are shown in Table 14 and 15. Using 6-hour liquid cultures did not yield a high number of translucent colonies for the isolates, except for isolate A1 (Table 14 and 15). Few translucent colonies were also observed for isolate A63, and none were observed for isolate A98 and *A. baumannii* strain ATCC17978. More translucent colonies were observed for isolate A1 and A63 when using 0.5X LB plates compared to regular LB plates. After 24 hours of incubation with the LB plate the switching frequency for isolate A1 was 0.94 %. In comparison, for the 0.5X LB plate the switching frequency was 1.97 %. After 48 hours the switching frequency was 1.80 % when plated on LB and 2.50 % for 0.5X LB plate, and after 72 hours it was 2.15 % and 2.75 % respectively. The switching frequency was also slightly higher for isolate A63 when using 0.5X LB plates, however the number of translucent colonies differed only by either one or two colonies depending on the incubation period for the plates. The main reason for the difference in the switching frequency for isolate A63 is due to the difference in the number of colonies on the plate with dilution x 10^{-6}.

An increase in switching to translucent colonies was observed for the 24-hour liquid cultures (Table 14 and 15). However, again, no translucent colonies were observed for *A. baumannii* strain ATCC17978. The switching frequency and the number of translucent colonies for isolate A63 and A98 was almost the same when using either LB or 0.5X LB for plating (Table 14 and 15). For isolate A1, more translucent colonies were observed when using 0.5X LB. After 24 hours of incubation with the LB plates the switching frequency was 4.6 % as opposed to 7.03 % for the 0.5X LB plates. After 48 hours the switching frequency was 5.1 % for LB and 7.35 % for 0.5X LB plate, and after 72 hours it was 5.4 % and 7.79 % respectively.

For the 48-hour liquid cultures an increase of the number of translucent colonies was yet again observed as compared to the 6 -and 24-hour liquid cultures, see Table 14 and 15. The reason why the number of colonies with the dilution factor of 10^{-6} was high after incubating the liquid cultures for 48 hours is not known. However, the switching frequency did not increase for isolate A1 or A63 compared to the switching frequencies determined for the isolates when the liquid cultures were incubated for 6 -and 24 hours. The switching frequencies were lower due to the high count of total colonies (plate with dilution x 10^{-6}), even though the number of translucent colonies was higher than observed previously. For isolate A1, the switching frequency was overall higher on the LB plates compared to 0.5X LB plates, as was the number of translucent colonies (Table 14 and 15). For isolate A98 the switching frequency and the number of translucent colonies were higher compared to the 6 - and 24-hour liquid cultures, despite the high count of total colonies. The switching frequencies were rather similar after 24 hours of incubation of the LB and 0.5X LB plates, 0.36 % compared to 0.33 %, however after 48 hours of incubation the switching frequency for the 0.5X LB plate doubled. This did not happen for the regular LB plate after 48 hours, and why this happened for the 0.5X LB plate is not known. Yet again, no translucent colonies were observed for *A. baumannii* ATCC17978, indicating that this strain does not possess detectable levels, if at all, of phase variation.

Overall, the switching frequencies and the number of translucent colonies seem to increase with length of incubation, both with respect to the liquid cultures ahead of plating and to the incubation of the LB plates. However, the increase in number of translucent colonies is not that high when incubating the plates for more than 24 hours, except for isolate A1 for the 6 - and 48-hour liquid cultures and for A98 for the 48-hour liquid culture (Table 14). A difference in the switching frequency was observed when using the different types of plates, however the difference was not very large, except for isolate A1, in which the results varied. For isolate A1, for the 6-hours liquid culture, the 0.5X LB plates seemed to yield a rather higher number of translucent colonies compared to the regular LB plates, while for the 48-hour culture the regular LB plates had definitely more translucent colonies than 0.5X LB plates. In sum, the switch from opaque to translucent colonies was shown to be highest and most optimal when incubating the liquid cultures for 48 hours. An increase of the number of translucent colonies was observed when incubating the plates longer than 24 hours. The type of plate used seemed to not have a substantial effect on the switching frequencies, however, it remains somewhat uncertain because of the variation in results seen for isolate A1 and A98.

Table 14. Measured switching frequencies from opaque to translucent colony morphology for 6, 24, and 48-hour liquid cultures of A1, A63, A98 and *A. baumannii* ATCC17978 in LB broth at 37 °C with shaking (180 rpm). The LB plates were incubated for 24, 48 and 72 hours to observe if there were any differences in the switching frequency.

	Number of colonies x 10^{-6}	**Number of translucent colonies x 10^{-4} (switching frequency %)**		
		6 hours liquid cultures		
		24h on LB plates	48h on LB plates	72h on LB plates
Isolate A1	69	65 (0.94 %)	124 (1.80 %)	148 (2.15 %)
Isolate A63	45	1 (0.02 %)	2 (0.04 %)	2 (0.04 %)
Isolate A98	38	0 (0 %)	0 (0 %)	0 (0 %)
ATCC 17978	19	0 (0 %)	0 (0 %)	0 (0 %)
		24 hours liquid cultures		
		24h on LB plates	48h on LB plates	72h on LB plates
Isolate A1	50	230 (4.6 %)	255 (5.1 %)	270 (5.4 %)
Isolate A63	46	3 (0.07 %)	4 (0.09 %)	4 (0.09 %)
Isolate A98	33	4 (0.12 %)	6 (0.18 %)	7 (0.21 %)
ATCC 17978	51	0 (0 %)	0 (0 %)	0 (0 %)
		48 hours liquid cultures		
		24h on LB plates	48h on LB plates	72h on LB plates
Isolate A1	134	357 (2.66 %)	390 (2.91 %)	415 (3.10 %)
Isolate A63	164	6 (0.04 %)	6 (0.04 %)	11 (0.07 %)
Isolate A98	109	39 (0.36 %)	46 (0.42 %)	48 (0.44 %)
ATCC 17978	128	0 (0 %)	0 (0 %)	0 (0 %)

Table 15. Measured switching frequencies from opaque to translucent colony morphology for 6, 24, and 48-hour liquid cultures of A1, A63, A98 and *A. baumannii* ATCC17978 in LB broth at 37 °C with shaking (180 rpm). The 0.5X LB plates were incubated for 24, 48 and 72 hours to check if there were any differences in the switching frequency.

	Number of colonies x 10^{-6}	**Number of translucent colonies x 10^{-4} (switching frequency %)**		
		6 hours liquid cultures		
		24h on 0.5X LB plates	48h on 0.5X LB plates	72h on 0.5X LB plates
Isolate A1	74	146 (1.97 %)	185 (2.50 %)	190 (2.57 %)
Isolate A63	33	3 (0.09 %)	4 (0.12 %)	4 (0.12 %)
Isolate A98	37	0 (0 %)	0 (0 %)	0 (0 %)
ATCC 17978	12	0 (0 %)	0 (0 %)	0 (0 %)
		24 hours liquid cultures		
		24h on 0.5X LB plates	48h on 0.5X LB plates	72h on 0.5X LB plates
Isolate A1	37	260 (7.03 %)	272 (7.35 %)	288 (7.79 %)
Isolate A63	55	6 (0.11 %)	7 (0.13 %)	7 (0.13 %)
Isolate A98	39	5 (0.13 %)	6 (0.15 %)	6 (0.15 %)
ATCC 17978	47	0 (0 %)	0 (0 %)	0 (0 %)
		48 hours liquid cultures		
		24h on 0.5X LB plates	48h on 0.5X LB plates	72h on 0.5X LB plates
Isolate A1	137	268 (1.96 %)	286 (2.09 %)	298 (2.18 %)
Isolate A63	170	8 (0.05 %)	17 (0.10 %)	18 (0.11 %)
Isolate A98	97	32 (0.33 %)	66 (0.68 %)	72 (0.74 %)
ATCC 17978	87	0 (0 %)	0 (0 %)	0 (0 %)

3.3.2 Investigating the complete set of *A. baumannii* chicken farm isolates for the ability to switch from opaque to translucent morphotypes

Most of the isolates can switch from the opaque to translucent colony morphology

The transition from the opaque to the translucent colony phase was investigated for all the *bla*$_{\text{OXA-51}}$ positive *A. baumannii* chicken farm isolates of A1-A176 (Table 16). The switching frequency was highly variable, ranging from 0 – 51 %. Of all the isolates tested, only one isolate (A3) did not show any translucent colonies. For isolate A73 I was not able to determinate switching frequency because the colonies were too large, so that I was not able to distinguish them from each other (thus non-countable). Other than this, all the chicken farm isolates showed the ability to switch between colony phenotypes. Due to the SARS-CoV-2 pandemic, I was not able to check all the *bla*$_{\text{OXA-51}}$ positive *A. baumannii* chicken farm isolates for their ability to switch from the opaque to translucent colony phase. The isolates having a switching frequency of 0, or the isolates I was not able to determine the switching

frequency due to some experimental error in one of the replicates, were supposed to be re-tested, but I was not able to because of the pandemic.

Table 16. An overview of the opaque to translucent switching frequencies of the *bla*$_{\text{OXA-51}}$ positive *A. baumannii* chicken farm isolates A1-A176. The switching frequencies for each isolate were measured twice, and the average switching frequency was calculated from the average of the two biological replicates.

Isolate	Switching frequency replicate 1	Switching frequency replicate 2	Average switching frequency
A1	2.018	4.984	3.501
A3	0.000	0.000	0.000
A5	0.000	0.032	-
A6	0.031	0.017	0.024
A7	0.021	0.020	0.021
A8	0.013	1.488	0.751
A9	0.388	0.614	0.501
A12	1.205	0.133	0.669
A13	0.022	0.043	0.032
A14	0.029	0.032	0.030
A15	0.209	0.478	0.344
A16	4.111	4.571	4.341
A18	0.558	0.048	0.303
A19	0.029	0.058	0.043
A20	8.634	7.559	8.097
A21	9.148	8.182	8.665
A22	0.019	0.148	0.084
A23	0.103	0.500	0.302
A24	3.902	3.288	3.595
A25	0.157	0.131	0.144
A26	0.107	0.021	0.064
A28	0.024	0.137	0.081
A29	0.162	0.065	0.114
A30	7.250	10.311	8.781
A31	1.493	2.086	1.789
A32	4.918	2.059	3.489
A33	1.917	1.059	1.488
A34	0.065	0.050	0.057
A37	1.041	0.524	0.782

A38	0.105	0.200	0.153
A39	50.880	42.483	46.681
A40	10.415	9.490	9.953
A41	17.551	13.677	15.614
A42	17.655	7.365	12.510
A43	37.600	40.571	39.086
A44	0.000	0.029	-
A45	0.035	0.179	0.107
A46	0.078	0.010	0.044
A47	0.222	0.011	0.117
A48	0.069	0.093	0.081
A49	0.240	0.306	0.273
A50	22.581	14.563	18.572
A51	0.028	0.283	0.155
A52	0.031	0.013	0.022
A53	0.367	26.609	13.488
A54	1.407	2.281	1.844
A56	0.050	0.017	0.034
A57	0.759	-	-
A58	0.029	0.045	0.037
A60	0.035	0.035	0.035
A61	0.038	0.020	0.029
A62	15.000	25.362	20.181
A63	0.164	0.209	0.187
A64	0.114	0.067	0.090
A65	0.277	0.114	0.195
A66	0.345	1.292	0.818
A67	1.120	0.636	0.878
A68	0.037	0.107	0.072
A69	1.411	6.167	3.789
A70	2.195	4.588	3.392
A71	8.968	8.762	8.865
A72	1.385	0.792	1.088
A73	-	-	-
A74	0.173	0.206	0.189
A75	0.045	0.963	0.504
A76	0.086	2.184	1.135
A77	0.102	0.240	0.171
A78	0.029	0.295	0.162

A79	0.267	-	-
A80	0.017	8.706	4.362
A81	0.082	0.114	0.098
A82	20.600	18.706	19.653
A83	0.028	0.079	0.053
A84	0.030	0.038	0.034
A85	29.306	22.310	25.808
A86	0.000	0.048	-
A87	0.044	0.480	0.262
A88	3.000	25.179	14.090
A89	0.432	0.896	0.664
A90	2.576	1.267	1.922
A92	0.014	0.018	0.016
A93	8.150	0.436	4.293
A94	0.160	0.596	0.378
A96	1.409	1.551	1.480
A97	0.115	2.535	1.325
A98	0.107	0.532	0.320
A100	0.080	0.100	0.090
A101	0.045	0.202	0.124
A102	24.078	17.878	20.978
A103	0.042	0.041	0.042
A104	0.068	0.019	0.043
A105	3.907	4.737	4.322
A106	10.179	23.784	16.981
A107	0.310	0.261	0.286
A108	0.274	0.098	0.186
A109	0.899	1.158	1.028
A110	0.015	0.024	0.020
A111	4.952	2.324	3.638
A112	8.389	0.286	4.337
A113	0.050	0.000	-
A114	4.571	3.860	4.216
A115	7.015	4.282	5.648
A116	9.333	5.559	7.446
A117	0.096	0.099	0.097
A118	1.017	0.508	0.763
A119	6.783	2.323	4.553
A120	0.486	0.020	0.253

A121	6.140	14.000	10.070
A122	0.038	0.182	0.110
A123	1.058	4.901	2.980
A124	0.796	0.000	-
A125	0.024	0.038	0.031
A126	15.088	4.000	9.544
A127	0.154	0.022	0.088
A128	0.429	0.025	0.227
A129	24.129	21.614	22.872
A130	0.306	0.309	0.307
A131	30.100	26.469	28.285
A132	0.018	0.014	0.016
A133	0.838	2.291	1.564
A134	0.089	0.058	0.074
A135	1.396	1.905	1.650
A136	17.882	6.330	12.106
A137	0.857	-	-
A138	2.425	-	-
A139	0.333	-	-
A140	0.456	0.671	0.563
A141	0.174	0.028	0.101
A142	1.590	0.385	0.988
A143	0.088	0.044	0.066
A145	10.240	24.000	17.120
A146	0.063	0.107	0.085
A147	21.833	12.500	17.167
A148	9.744	6.431	8.087
A149	6.923	5.511	6.217
A150	3.068	0.556	1.812
A151	0.000	0.136	-
A152	0.045	0.029	0.037
A153	0.547	1.885	1.216
A154	0.020	0.071	0.046
A155	0.074	3.415	1.744
A156	0.045	0.011	0.028
A157	0.038	0.023	0.031
A158	7.347	11.667	9.507
A159	0.178	-	-
A160	0.155	-	-

A161	0.033	-	-
A162	7.769	-	-
A163	6.380	-	-
A164	0.044	-	-
A165	0.333	-	-
A166	-	-	-
A167	0.032	-	-
A168	0.507	-	-
A169	20.750	-	-
A170	18.581	-	-
A171	0.013	-	-
A172	-	-	-
A173	10.222	-	-
A174	0.156	-	-
A175	0.067	-	-
A176	0.394	-	-

Shown in Figure 17 is a pie chart showing the distribution of the average switching frequencies of the 132 chicken farm isolates. The average switching frequency was determined by two biological replicates, not including the replicates with a frequency of 0 %. 75 (57 %) of the isolates were shown to have a switching frequency of 0 % or between 0 % and 1 %. 39 isolates (29 %) had a switching frequency between 1 % and 10 %, while the remaining 18 isolates (14 %) had a switching frequency above 10 %. Of the remaining isolates with a switching frequency from only one replicate, 21 isolates have a frequency of 0 % or between 0 % and 1 %, four isolates between 1 % and 10 %, and three isolates above 10 %. Including these data, 96 isolates (59 %) have a switching frequency of 0 % or between 0 % and 1 %, 43 isolates (27 %) have a switching frequency between 1 % and 10 %, while 21 isolates (13 %) have a switching frequency above 10 %.

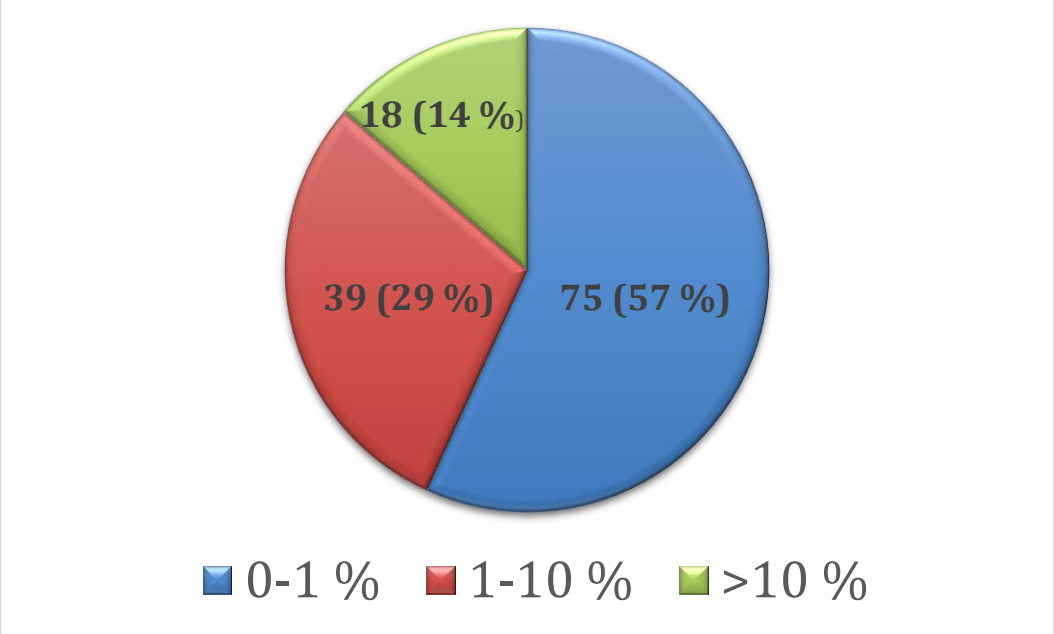

Figure 17. A pie chart of the 132 isolates having an average opaque to translucent switching frequency value from two replicates. The blue color represents the isolates having a switching frequency of 0 or between 0 and 1 %. The red color represents the isolates having a switching frequency between 1 and 10 %, while the green color represents the isolates having a switching frequency above 10 %. The number of isolates belonging to each color code are written in the chart with the percentage written in parentheses.

Whilst measuring the opaque to translucent switching frequencies of the chicken farm isolates, it was observed that several of the isolates displayed striking colony morphologies as shown in Figure 18. Originally, this was thought to be caused by some experimental error, however since this phenotype was observed for at least 11 isolates, it promoted a further investigation of the matter. Literature searched indicated that this could be some sort of *rugose* phenotype in *A. baumannii*, which is a phenotype characterized by yet another phase variable mechanism, and linked to biofilm formation and the cyclic-di-GMP network in some of the *Vibrio* species (Yildiz and Visick, 2009).

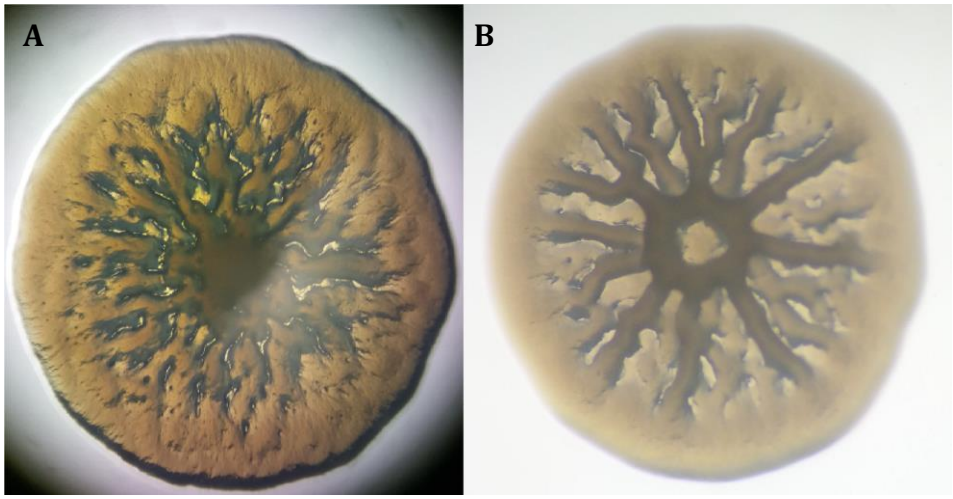

Figure 18. Possible *rugose* phenotype in (A) Isolate A7 and (B) Isolate A132.

4 Discussion

In this work, increased knowledge about strains of *A. baumannii* circulating outside the hospital environment in Norway have been acquired. Additionally, new insights about the phylogenetic relationships of environmental strains of the species have been gained. The findings in this work indicate both close and distant relationships between the chicken farm isolates found in Norway. From this work, there are no indications that chicken farms represent a reservoir for drug resistant *A. baumannii* at this point, which also fits with the knowledge of most multidrug resistant *A. baumannii* infections in Norway being a result of imported cases. Furthermore, the isolates were tested for their susceptibility against several clinically relevant antibiotics; however, it was determined that none of them were resistant against any of the agents tested for. In this work, for the first time, it is shown that non-clinical isolates of *A. baumannii* can switch from the opaque to translucent colony phase, and a broad mapping of switching frequencies.

4.1 The source of the bacteria

As described in the methods section (section 2.1), the *A. baumannii* isolates were collected by a sock sampling method which targets the litter of the chickens, thought to represent their intestinal environment. This method is commonly used by the Norwegian Veterinary Institute to detect the presence of *Salmonella* in chicken flocks, however when sampling for *Salmonella* spp. during 2016, *A. baumannii* was also detected during growth on McConkey agar. Consequently, the *A. baumannii* isolates were kept and stored. Given the nature of the sock sampling method, one cannot however know with absolute certainty that the litter is the only source of the bacteria sampled. Since boot swabs are used for sampling, other sources than the chicken litter may contribute to the bacteria sampled from the floors in the chicken farms. Such sources may include the food, or the water provided to the chickens, the soil brought in by shoes, farmers, veterinarians, or vermin. Therefore, the samples may be defined as environmental samples because the floor may contain bacteria from several sources. Considering that *A. baumannii* has been isolated previously from soil, water as well as the human normal flora, the fact that the bacteria may originate from other sources than the chickens themselves has to be taken into account (Dijkshoorn, Nemec and Seifert, 2007; Pailhoriès *et al.*, 2015; Rafei, Hamze, *et al.*, 2015; Wilharm *et al.*, 2017). Additionally, several of the previously known STs to which chicken farm isolates were mapped, have

previously been found in samples retrieved from water, humans, and other animals, which could to some extent indicate that not only the litter of the chickens may represent the origin of the bacteria.

4.2 Identifying *A. baumannii* chicken farm isolates by MALDI-TOF and *bla*$_{\text{OXA-51}}$

Differentiating species of *Acinetobacter* by phenotypic tests are difficult and unreliable, especially the species in the Acb complex (Seifert and Dijkshoorn, 2008). Rapid identification of *A. baumannii* can be done by both MALDI-TOF and *bla*$_{\text{OXA-51}}$ screening, however both methods suffers from difficulties in distinguishing the species within the Acb complex. The lack of reference spectra and the similar mass spectra between some species in the Acb complex, are some of the problems associated with MALDI-TOF. Furthermore, MALDI-TOF is only as good as the database that is used (Espinal *et al.*, 2012; Šedo *et al.*, 2013; van der Kolk *et al.*, 2019). Detection of *bla*$_{\text{OXA-51-like}}$ genes in non-*A. baumannii* species, makes screening for *bla*$_{\text{OXA-51}}$ somewhat unreliable on its own (Zander *et al.*, 2013). Additionally, disruption of the *bla*$_{\text{OXA-51}}$ gene by IS sequences have also been reported (Lee *et al.*, 2012; Zander *et al.*, 2013). A combination of these two methods gives increased reliability and specificity, verified by the MLST mapping.

Out of the 200 *A. baumannii* isolates retrieved, all of which were identified by MALDI-TOF, 180 (90 %) tested positive for *bla*$_{\text{OXA-51}}$. The *bla*$_{\text{OXA-51}}$ screening supports earlier findings and indicates, that MALDI-TOF by itself is probably not a sufficiently specific method to be used in isolation for accurately identifying *A. baumannii*. Species determination of the 20 isolates that failed the *bla*$_{\text{OXA-51}}$ PCR screening will be necessary to fully confirm this finding. A BLAST search with all the *rpoB* sequences for the chicken farm isolates revealed that the closest match was *A. baumannii* (results not shown), and the MLST mapping confirmed that all 180 isolates were indeed *A. baumannii*. One of the *rpoB* BLAST matches was indicated to be *A. calcoaceticus* NCTC7364, however this isolate is now known as *A. baumannii* NCTC7364. For five of the isolates that were not *bla*$_{\text{OXA-51}}$ positive, sequencing was performed of the *gltA* and *pyrG* genes to confirm that they were not in fact *A. baumannii* (done by PhD candidate Claus Michael Goul Larsen). The subsequent BLAST search revealed that they were not *A. baumannii*, the closest match being either *A. nosocomialis* or *A. pittii* (results not shown). The results discussed here strongly suggest that combining

MALDI-TOF with *bla*$_{OXA-51}$ screening provides identification *A. baumannii*. However, since the *rpoB* gene was included for the MLST mapping, one may in retrospect also have considered replacing the *bla*$_{OXA-51}$ screening by sequencing of the *rpoB* gene to verify the species identification done by MALDI-TOF. This requires however that the first step with MALDI identification is done with reasonable accuracy.

4.3 Chicken farms as a possible clinical reservoir of *A. baumannii*

The MLST data analysis identified 36 new and 18 previously existing STs among the 170 isolates analyzed (Table 7 and 8). The identification of several new STs in this study was expected, as most studies on *A. baumannii* have focused on clinical isolates. Consequently, the pubMLST database will most probably be biased towards having more STs from clinical samples. Among the isolates in the current study, 76 % (n = 129) belonged to newly identified STs, indicating that other sources than patient samples and the hospital environment may contain a rather big pool of unidentified STs. To avoid this bias, more studies should focus on using a One Health approach for *A. baumannii* in the future, such as focusing on animals isolates and/or environmental isolates, not only looking in on the hospital setting. This in return might give more insight and broaden our knowledge into the natural habitats and the potential reservoirs of *A. baumannii*. Furthermore, it will contribute to an improved understanding of the population evolution of this clinically important bacterium.

Overall, most STs found in this work did not exhibit close relationship to each other. However, five small clonal complexes containing related STs were found (Figure 11). Among the five clonal complexes, three consisted of entirely new STs while the other two consisted of pre-existing STs. The clonal complex consisting of ST46, ST149 and ST1032 might be a novel clonal complex in the phylogeny of *A. baumannii* (Shrestha et al., 2015). ST46 has been identified in clinical samples from both China, the Czech Republic and Lebanon (Rafei, Pailhoriès, *et al.*, 2015). Similarly, ST149 has been identified in clinical samples from Japan and Nepal (Shrestha *et al.*, 2015). ST1032 has only been identified once previously, in Germany in an animal sample. Shrestha et al. (2015) indicated that the complex might be a novel complex in Asia, however as seen in this work it may occur elsewhere as well. When these STs were examined in greater detail using the STs in the *A.*

baumannii database, a larger clonal complex emerged (Figure 19). As indicated by Shrestha et al. (2015), this complex is a novel clonal complex of *A. baumannii*, and a larger complex seems to be developing from these STs. However, ST149 is not the central ST in this clonal complex and should therefore probably not be named CC149 as Shrestha *et al.* (2015) suggested. Instead ST46 seem to be the central founder, and the complex should thus for the future be named CC46 (Figure 19).

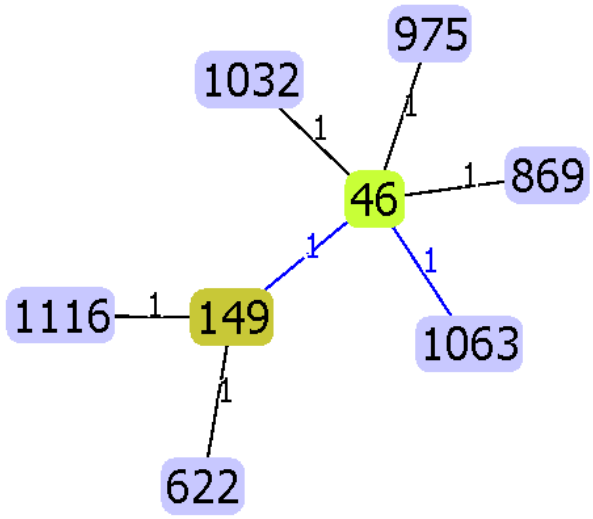

Figure 19: Clonal complex 46 consisting of ST46, ST149, ST622, ST869, ST975, ST1032, ST1063 and ST1116. The light green node represents the current probable founder of the clonal complex (ST46). The dark green node represents the current sub-group founder of the clonal complex (ST149). The light blue nodes represent common nodes. The number between the different STs indicate the number of allelic differences. The blue lines indicate a tie for the position as the founder of the clonal complex. In the case of a tie, the founder becomes the ST with greater number of single locus variants, double locus variants, and triple locus variants. The clonal complex was identified using the goeBURST algorithm with the criterion of SLVs in PHYLOViZ 2.0. The figure was made from the publicly available data on the pubMLST database (as of 24.04.2020).

Interestingly, when analyzing the UPGMA dendrogram in Figure 12, three of the five clonal complexes were observed to cluster together to form a big clade. Such a connection was not seen with the MST. Even more interesting is that ST923 seems to be one of the central founders of this clade. This ST was originally identified in a white stork from Poland (Wilharm *et al.*, 2017). Among the three registered isolates within this ST in the pubMLST database, two are isolated from birds while isolate A166B from Australia is a human clinical isolate. When examining the clonal complex, consisting of ST602 and ST923, in more detail using the pubMLST database, a fascinating pattern was seen (Figure 20). All the STs in this complex, except for ST877 for which there is no information about the source, contain isolates that have either been isolated directly or indirectly from birds. This is interesting since it has been speculated that *A. baumannii* may be carried by birds (including chickens),

as this species readily grows at the body temperatures of birds (Wilharm *et al.*, 2017). More studies are however needed to further investigate this hypothesis.

Compared to the results of the MST analysis shown in Figure 10, the clonal complex shown in Figure 20 contains ST821, which seems to be the missing ST which connects ST923 with ST1357. In this study ST821 was not identified among the chicken farm isolates, however the analysis indicates that ST923 and ST1357 are relatively closely related despite having two allelic mismatches when compared to each other. Furthermore, ST1357, which was identified in this work, seems to be the founder of this group. The identification of this ST within this work caused several of the STs seen in Figure 20 to be linked. This demonstrates that isolating samples from other sources than the clinic contributes to an improved understanding of the population evolution of *A. baumannii*.

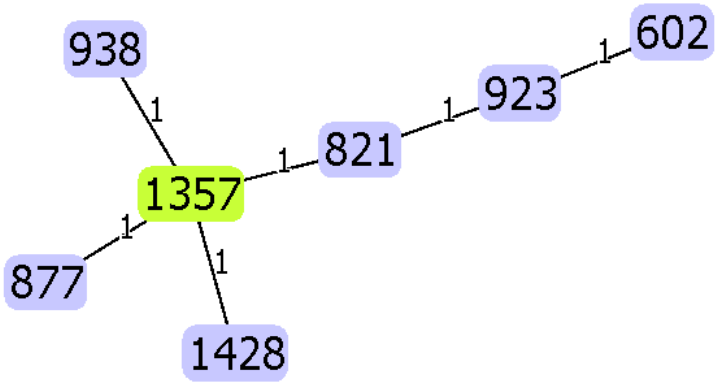

Figure 20: Clonal complex 1357 consisting of ST602, ST821, ST877, ST923, ST938, ST1357, and ST1428. The light green node represents the current founder of the clonal complex (ST1357). The light blue nodes represent common nodes. The number between the different STs indicate the number of allelic differences. The clonal complex was identified using the goeBURST algorithm with the criterion of SLVs in PHYLOViZ 2.0. The figure was made from the publicly available data on the pubMLST database (as of 24.04.2020).

In addition to making the dendrogram containing only the chicken farm isolates, a dendrogram was made including the central STs of the international clonal lineages (Figure 13). These were included to see if any of the chicken farm isolates could in theory be related to the lineages harboring MDR isolates. As it turned out, IC8 (ST10) showed to be, potentially, very close to both ST575 and ST1370 (Figure 13). Strikingly, when in a separate study analyzing clinical samples of non-MDR *A. baumannii* collected from patients in Norwegian hospitals and originating from the same time period as when the chicken farm isolates were sampled, a clinical sample with ST10 (IC8) was identified (PhD candidate Claus Michael Goul Larsen (UiO); personal communication, April 14, 2020). However, we

do not know if these isolates containing these STs are clonal even if the evidence indicate a close relationship. On the other hand, discovering that these STs are present in Norway, and that there seems to be a connection between them based on the MLST, one may speculate that the chicken farms may be a reservoir of clinical isolates. Future whole genome sequencing and comparative genomic analysis of the isolates containing belonging to these STs, will reveal their degree of genomic similarity. A clinical sample with ST25 (IC7) was also identified, however this ST was predicted not to have any close relationship to the chicken farm isolates (Figure 13). It is worth mentioning that none of the human clinical isolates mentioned above had any STs that overlapped with the STs for the chicken farm isolates identified in the current work.

To further speculate on the topic that chicken farms may be a reservoir of clinical isolates, one of the clinical samples from one of the Norwegian hospitals was found to belong to ST388 (PhD candidate Claus Michael Goul Larsen (UiO); personal communication, April 22, 2020). Interestingly, according to the literature, this ST has been found in water samples recovered from eviscerators from a German poultry slaughterhouse (Savin *et al.*, 2019). Furthermore, Wilharm *et al.* (2017) identified a close relationship between one of their chicken isolates and a clinical isolate from China assoicated with MDR. Both these isolates belong to ST23, which is an SLV of ST10 and a double locus variant (DLV) of ST1370 (Figure 21). Thus, previous data further connect the STs found in this work with STs that are associated with chicken farms in Germany and a clinical isolate from China.

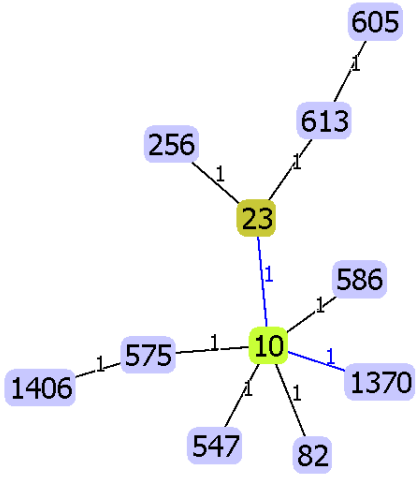

Figure 21: Clonal complex 10 consisting of ST10, ST23, ST82, ST256, ST575, ST586, ST605, ST613, ST1370 and ST1406. The light green node represents the current founder of the clonal complex (ST10). The dark green node represents the current sub-group founder of the clonal complex (ST23). The light blue nodes represent common nodes. The number between the different STs indicate the number of allelic differences. The blue lines indicate a tie for the position as the founder of the clonal complex. In the case of a tie, the founder becomes the ST with greater number of single locus variants, double locus variants, and triple locus variants. The clonal

complex was identified using the goeBURST algorithm with the criterion of SLVs in PHYLOViZ 2.0. The figure was made from the publicly available data on the pubMLST database (as of 24.04.2020).

Wilharm *et al.* (2017) further discovered in their earlier study that several of the avian isolates in their work were highly diverse and did not form a distinct clade within the phylogeny of *A. baumannii*. This may also be the true for the chicken farm isolates from Norway since many different clades are formed in the dendrograms, and the different clades have different relationships to the international clones (Figures 12 and 13). Additionally, few close relationships are seen between the STs for the chicken farm isolates. A large-scale whole genome sequencing project and comparative genomics analyses would however be needed to provide the best resolution to make the best possible conclusions about the diversity of the chicken farm isolates.

The obvious weakness with the regular MLST approach is that the relatedness of the isolates is only based on seven genes. This allows the isolates to only be assigned to lineages or to clonal complexes. However, the genes used are housekeeping genes, which are rather conserved, but do not reveal anything about the diversity within the different genomes of the isolates. Consequently, MLST does not provide the best resolution for determining the exact relationship between isolates. Therefore, some isolates that be may considered close and assigned to the same clonal complex, could be more distantly related when analyzing relationships in more detail. To circumvent this problem however, one could perform ribosomal MLST (rMLST) or sequence the core genome of the isolates (core genome; cgMLST) to better determine the relationship between the isolates (Maiden *et al.*, 2013). Ribosomal MLST can determine the genealogical relationships down to the strain level, while cgMLST can determine bacterial relationships down to the level of single clones (Maiden *et al.*, 2013). Nevertheless, since sequencing can be very costly, especially for many isolates, rMLST or cgMLST was not performed within this work.

Out of the known STs identified in this work, ST138, ST155, ST285, ST923 and ST961 have been found both in the clinic and in animals. This is interesting as it further associates some of the STs which have been found in among clinical isolates with STs found outside the hospital setting. Furthermore, ST149, ST150, ST154, ST575, ST602, ST608 and ST1222 which have only been found in the clinic, is now through the current study associated with the environment of chicken farms. Additionally, ST46 which has been found in biogas

isolates as well as in the clinic, is now associated with the environment of chickens. These findings altogether further suggest that there is a link between the STs found in the hospital and the STs found in animals and the environment.

4.4 None of the *A. baumannii* chicken farm isolates were resistant to the clinically relevant antibiotics tested

None of the chicken farm isolates were found to be resistant to neither carbapenems nor any of other antibiotics tested for. The disc diffusion initially indicated that some of the isolates were resistant to tobramycin (TOB) and gentamicin (GEN), however the broth microdilution method verified that they were in fact not resistant to these agents.

As observed in Table 9 and Figure 15, the R category for TOB and GEN for the disc diffusion was defined as having a zone of inhibition with a diameter below 17 mm. The isolates being defined as resistant only had a diameter one or two mm below the clinical and ECOFF breakpoint. Measuring the zone of inhibition can be an error-prone process, and such errors may cause the difference in defining the isolates as either susceptible or resistant. However, despite these errors, one may question the concept of breakpoints. Is it feasible to define bacteria into either of two categories, susceptible or resistant? Potentially not. In the clinic this surely provides vitally important information guiding choice of therapy, since clinical isolates show a lot of variation in their resistance patterns. A range of different values for the diameters for the zones of inhibition was observed for the chicken farm isolates. For *A. baumannii*, the differential expression of the intrinsic $bla_{\text{OXA-51}}$ gene may lead one isolate into being "more resistant" towards carbapenems than others, causing the different isolates to fall into the same category. For imipenem, the diameters for the chicken farm isolates were in the range of 23 - 40 mm (Figure 15). The difference in having a diameter of 40 mm compared to 23 mm is large, however, the isolates having these diameters fall into the same category, being susceptible. Nonetheless, one would assume that the isolate having a zone diameter of 23 mm would be "more resistant" towards imipenem than the isolate with a diameter of 40 mm. This could be caused, as mentioned above, by the differential expression of $bla_{\text{OXA-51}}$ alone, or by additional bla_{OXA} genes.

For ceftazidime there are currently no data on the zone diameters for the disc diffusion method for *A. baumannii* when using 10 µg ceftazidime disks. Because of this, it could not be

determined if these isolates are clinically susceptible nor resistant towards this antibiotic. At the same time, according to EUCAST susceptibility testing of *Acinetobacter spp.* to penicillins is unreliable (EUCAST, 2020a, 2020b). Consequently, it is assumed that most *Acinetobacter spp.* are resistant towards penicillins and cephalosporins. The reason for this is because of the low permeability of the outer-membrane and the presence of several intrinsic mechanisms towards β-lactams. For *A. baumannii* this includes the production β-lactamases such as AmpC and OXA proteins, absence of large porins in the outer membrane, and the efflux pump AdeABC (Van Looveren *et al.*, 2004; Perez *et al.*, 2007; Peleg, Seifert and Paterson, 2008; Zahn *et al.*, 2016). However, as mentioned before, the *Acinetobacter* community is heavily biased towards clinical isolates. Thus, what might be considered intrinsic in clinical isolates may possibly not be intrinsic in non-clinical strains. One might expect that several of the genes conferring β-lactam resistance will be intrinsic to the species, however this does not explain the inconsistent detection of the *AdeABC* pump, as will be discussed in the next section.

To verify and extend the results from the disc diffusion testing, the broth microdilution method was used to test for resistance towards TOB and GEN. This method verified that none of the chicken farm isolates are resistant towards these antibiotics. The MIC values identified were either 2 μg/mL, 4 μg/mL or somewhere between. As all MIC values ≤4 μg/mL are regarded as susceptible for both TOB and GEN, none were defined as clinically resistant. However, every isolate had a close MIC value compared to the R breakpoint. One intriguing question is then why is that so? Could for instance all the isolates express the AdeABC pump causing intrinsic resistance to both aminoglycosides? In a study by Huys et al. (2005), the authors stated that when trying to amplify the *adeB* gene in 32 environmental isolates of *A. baumannii*, it was found that none of these strains harbored this gene, possibly indicating the absence of the *AdeABC* pump in these isolates – although the authors stated that this needs to be investigated further in more extended strain collections to obtain more insight of the distribution of *adeB* (Huys *et al.*, 2005). Furthermore, the evidence presented was based on PCR which on its own may not be the most reliable method to show this. Bad primer design or wrong annealing temperatures may give false negatives. Even in clinical isolates the detection rate of either *adeA, adeB* and *adeC* by PCR is inconsistent (Coyne, Courvalin and Périchon, 2011; Xu, Bilya and Xu, 2019). Thus, one may wonder if the *AdeABC* pump is intrinsic or not to *A. baumannii*. If the AdeABC pump does not cause the

elevated MIC seen for the chicken farm isolates, other contributing factors may yet remain to be characterized.

As antibiotic growth promoters (AGPs) are phased out of use in Norway, and considering the strict regulations of antibiotic usage (NORM, 2019), it was perhaps not surprising to discover that none of the isolates from the chicken farm environment were clinically resistant. Likewise, Wilharm *et al.* (2017) did generally not find their chicken isolates to be resistant either, except for two isolates displaying resistance to kanamycin and gentamicin. None of their isolates displayed resistance towards ciprofloxacin or meropenem. The data presented here cannot be directly compared with the data of Wilharm *et al.* (2017), since we do not conclusively know if our isolates originate from the chicken themselves (although sampling method targets the chicken litter) or if contributions are made by contaminants from other sources in the chicken farm.

4.5 The chicken farm isolates can switch from the opaque to translucent colony phase

To date, phase variation in *A. baumannii* has only been shown to be present in clinical isolates (Tipton, Dimitrova and Rather, 2015; Ahmad et al., 2019). However, in this work it has been demonstrated that non-clinical isolates of *A. baumannii* are also able to switch from the opaque to the translucent phenotype (all isolates tested except for isolate A3).

For the modified protocol of phase variation, which was used in this work, it was decided that liquid cultures were to be incubated for 48 hours and that LB plates were to be incubated for approximately 24 hours. Only after 24 hours and 48 hours preculture, was switching from opaque to translucent colonies detected for all the isolates (following plating and colony growth), except for ATCC17978. However, to increase the chance of detecting low frequency switching from opaque to translucent phase, the timepoint chosen, was after 48 hours of preculture of the liquid cultures. Furthermore, as colony density seem to be a factor determining the switching frequency, having a rather high optical density was also important (Tipton, Dimitrova and Rather, 2015). This was achieved with the timepoint chosen.

LB plates were used in this study, instead of 0.5X LB plates. 0.5X LB plates were used in the original protocol, however switching from opaque to translucent colony morphology was in

our hands not as easily observable on 0.5X LB plates compared to regular LB. This is not in agreement with Tipton, Dimitrova and Rather (2015) which stated that both could be used to detect phase variation but that it was easier to observe phase variation for 0.5X LB plates. Regular LB plates were used within this work, mainly because it was easier to detect the switching frequency and since the choice of growth medium after plating did not seem to have a major effect on switching frequencies (Table 14 and 15). LB plates were only incubated for 24 hours, such that the protocol used did not differ too much from the original protocol. Also, no major difference was observed in switching frequencies when incubating the LB plates for additional days (Table 14 and 15).

In sum, the major differences between the original protocol and the modified protocol used in this work are: the incubation time (which was 48 hours for the protocol in this work), the type of LB plates used and that the switching frequencies back from translucent to opaque were not determined. Since there are data available on the switching frequency of *A. baumannii* AB5075, it would be interesting to compare the previously determined switching frequency of that strain to those achieved with the protocol used in this work. Due to the SARS-CoV-2 pandemic I was however not able to perform this experiment, due to lab shutdown.

In this work, it was shown that different isolates possess highly different switching frequencies ranging from 0-51 % (Table 16). Even more intriguing is that in the pilot study whilst trying to establish a modified protocol of phase variation for the chicken farm isolates, it was shown that the reference strain ATCC17978 was not able to switch from the opaque to the translucent variant. This corresponds well with the results from Tipton, Dimitrova and Rather (2015) who could not detect phase variation in *A. baumannii* ATCC17978. This strain was already isolated in the 1950s, and potentially, this strain may have lost the ability to undergo phase variation because of numerous *in vitro* passages in the laboratory (strain domestication). This may have caused several genetic alterations in the genome of this strain, causing it to lose its ability to undergo phase variation (Fux *et al.*, 2005). A second possibility is that the difference of the opaque and translucent phenotype is too subtle to detect, or that switching frequencies are very low, beyond the resolution of our assay (Tipton, Dimitrova and Rather, 2015).

As there are few articles in the literature about phase variation in *A. baumannii*, there are not much data available about the switching frequencies. The first paper reporting on the phase

variation phenomenon states that the switching frequency (opaque to translucent) of several clinical isolates were found to be in the range of 0.001 % to 1 % (Tipton, Dimitrova and Rather, 2015). On the other hand, the switching frequency (opaque to translucent) of *A. baumannii* AB5075 was determined to be 6.22 ± 2.9 % (Pérez-Varela *et al.*, 2020). Furthermore, Ahmad *et al.* (2019) have reported switching frequencies (opaque to translucent) from between 0 and 10 % for their clinical isolates. Isolate A100 in their study had the highest switching frequency of 8.02 ± 1.90 %, while the lowest switching frequency was 0.05 ± 0.02 %. Taken together, as most of the chicken farm isolates do have a switching frequency between 0 and 10 %, the data presented in this work is consistent with earlier findings.

Demonstrating that environmental isolates of *A. baumannii* are also capable of switching from the opaque- to translucent phenotype, this mechanism is clearly also present in environmental isolates of this species. More work should be done to try to establish a universal protocol for phase variation. If this is not possible, perhaps two protocols should be established, one for detecting low switching frequencies and one for detecting high switching frequencies. As many isolates of *A. baumannii* may have low switching frequencies, as demonstrated here, a protocol like the one established in this work may be needed. The weakness however with the current protocol (this work) is that several thousands of colonies are needed to be screened to exactly determine the switching frequency. This is ideal if one can easily distinguish the colonies from one another but is not always sufficiently processive under a stereo microscope. One way to circumvent this challenge may be to use larger petri dishes, to ensure that the bacteria are evenly spread on the LB plates such that the colonies might be more easily distinguished. In addition, several dilutions could also be plated out such that isolates with high switching frequencies are easier to determine.

While measuring the opaque to translucent switching frequencies of the chicken farm isolates, a striking colony morphology was identified (Figure 18). A collaborator suggested that this might be some form of *rugose* phenotype, which is also found in other bacteria (Associate Professor Roger Simm (UiO); personal communication, February 8, 2020). Upon further investigation and literature comparisons, similarities were seen with the species of the genus *Vibrio* (Yildiz and Visick, 2009). In fact, just like *A. baumannii*, the species of *Vibrio parahaemolyticus* and *Vibrio vulnificus* can undergo a reversible phase variation between opaque and translucent colony morphologies. Moreover, these species are also able to switch

from smooth to the *rugose* colony morphology in addition to the phase variable mechanism of the opaque and translucent phenotypes. In contrast, the related species of *Vibrio cholerae* is only able to switch between smooth and *rugose* colony morphotypes (Yildiz and Visick, 2009). Furthermore, a recent study in Scientific Reports identified that a cyclic-di-GMP network is present in *A. baumannii* (Ahmad *et al.*, 2020). This finding is interesting because a single nucleotide change in the diguanylate cyclase gene *vpvC* in *V. cholerae* has been associated with the generation of the *rugose* phenotype by elevated cyclic-di-GMP levels. Disruption of the *vpvC* gene reduced the cyclic-di-GMP levels and caused the cells to display the smooth variant (Beyhan and Yildiz, 2007). Likewise, in *V. vulnificus*, the presence and expression of the diguanylate cyclase DcpA in several strains caused the formation of the *rugose* phenotype (Nakhamchik, Wilde and Rowe-Magnus, 2008).

As both STs and switching frequency of opaque- to translucent colonies were determined for the chicken farm isolates, a question for future systematic analysis could be to investigate whether there could be a connection between STs and average switching frequencies. For ST1369, the switching frequency was in the range of 0.016 – 0.818 % except for two isolates having a frequency of 4.337 % and 9.544 %. On the other hand, for ST1370, the switching frequency was in the range of 16.981 – 28.285 % except for one isolate having a frequency of 4.216 %. ST154, ST1356 and ST1371 had a switching frequency in the range of 0.097 – 1.744 %, 0.162 – 1.325 % and 0.03 – 0.664 %, respectively. As these STs are some of the major STs found in this work, there may potentially be a connection between the STs and the range of the average switching frequency. In contrast, however, isolates within ST1354 varied quite substantially in switching frequencies, from 0,988 % to 19,653 %, showing that switching frequencies are not universally linked within an ST.

4.6 Concluding remarks and future perspectives

In this work, it has been demonstrated that Norwegian chicken farms harbor the opportunistic pathogen *A. baumannii*. Since previous studies have shown that *A. baumannii* have been isolated from sewage water from a chicken slaughterhouse, raw chicken meat and live chickens, this was perhaps not highly surprising (Lupo *et al.*, 2014; Wilharm *et al.*, 2017; Savin *et al.*, 2019). A possible connection between some of the chicken farm isolates and a non-MDR clinical isolate from a Norwegian hospital was established. One can therefore not exclude previous findings, indicating the dissemination of *A. baumannii* from chicken farms

with possible consequences for the general public health (Lupo *et al.*, 2014; Wilharm *et al.*, 2017). Any firm conclusion would require whole genome sequencing of the isolates, which is currently ongoing. A subselection of the chicken farm isolates and all the non-MDR clinical samples are currently being sequenced. Norwegian chicken farms do however not seem to contain carbapenem resistant *A. baumannii*, to the extent detectable by the current sampling scheme, nor isolates with clinical resistance to other drugs tested in this study. The prevalence of *A. baumannii* in chickens and in food production should however be investigated further, such that the role of chickens and chicken farms can be better understood as a role as an environmental or animal reservoir, and potentially in the ecology and dissemination of *A. baumannii*. Furthermore, this should not only be limited to chickens, but other livestock animals as well. Increasing evidence internationally indicates that there may be a connection between the *A. baumannii* isolates found in hospitals and isolates found in animals and the environment. Future studies should investigate and address this by using a One Health approach, in order to get more insight into this matter. This can e.g. be done by implementing and integrating the One Health approach into surveillance systems such that livestock animals and the environment can be sampled more frequently for *A. baumannii*. Alternatively, studies can be designed such that both clinical isolates and animal and/or environmental isolates are sampled in the same period.

Almost all the chicken farm isolates were able to switch from the opaque- to translucent colony phase, strongly suggesting that phase variation is present in non-clinical isolates and that phase variation may be an intrinsic phenomenon to (undomesticated isolates of) the species. In future studies it will be of important to further elucidate what function this mechanism has in *A. baumannii* biology, to determine what role it has outside the hospital environment, and to further determine how this mechanism contributes to the persistence of this pathogen in different environments. Additionally, the chicken farm isolates should be examined for their ability to switch back from translucent- to opaque colonies as well, to confirm that true phase variation is present in these isolates. Further optimization of the protocol might also be required. As phase variation has been shown to be present in *A. baumannii*, it would also be possible to investigate other closely related species of *A. baumannii* to see if they possess this mechanism. Finally, further investigation into the possible *rugose* phenotype of *A. baumannii* should be continued. This phenotype was observed for several of the chicken farm isolates, potentially indicating that another mechanism of phenotype switching may be present in *A. baumannii*. Since other Gram-

negative bacteria such as *Vibrio* species possess both the smooth to *rugose* transition and the opaque to translucent phase variable mechanism, it does not seem unlikely that this may also be the case for *A. baumannii* as well (Yildiz and Visick, 2009). Additionally, the cyclic-di-GMP system seem to be connected to the switching of the smooth to the *rugose* colony morphology in some of the *Vibrio* species (Beyhan and Yildiz, 2007; Nakhamchik, Wilde and Rowe-Magnus, 2008). The finding that this system is also present in *A. baumannii* and its connection to the smooth to *rugose* phase variable mechanism in some of the species of *Vibrio,* further suggests that this mechanism may exist in *A. baumannii*. Since the *rugose* phenotype has not been reported in the literature before for *A. baumannii*, further investigation into its molecular regulation would most likely bring new important biological insights for the species.

References

Abhari, S. S. *et al.* (2019) 'Circulation of imipenem-resistant *Acinetobacter baumannii* ST10, ST2 and ST3 in a university teaching hospital from Tehran, Iran', *Journal of Medical Microbiology*, 68(6), pp. 860–865. doi: 10.1099/jmm.0.000987.

Abraham, E. P. and Chain, E. (1940) 'An Enzyme from Bacteria able to Destroy Penicillin', *Nature*, 146(837). doi: 10.1038/146837a0.

Ahmad, I. *et al.* (2019) 'Analysis of colony phase variation switch in *Acinetobacter baumannii* clinical isolates', *PLoS ONE*, 14(1). doi: 10.1371/journal.pone.0210082.

Ahmad, I. *et al.* (2020) 'A Cyclic-di-GMP signalling network regulates biofilm formation and surface associated motility of *Acinetobacter baumannii* 17978', *Scientific Reports*, 10(1991). doi: 10.1038/s41598-020-58522-5.

American Veterinary Medical Association (2008) *One health: A new professional imperative*. Available at: https://www.avma.org/sites/default/files/resources/onehealth_final.pdf (Accessed: 10 January 2020).

Anderson, S. E. and Rather, P. N. (2019) 'Distinguishing Colony Opacity Variants and Measuring Opacity Variation in *Acinetobacter baumannii*', in *Acinetobacter Baumannii: Methods and Protocols*. New York, NY: Humana Press, pp. 151–157. doi: 10.1007/978-1-4939-9118-1_14.

Atrouni, A. Al *et al.* (2016) 'Reservoirs of non-baumannii *Acinetobacter* species', *Frontiers in Microbiology*, 7(49). doi: 10.3389/fmicb.2016.00049.

Baumann, P., Doudoroff, M. and Stanier, R. Y. (1968) 'A Study of the *Moraxella* Group II. Oxidase-negative Species (Genus *Acinetobacter*)', *Journal of bacteriology*, 95(5), pp. 1520–1541.

Beyhan, S. and Yildiz, F. H. (2007) 'Smooth to rugose phase variation in *Vibrio cholerae*

can be mediated by a single nucleotide change that targets c-di-GMP signalling pathway', *Molecular Microbiology*, 63(4), pp. 995–1007. doi: 10.1111/j.1365-2958.2006.05568.x.

Bonnin, R. A., Nordmann, P. and Poirel, L. (2013) 'Screening and deciphering antibiotic resistance in *Acinetobacter baumannii*: A state of the art', *Expert Review of Anti-Infective Therapy*, 11(6), pp. 571–583. doi: 10.1586/eri.13.38.

Bouvet, P. J. M. and Grimont, P. A. D. (1986) 'Taxonomy of the Genus *Acinetobacter* with the Recognition of *Acinetobacter baumannii* sp. nov. *Acinetobacter haemolyticus* sp. nov. *Acinetobacter johnsonii* sp. nov. and *Acinetobacter junii* sp. nov. and Emended Descriptions of *Acinetobacter calcoaceticus* and ', *International Journal of Systematic Bacteriology*, 36(2), pp. 228–240. doi: 10.1099/00207713-36-2-228.

Brundtland, G. H. (2003) *Dr Brundtland's speech to the International Conference on Public Health*. Available at: https://www.who.int/dg/brundtland/speeches/2003/bergen/en/ (Accessed: 13 January 2020).

Calistri, P. *et al.* (2013) 'The Components of "One World - One Health" Approach', *Transboundary and Emerging Diseases*, 60(s2), pp. 4–13. doi: 10.1111/tbed.12145.

Cantas, L. and Suer, K. (2014) 'Review: The important bacterial zoonoses in "One Health" concept', *Frontiers in Public Health*, 2(144). doi: 10.3389/fpubh.2014.00144.

Cerezales, M. *et al.* (2019) '*Acinetobacter baumannii* analysis by core genome multi-locus sequence typing in two hospitals in Bolivia: endemicity of international clone 7 isolates (CC25)', *International Journal of Antimicrobial Agents*, 53(6), pp. 844–849. doi: 10.1016/j.ijantimicag.2019.03.019.

Chin, C. Y. *et al.* (2018) 'A high-frequency phenotypic switch links bacterial virulence and environmental survival in *Acinetobacter baumannii*', *Nature Microbiology*, 3(5), pp. 563–569. doi: 10.1038/s41564-018-0151-5.

Cogliani, C., Goossens, H. and Greko, C. (2011) 'Restricting antimicrobial use in food animals: Lessons from Europe', *Microbe*, 6(6), pp. 274–279. doi: 10.1128/microbe.6.274.1.

Cosgaya, C. *et al.* (2016) '*Acinetobacter dijkshoorniae* sp. Nov., a member of the *Acinetobacter calcoaceticus–Acinetobacter baumannii* complex mainly recovered from clinical samples in different countries', *International Journal of Systematic and Evolutionary Microbiology*, 66(10), pp. 4105–4111. doi: 10.1099/ijsem.0.001318.

Coyne, S., Courvalin, P. and Périchon, B. (2011) 'Efflux-mediated antibiotic resistance in *Acinetobacter spp.*', *Antimicrobial Agents and Chemotherapy*, 55(3), pp. 947–953. doi: 10.1128/AAC.01388-10.

Diancourt, L. *et al.* (2010) 'The population structure of *Acinetobacter baumannii*: Expanding multiresistant clones from an ancestral susceptible genetic pool', *PLoS ONE*, 5(4). doi: 10.1371/journal.pone.0010034.

Dijkshoorn, L., Nemec, A. and Seifert, H. (2007) 'An increasing threat in hospitals: Multidrug-resistant *Acinetobacter baumannii*', *Nature Reviews Microbiology*, 5(12), pp. 939–951. doi: 10.1038/nrmicro1789.

Doi, Y., Murray, G. and Peleg, A. (2015) '*Acinetobacter baumannii*: Evolution of Antimicrobial Resistance—Treatment Options', *Seminars in Respiratory and Critical Care Medicine*, 36(01), pp. 085–098. doi: 10.1055/s-0034-1398388.

Doughari, H. J. *et al.* (2011) 'The ecology, biology and pathogenesis of *Acinetobacter* spp.: An overview', *Microbes and Environments*, 26(2), pp. 101–112. doi: 10.1264/jsme2.ME10179.

Dunlap, C. A. and Rooney, A. P. (2018) '*Acinetobacter dijkshoorniae* is a later heterotypic synonym of *Acinetobacter lactucae*', *International Journal of Systematic and Evolutionary Microbiology*, 68(1), pp. 131–132. doi: 10.1099/ijsem.0.002470.

Espinal, P. *et al.* (2012) 'Rapid and accurate identification of genomic species from the *Acinetobacter baumannii* (Ab) group by MALDI-TOF MS', *Clinical Microbiology and Infection*, 18(11), pp. 1097–1103. doi: 10.1111/j.1469-0691.2011.03696.x.

EUCAST (2020a) *Breakpoint tables for interpretation of MICs and zone diameters version 10.0*. Available at: https://www.eucast.org/fileadmin/src/media/PDFs/EUCAST_files/Breakpoint_tables/v_10.0_Breakpoint_Tables.pdf (Accessed: 25 March 2020).

EUCAST (2020b) *Intrinsic Resistance and Unusual Phenotypes version 3.2*. Available at: https://www.eucast.org/fileadmin/src/media/PDFs/EUCAST_files/Expert_Rules/2020/Intrinsic_Resistance_and_Unusual_Phenotypes_Tables_v3.2_20200225.pdf (Accessed: 1 June 2020).

Feil, E. J. *et al.* (2004) 'eBURST: Inferring Patterns of Evolutionary Descent among Clusters of Related Bacterial Genotypes from Multilocus Sequence Typing Data', *Journal of Bacteriology*, 186(5), pp. 1518–1530. doi: 10.1128/JB.186.5.1518-1530.2004.

Francisco, A. P. *et al.* (2009) 'Global optimal eBURST analysis of multilocus typing data using a graphic matroid approach', *BMC Bioinformatics*, 10(152). doi: 10.1186/1471-2105-10-152.

Fux, C. A. *et al.* (2005) 'Can laboratory reference strains mirror "real-world" pathogenesis?', *Trends in Microbiology*, 13(2), pp. 58–63. doi: 10.1016/j.tim.2004.11.001.

Gaiarsa, S. *et al.* (2019) 'Comparative analysis of the two *Acinetobacter baumannii* multilocus sequence typing (MLST) schemes', *Frontiers in Microbiology*, 10(930). doi: 10.3389/fmicb.2019.00930.

Garrity, G. *et al.* (eds) (2005) *Systematic Bacteriology: Volume Two: The Proteobacteria Part C: The Alpha-, Beta-, Delta-, and Epsilonproteobacteria*. New York, NY: Springer New York.

Gerner-Smidt, P., Tjernberg, I. and Ursing, J. (1991) 'Reliability of phenotypic tests for identification of *Acinetobacter* species', *Journal of Clinical Microbiology*, 29(2), pp. 277–282.

Giannouli, M. *et al.* (2010) 'Molecular epidemiology of multidrug-resistant *Acinetobacter baumannii* in a tertiary care hospital in Naples, Italy, shows the emergence of a novel epidemic clone', *Journal of Clinical Microbiology*, 48(4), pp. 1223–1230. doi: 10.1128/JCM.02263-09.

Gootz, T. D. and Marra, A. (2008) '*Acinetobacter baumannii*: An emerging multidrug-resistant threat', *Expert Review of Anti-Infective Therapy*, 6(3), pp. 309–325. doi: 10.1586/14787210.6.3.309.

Helse-Bergen (2016) *Funn av multiresistent bakterie på Brannskadeavdelinga på Haukeland*. Available at: https://helse-bergen.no/nyheiter/funn-av-multiresistent-bakterie-pa-brannskadeavdelinga-pa-haukeland (Accessed: 7 May 2020).

Henderson, I. R., Owen, P. and Nataro, J. P. (1999) 'Molecular switches - The ON and OFF of bacterial phase variation', *Molecular Microbiology*, 33(5), pp. 919–932. doi: 10.1046/j.1365-2958.1999.01555.x.

Higgins, P. G. *et al.* (2009) 'Global spread of carbapenem-resistant *Acinetobacter baumannii*', *Journal of Antimicrobial Chemotherapy*, 65(2), pp. 233–238. doi: 10.1093/jac/dkp428.

Higgins, P. G. *et al.* (2017) 'Development and evaluation of a core genome multilocus typing scheme for whole-genome sequence-based typing of *Acinetobacter baumannii*', *PLoS ONE*, 12(6). doi: 10.1371/journal.pone.0179228.

Howard, A. *et al.* (2012) '*Acinetobacter baumannii* An emerging opportunistic pathogen', *Virulence*, 3(3), pp. 243–250. doi: 10.4161/viru.19700.

Huys, G. *et al.* (2005) 'Sequence-based typing of *adeB* as a potential tool to identify intraspecific groups among clinical strains of multidrug-resistant *Acinetobacter baumannii*', *Journal of Clinical Microbiology*, 43(10), pp. 5327–5331. doi: 10.1128/JCM.43.10.5327-5331.2005.

IACG (2019) *No Time To Wait: Infections From Drug-Resistant Securing the Future*. Available at: https://www.who.int/antimicrobial-resistance/interagency-coordination-group/IACG_final_report_EN.pdf?ua=1 (Accessed: 1 November 2019).

Johnson, J. L., Anderson, R. S. and Ordal, E. J. (1970) 'Nucleic Acid Homologies Among Oxidase-Negative *Moraxella* Species', *Journal of Bacteriology*, 101(2), pp. 505–512.

Karah, N., Haldorsen, B., Hermansen, N. O., *et al.* (2011) 'Emergence of OXA-carbapenemase- and 16S rRNA methylase-producing international clones of *Acinetobacter baumannii* in Norway', *Journal of Medical Microbiology*, 60(4), pp. 515–521. doi: 10.1099/jmm.0.028340-0.

Karah, N., Haldorsen, B., Hegstad, K., *et al.* (2011) 'Species identification and molecular characterization of *Acinetobacter* spp. blood culture isolates from Norway', *Journal of Antimicrobial Chemotherapy*, 66(4), pp. 738–744. doi: 10.1093/jac/dkq521.

van der Kolk, J. H. *et al.* (2019) '*Acinetobacter* in veterinary medicine, with an emphasis on *Acinetobacter baumannii*', *Journal of Global Antimicrobial Resistance*, 16, pp. 59–71. doi: 10.1016/j.jgar.2018.08.011.

Lee, C. R. *et al.* (2017) 'Biology of *Acinetobacter baumannii*: Pathogenesis, antibiotic resistance mechanisms, and prospective treatment options', *Frontiers in Cellular and Infection Microbiology*, 7(55). doi: 10.3389/fcimb.2017.00055.

Lee, Y. T. *et al.* (2012) 'Emergence of carbapenem-resistant non-baumannii species of *Acinetobacter harboring* a $bla_{\text{OXA-51-like}}$ gene that is intrinsic to *A. baumannii*', *Antimicrobial Agents and Chemotherapy*, 56(2), pp. 1124–1127. doi: 10.1128/AAC.00622-11.

Lobanovska, M. and Pilla, G. (2017) 'Penicillin's discovery and antibiotic resistance: Lessons for the future?', *Yale Journal of Biology and Medicine*, 90(1), pp. 135–145.

Van Looveren, M. *et al.* (2004) 'Antimicrobial resistance of *Acinetobacter* spp. in Europe', *Clinical Microbiology and Infection*, 10(8), pp. 684–704. doi: 10.1111/j.1469-

0691.2004.00942.x.

Lupo, A. *et al.* (2014) ‘Antibiotic resistance and phylogenetic characterization of *Acinetobacter baumannii* strains isolated from commercial raw meat in Switzerland’, *Journal of Food Protection*, 77(11), pp. 1976–1981. doi: 10.4315/0362-028X.JFP-14-073.

Maiden, M. C. J. *et al.* (2013) ‘MLST revisited: The gene-by-gene approach to bacterial genomics’, *Nature Reviews Microbiology*, 11(10), pp. 728–736. doi: 10.1038/nrmicro3093.

Marshall, B. M. and Levy, S. B. (2011) ‘Food Animals and Antimicrobials : Impacts on Human Health’, *Clinical Microbiology Reviews*, 24(4), pp. 718–733. doi: 10.1128/CMR.00002-11.

Matuschek, E., Brown, D. F. J. and Kahlmeter, G. (2014) ‘Development of the EUCAST disk diffusion antimicrobial susceptibility testing method and its implementation in routine microbiology laboratories’, *Clinical Microbiology and Infection*, 20(4). doi: 10.1111/1469-0691.12373.

Moffatt, J. H. *et al.* (2010) ‘Colistin resistance in *Acinetobacter baumannii* is mediated by complete loss of lipopolysaccharide production’, *Antimicrobial Agents and Chemotherapy*, 54(12), pp. 4971–4977. doi: 10.1128/AAC.00834-10.

Nakhamchik, A., Wilde, C. and Rowe-Magnus, D. A. (2008) ‘Cyclic-di-GMP regulates extracellular polysaccharide production, biofilm formation, and rugose colony development by *Vibrio vulnificus*’, *Applied and Environmental Microbiology*, 74(13), pp. 4199–4209. doi: 10.1128/AEM.00176-08.

Nemec, A. *et al.* (2015) ‘*Acinetobacter seifertii* sp. nov., a member of the *Acinetobacter calcoaceticus-Acinetobacter baumannii* complex isolated from human clinical specimens’, *International Journal of Systematic and Evolutionary Microbiology*, 65(3), pp. 934–942. doi: 10.1099/ijs.0.000043.

Nemec, A. (2018) *Classification and nomenclature of species in the genus Acinetobacter*. Available at: http://apps.szu.cz/anemec/Classification.pdf (Accessed: 5 May 2020).

NORM (2019) *Norm/Norm-Vet 2018: Usage of Antimicrobial Agents and Occurrence of Antimicrobial Resistance in Norway*. Oslo/Tromsø.

O'Neill, J. (2014) *Review on Antibiotic resisitance. Antimicrobial Resistance : Tackling a crisis for the health and wealth of nations*. Available at: https://amr-review.org/sites/default/files/AMR Review Paper - Tackling a crisis for the health and wealth of nations_1.pdf (Accessed: 8 February 2019).

Onarheim, H. *et al.* (2000) 'Outbreak of multiresistant *Acinetbacter baumannii* infection', *Tidsskr Nor Laegeforen*, 120(9), pp. 1028–1033. Available at: https://tidsskriftet.no/2000/04/klinikk-og-forskning/utbrudd-av-infeksjon-med-multiresistent-acinetobacter-baumannii.

Pailhoriès, H. *et al.* (2015) 'Diversity of *Acinetobacter baumannii* strains isolated in humans, companion animals, and the environment in Reunion Island: An exploratory study', *International Journal of Infectious Diseases*, 37, pp. 64–69. doi: 10.1016/j.ijid.2015.05.012.

Peleg, A. Y., Seifert, H. and Paterson, D. L. (2008) '*Acinetobacter baumannii*: Emergence of a successful pathogen', *Clinical Microbiology Reviews*, 21(3), pp. 538–582. doi: 10.1128/CMR.00058-07.

Pérez-Varela, M. *et al.* (2020) 'Characterization of RelA in *Acinetobacter baumannii*', *Journal of Bacteriology*. doi: 10.1128/jb.00045-20.

Perez, F. *et al.* (2007) 'Global challenge of multidrug-resistant *Acinetobacter baumanni*', *Antimicrobial Agents and Chemotherapy*, 51(10), pp. 3471–3484. doi: 10.1128/AAC.01464-06.

Rafei, R., Hamze, M., *et al.* (2015) 'Extrahuman epidemiology of *Acinetobacter baumannii* in Lebanon', *Applied and Environmental Microbiology*, 81(7), pp. 2359–2367. doi: 10.1128/AEM.03824-14.

Rafei, R., Pailhoriès, H., *et al.* (2015) 'Molecular epidemiology of *Acinetobacter baumannii* in different hospitals in Tripoli, Lebanon using bla OXA-51-like sequence based typing',

BMC Microbiology, 15(103). doi: 10.1186/s12866-015-0441-5.

Richardson, E. J. *et al.* (2018) 'Gene exchange drives the ecological success of a multi-host bacterial pathogen', *Nature Ecology and Evolution*, 2(9), pp. 1468–1478. doi: 10.1038/s41559-018-0617-0.

Rooney, A. P., Dunlap, C. A. and Flor-Weiler, L. B. (2016) '*Acinetobacter lactucae* sp. nov., isolated from iceberg lettuce (Asteraceae: Lactuca sativa)', *International Journal of Systematic and Evolutionary Microbiology*, 66(9), pp. 3566–3572. doi: 10.1099/ijsem.0.001234.

Savin, M. *et al.* (2019) 'Draft Genome Sequences of *Acinetobacter baumannii* Isolates Recovered from Sewage Water from a Poultry Slaughterhouse in Germany', *Microbiology Resource Announcements*, 8(28). doi: 10.1128/mra.00553-19.

Schleicher, X. *et al.* (2013) 'Molecular epidemiology of *Acinetobacter baumannii* and *Acinetobacter nosocomialis* in Germany over a 5-year period (2005-2009)', *Clinical Microbiology and Infection*. European Society of Clinical Microbiology and Infectious Diseases, 19(8), pp. 737–742. doi: 10.1111/1469-0691.12026.

Šedo, O. *et al.* (2013) 'Improvement of MALDI-TOF MS profiling for the differentiation of species within the *Acinetobacter calcoaceticus-Acinetobacter baumannii* complex', *Systematic and Applied Microbiology*, 36(8), pp. 572–578. doi: 10.1016/j.syapm.2013.08.001.

Seifert, H. and Dijkshoorn, L. (2008) '*Acinetobacter* Biology and Pathogenesis: Overview of the Microbial Characteristics, Taxonomy, and Epidemiology of *Acinetobacter*', in *Acinetobacter Biology and Pathogenesis*. doi: 10.1007/978-0-387-77944-7.

Shrestha, S. *et al.* (2015) 'Molecular epidemiology of multidrug-resistant *Acinetobacter baumannii* isolates in a university hospital in Nepal reveals the emergence of a novel epidemic clonal lineage', *International Journal of Antimicrobial Agents*, 46(5), pp. 526–531. doi: 10.1016/j.ijantimicag.2015.07.012.

Da Silva, K. E. *et al.* (2018) 'A high mortality rate associated with multidrug-resistant *Acinetobacter baumannii* ST79 and ST25 carrying OXA-23 in a Brazilian intensive care unit', *PLoS ONE*, 13(12). doi: 10.1371/journal.pone.0209367.

***Sir Alexander Fleming – Nobel Lecture* (2019)**. NobelPrize.org. Nobel Media AB 2019. Available at: https://www.nobelprize.org/uploads/2018/06/fleming-lecture.pdf (Accessed: 23 August 2019).

Tacconelli, E. *et al.* (2018) 'Discovery, research, and development of new antibiotics: the WHO priority list of antibiotic-resistant bacteria and tuberculosis', *The Lancet Infectious Diseases*, 18(3), pp. 318–327. doi: 10.1016/S1473-3099(17)30753-3.

Tipton, K. A., Dimitrova, D. and Rather, P. N. (2015) 'Phase-variable control of multiple phenotypes in *Acinetobacter baumannii* strain AB5075', *Journal of Bacteriology*, 197(15), pp. 2593–2599. doi: 10.1128/JB.00188-15.

Touchon, M. *et al.* (2014) 'The genomic diversification of the whole *Acinetobacter* genus: Origins, mechanisms, and consequences', *Genome Biology and Evolution*, 6(10), pp. 2866–2882. doi: 10.1093/gbe/evu225.

Turton, J. F. *et al.* (2006) 'Identification of *Acinetobacter baumannii* by detection of the *bla* $_{\text{OXA-51-like}}$ carbapenemase gene intrinsic to this species', *Journal of Clinical Microbiology*, 44(8), pp. 2974–2976. doi: 10.1128/JCM.01021-06.

Urwin, R. and Maiden, M. C. J. (2003) 'Multi-locus sequence typing: A tool for global epidemiology', *Trends in Microbiology*, 11(10), pp. 479–487. doi: 10.1016/j.tim.2003.08.006.

Waterhouse, A. M. *et al.* (2009) 'Jalview Version 2-A multiple sequence alignment editor and analysis workbench', *Bioinformatics*, 25(9), pp. 1189–1191. doi: 10.1093/bioinformatics/btp033.

Watson, J. D. *et al.* (2013) *Molecular Biology of the Gene, 7th edition*. Pearson.

WHO (2014) *Antimicrobial resistance: global report on surveillance, WHO*. Available at: https://www.who.int/antimicrobial-resistance/publications/surveillancereport/en/ (Accessed: 27 November 2019).

WHO (2015) *Global action plan on antimicrobial resistance, WHO*. Available at: https://www.who.int/antimicrobial-resistance/publications/global-action-plan/en/ (Accessed: 8 May 2019).

Wilharm, G. *et al.* (2017) 'Relatedness of wildlife and livestock avian isolates of the nosocomial pathogen *Acinetobacter baumannii* to lineages spread in hospitals worldwide', *Environmental Microbiology*, 19(10), pp. 4349–4364. doi: 10.1111/1462-2920.13931.

Wisniewski-Dyé, F. and Vial, L. (2008) 'Phase and antigenic variation mediated by genome modifications', *Antonie van Leeuwenhoek, International Journal of General and Molecular Microbiology*, 94(4), pp. 493–515. doi: 10.1007/s10482-008-9267-6.

World Bank (2017) *Drug-Resistant Infections: A Threat to Our Economic Future, World Bank*. Available at: http://documents.worldbank.org/curated/en/323311493396993758/pdf/final-report.pdf (Accessed: 27 November 2019).

Xiong, J. (2006) *Essentials of Bioinformatics*. Cambridge University Press.
Xu, C., Bilya, S. R. and Xu, W. (2019) 'adeABC efflux gene in *Acinetobacter baumannii*', *New Microbes and New Infections*, 30(100549). doi: 10.1016/j.nmni.2019.100549.

Zahn, M. *et al.* (2016) 'Structural Insights into Outer Membrane Permeability of *Acinetobacter baumannii*', *Structure*, 24(2), pp. 221–231. doi: 10.1016/j.str.2015.12.009.

Zaman, S. Bin *et al.* (2017) 'A Review on Antibiotic Resistance: Alarm Bells are Ringing', *Cureus*, 9(6). doi: 10.7759/cureus.1403.

Zander, E. *et al.* (2013) 'Detection of intrinsic $bla_{\text{OXA-51-like}}$ by multiplex PCR on its own is not reliable for the identification of *Acinetobacter baumannii*', *International Journal of Medical Microbiology*, 303(2), pp. 88–89. doi: 10.1016/j.ijmm.2012.12.007.

Appendices

Appendix 1, Recipes: Buffers and solutions

dNTP-mix with a final concentration of 10 mM

50 µL dATP (100 mM) (Thermo Fisher Scientific)

50 µL dGTP (100 mM) (Thermo Fisher Scientific)

50 µL dTTP (100 mM) (Thermo Fisher Scientific)

50 µL dCTP (100 mM) (Thermo Fisher Scientific)

300 µL MQ-dH2O

The components were mixed and stored at -20 °C.

Primer-mix with a final concentration of 10 µM

50 µL Forward-Primer (100 µM) (Thermo Fisher Scientific)

50 µL Reverse-Primer (100 µM) (Thermo Fisher Scientific)

400 µL MQ-dH2O

Ethidium bromide (5 mg/mL)

0.5 g of ethidium bromide (Sigma-Aldrich/Merck) was added to 100 mL MQ-dH_2O. The container was wrapped in aluminum foil and the mixture was stirred magnetically for several hours to ensure dissolution of the dye. The solution was stored at 4 °C.

Orange mix

10 g Ficoll 400 (Sigma-Aldrich/Merck)

0.125 g Orange G (Sigma-Aldrich/Merck)

2 mL EDTA (0.5 M, pH 8.0)

The components were dissolved in 50 ml MQ-dH_2O and sterile-filtrated. The solution was aliquoted in sterile Eppendorf tubes and stored at -20 °C.

50 × TAE (Tris/acetat/EDTA buffer)

242 g Tris-Base (Sigma-Aldrich/Merck)

57.1 mL acetic acid (17.5 M) (VWR)

100 mL EDTA (0.5 M, pH 8.0)

MQ-dH2O added to 1 L

The solution was stored at room temperature.

1 × TAE (Tris/Acetate/EDTA buffer)

20 mL 50 x TAE buffer

980 mL MQ-dH2O

The solution was stored at room temperature.

1 % agarose gel

0.075 L/0.2 L/0.4 L 1 X TAE buffer

0.75 g/2.0 g/4.0 g Agarose (Life Technologies/Thermo Fisher Scientific or FMC bioproducts)

7.5 µL/20 µL/40 µL EtBr or GelRed (Sigma-Aldrich/Merck or Biotium)

0.5X LB agar medium for plates (1 L)

5 g Tryptone (Oxoid/Thermo Fisher Scientific)

2.5 g Yeast extract (Oxoid/Thermo Fisher Scientific)

5 g NaCl (VWR)

12.5 g Agar (Oxoid/Thermo Fisher Scientific)

Water is added up to the 1 L mark

The pH is adjusted if needed to 7 with 5.8 M HCl.

The solution was sterilized by using an autoclave. Afterwards it was cooled in a water bath at 45-50 °C.

LB agar medium for plates (1 L)

10 g Tryptone (Oxoid/Thermo Fisher Scientific)

5 g Yeast extract (Oxoid/Thermo Fisher Scientific)

10 g NaCl (VWR)

12.5 g Agar (Oxoid/Thermo Fisher Scientific)

Water is added up to the 1 L mark

The pH is adjusted if needed to 7 with 5.8 M HCl.

The solution was sterilized by using an autoclave. Afterwards it was cooled in a water bath at 45-50 °C.

LB medium (1 L)

10 g Tryptone (Oxoid/Thermo Fisher Scientific)

5 g Yeast extract (Oxoid/Thermo Fisher Scientific)

10 g NaCl (VWR)

Water is added up to the 1 L mark

The pH is adjusted if needed to 7 with 5.8 M HCl.

The solution was sterilized by using an autoclave.

Mueller-Hinton agar 2 medium for plates (1 L medium)

38 grams of premade mix Mueller-Hinton agar 2 powder (Sigma-Aldrich/Merck).

Water is added up to the 1 L mark.

The solution was sterilized by using an autoclave. Afterwards it was cooled in a water bath at 45-50 °C.

Mueller-Hinton broth medium (1 L medium)

21 g of premade mix Mueller-Hinton broth powder (Sigma-Aldrich/Merck).

Water is added up to the 1 L mark.

The solution was sterilized by using an autoclave. Afterwards it was cooled in a water bath at 45-50 °C.

Saline solution (0.85 %) (1 L)

8.5 g NaCl (VWR)

Water is added up to the 1 L mark.

The solution was sterilized by using an autoclave.

Tobramycin solution (10.88 mg/mL)

13.77 mg of tobramycin sulfate (Sigma-Aldrich/Merck) was dissolved in 1 mL of autoclaved water. The solution was aliquoted in sterile Eppendorf tubes and stored at -20 °C.

Gentamicin solution (12.94 mg/mL)

15.60 mg of gentamicin sulfate (Sigma-Aldrich/Merck) was dissolved in 1 mL of autoclaved water. The solution was aliquoted in sterile Eppendorf tubes and stored at -20 °C.

Appendix 2, Oligonucleotide primer sequences

Gene	Direction	Sequence
60-kDa chaperonin (*cpn60*)	F	ACTGTACTTGCTCAAGC
60-kDa chaperonin (*cpn60*)	R	TTCAGCGATGATAAGAAGTGG
Elongation factor EF-G (*fusA*)	F	ATCGGTATTTCTGCKCACATYGAT
Elongation factor EF-G (*fusA*)	R	CCAACATACKYTGWACACCTTTGTT
Citrate synthase (*gltA*)	F	AATTTACAGTGGCACATTAGGTCCC
Citrate synthase (*gltA*)	R	GCAGAGATACCAGCAGAGATACACG
CTP synthase (*pyrG*)	F	GGTGTTGTTTCATCACTAGGWAAAGG
CTP synthase (*pyrG*)	R	ATAAATGGTAAAGAYTCGATRTCACCMA
Homologous recombination factor (*recA*)	F	CCTGAATCTTCYGGTAAAAC
Homologous recombination factor (*recA*)	R	GTTTCTGGGCTGCCAAACATTAC
50S ribosomal protein L2 (*rplB*)	F	GTAGAGCGTATTGAATACGATCCTAACC
50S ribosomal protein L2 (*rplB*)	R	CACCACCACCRTGYGGGTGATC
RNA polymerase subunit B (*rpoB*)	F	GGCGAAATGGC(AGT)GA(AG)AACCA
RNA polymerase subunit B (*rpoB*)	R	GA(AG)TC(CT)TCGAAGTTGTAACC

The primer sequences were retrieved from:

https://pubmlst.org/abaumannii/info/primers_Pasteur.shtml

Appendix 3, template sequences for MLST

cpn60 (405 bp):

ATGAACCCAA TGGATTTAAA ACGCGGTATC GACATTGCAG TAAAAACTGT AGTTGAAAAT ATCCGTTCTA
TTGCTAAACC AGCTGATGAT TTCAAAGCAA TTGAACAAGT AGGTTCAATC TCTGCTAACT CTGATACTAC
TGTTGGTAAA CTTATTGCTC AAGCAATGGA AAAAGTAGGT AAAGAAGGCG TAATCACTGT AGAAGAAGGT
TCTGGCTTCG AAGACGCATT AGACGTTGTA GAAGGTATGC AGTTTGACCG TGGTTATATC TCTCCGTACT
TTGCAAACAA ACAAGATACT TTAACTGCTG AACTTGAAAA TCCGTTCATT CTTCTTGTTG ATAAAAAAAT
CAGCAACATT CGTGAATTGA TTTCTGTTTT AGAAGCAGTT GCTAAAACTG GTAAA

fusA (633 bp):

ATTGGTGAAG TACACGACGG TGCAGCAACA ATGGACTGGA TGGAACAAGA GCAAGAGCGT GGTATTACAA
TTACCTCTGC TGCAACAACT TGTTTCTGGT CTGGTATGGG TAACCAATTC CCACAACACC GTATCAACGT
AATTGATACA CCGGGACACG TTGACTTCAC AATCGAAGTT GAGCGTTCTA TGCGTGTTCT TGACGGTGCT
TGCATGGTTT ACTGTGCAGT TGGTGGTGTA CAGCCTCAGT CTGAAACTGT ATGGCGTCAG GCTAACAAAT
ATAAAGTGCC TCGTTTAGCA TTCGTGAACA AGATGGACCG TACTGGTGCA AACTTCTTCC GTGTTGTTGA
ACAAATGAAA ACACGTCTTG GTGCGAATCC TGTGCCAATC GTTGTGCCAA TCGGTGCTGA AGACACATTC
ACTGGTGTAG TTGACCTTAT CGAAATGAAG GCAATTATCT GGGATGAAGC TTCTCAAGGT ATGAAGTTTG
AATACGGCGA GATTCCAGCT GACCTAGTTG ATACTGCTCA AGAATGGCGT ACAAACATGG TTGAAGCTGC
TGCTGAAGCT TCTGAAGAGT TAATGGACAA GTACCTTGAA GAGGGTGATC TTTCTAAAGA AGACATCATC GCA

gltA (483 bp):

GATCCTGGTT TTATGGCGAC AGCTTCATGC GAGTCTAAAA TCACATTTAT CGATGGTGAC AAAGGTATTT
TATTACACCG CGGTTACCCG ATTGACCAGT TAGCGACTCA AGCAGACTAC CTTGAAACTT GTTATTTATT
ATTAAATGGC GAGTTACCAA CTGCTGAACA AAAAGTTGAG TTCGATGCGA AAGTTCGTGC TCATACTATG
GTTCATGATC AAGTTAGCCG TTTCTTCAAT GGTTTCCGTC GTGATGCTCA CCCTATGGCA ATCATGGTTG
GTGTAGTAGG CGCATTATCT GCTTTCTATC ACAACAACCT TGACATTGAA GACATCAATC ACCGCGAAAT
TACTGCGATT CGTTTGATTG CTAAAATTCC AACGCTTGCT GCTTGGAGCT ACAAATATAC TGTAGGTCAG
CCATTCATCT ATCCACGTAA TGACTTAAAT TATGCGGAAA ACTTCTTACA CATGATGTTT GCA

pyrG (297 bp):

AAAGTCACAA TGGTTAAAAT GGATCCTTAT ATTAATGTCG ATCCAGGGAC AATGAGCCCA TTCCAGCATG
GTGAAGTTTT TGTTACCGAA GATGGTGCAG AAACAGATCT GGATCTGGGT TATTACGAAC GTTTCTTACG
TCGCGCGAAA ATGACCAAAC TAAACAACTT CACTAGTGGT CGTGTATATC AAGACGTTTT AAATAAAGAG
CGTCGTGGTG ATTACTTAGG TGGTACAGTT CAGGTTATTC CTCATATTAC CGACAATATT AAAGAACGTG
TACTCCGCGC AGGCGAA

recA (372 bp):

TTACAAGCAA TTGCTCAATG TCAAAAATCT GGTGGTACAT GTGCCTTCAT TGATGCTGAG CACGCCCTAG
ACCCTCAATA TGCACGCAAA CTTGGTGTAG ATATTGATAA CCTACTTGTT TCACAACCCG ACAATGGTGA
GCAAGCACTT GAAATTGCTG ACATGCTTGT CCGTTCAGGC GCAATTGATT TAATCGTTGT GGACTCGGTG
GCTGCACTTA CGCCTAAAGC AGAAATCGAA GGTGAGATGG GTGACTCTCA TATGGGTCTA CAAGCGCGTC
TTATGAGCCA GGCACTTCGT AAAATTACGG GTAATGCTAA ACGTTCAAAC TGTATGGTTA TCTTCATTAA
CCAGATTCGT ATGAAAATTG GT

rplB (330 bp):

CGTCGTTATA TCATTGCGCC TAAAGGCTTA CGTGCTGGTG ATAAAGTACA ATCTGGTAAC GATGCTCCAA
TTCGTCCAGG TAACTGTTTA CCACTTCGTA ACATGCCAAT CGGTTCTACA CTTCATAACG TTGAACTTAA
AATCGGTAAA GGTGCTCAAT TAGCACGTTC TGCTGGTGCT TCTGTTCAAT TGTTGGGTCG TGATGGTTCT
TACGCAATCA TTCGTCTTCG TTCAGGCGAA ATGCGTAAAG TACACGTTGA ATGCCGCGCT GTAATTGGTG
AAGTTTCTAA CCAAGAAAAC AACCTTCGCT CATTAGGTAA AGCTGGTGCT

rpoB (456 bp):

CAAACTCACT ATGGTCGTGT TTGTCCAATT GAAACTCCTG AAGGTCCAAA CATTGGTTTG ATCAACTCGC
TTTCTGTATA CGCAAAAGCG AATGACTTCG GTTTCTTGGA AACTCCATAC CGCAAAGTTG TAGATGGTCG
TGTAACTGAT GATGTTGAAT ATTTATCTGC AATTGAAGAA GTAGGCACTG TTATTGCACA GGCCGACTCT
GCAGTAGATA AAGATGGCAA CTTAACAGAA GAATTCGTTT CTGTTCGTCA TCAAGGTGAA TTCGTACGTA
TGCCGCCTGA AAAAGTAACG CATATGGACG TTTCTGCACA GCAGGTAGTA TCTGTTGCTG CATCACTTAT
TCCATTCCTT GAACACGATG ACGCAAACCG TGCGCTCATG GGTTCAAACA TGCAACGTCA GGCAGTTCCT
ACTTTACGTG CGGATAAACC GCTTGTAGGT ACAGGT

The templates were retrieved from:

https://pubmlst.org/abaumannii/info/primers_Pasteur.shtml